Westfälische Wilhelms-Universität Münster
Institute for theoretical physics

Jet radius dependence in aNNLO in DIS and photoproduction

Master thesis

Author: Jonas Potthoff

First supervisor: Prof. Dr. Michael Klasen

Second supervisor: Dr. Karol Kovarik

March 27, 2018

Stephen Hawking

1942 – 2018

Contents

1. Introduction

This thesis focuses on the perturbative calculation of cross sections for inclusive jet production in deep-inelastic scattering (DIS). It provides an extension of previous work on this topic ([1,2]) which analysed data of the HERA collider numerically based on the program JetVip [3] which computes inclusive DIS cross sections in full next-to-leading order (NLO). In [1] the associated code was extended to approximate next-to-next-to-leading order (aNNLO) by implementing a NNLO master formula stemming from a unified threshold resummation formalism [4].
The spirit underlying this subsequent study originates from findings concerning the invariant mass of the produced jet that were presented in [5,6]. In NLO it is commonly defined as $m^2 = (p_j + p_k)^2 = 2p_j \cdot p_k$ considering massless final-state partons j, k as they occur in DIS. At partonic threshold, i.e. the kinematical region where one of the momenta p_j, p_k tends to zero, this invariant mass is usually supposed to vanish. In experiment, it was shown, however, that a jet may have a non-vanishing invariant mass even at partonic threshold which affects its theoretical description significantly. Assuming the latter it becomes possible to calculate contributions $d\sigma_{jk}$ expressing the joint formation of the jet by two partons by integrating the associated phase space up to an upper limit of the jet invariant mass which depends on the chosen jet algorithm. This procedure leads to the situation that the contributions of the former NLO calculation get novel terms which partly depend on the cone opening δ of the jet or, what is qualitatively the same, on the jet radius R. Terms like these are so far not included in the code that was employed in [1,2]. Therefore, the presentation and implementation of them is topic of this thesis. It will not be the aim, however, to apply them in NLO what would mean to change parts of the original JetVip code. The basic idea is to use several contributions which are logarithmically enhanced at partonic threshold just within the framework of the aNNLO approach of the resummation formalism by adding them to the latter. This type of contributions shows the feature to be present in the full NLO calculation of JetVip as well as in the NNLO master formula which justifies the proceeding of this study. In particular, the numerical change induced by the NNLO master formula was found to be sizeable in [1,2].
By checking the available literature on the topic presented before it turns out that, essentially, all necessary theoretical computations have already been done so that we could directly start the numerical study. But to make this thesis self-contained, we will indeed do the exact opposite and present all important steps of the calculation in detail as it cannot be found in the literature so far. This also applies to quite basic calculations of LO cross sections and one-loop soft anomalous dimensions in the following chapter. In that regard, the crucial hard scattering events of DIS, namely QCD Compton scattering where the photon scatters a quark leading to a quark and a gluon in the final state, and boson gluon fusion where the photon merges with a gluon leaving a quark-antiquark pair, will constitute the common thread. In addition, the processes of quark-antiquark annihilation and light quark production will appear once although it is not relevant for our purposes - it will in a way serve as an 'educational method' to demonstrate the striking increase of theoretical complexity just caused by 'substituting' the photon (described

by the theory of quantum electrodynamics (QED)) by another parton (described by the theory of quantum chromodynamics (QCD)).
This work is structured as follows. In chapter 2 we are going to introduce the reader into the theoretical background and present a short review of the results in [1,2] on which this thesis will build on. Chapter 3 contains the main theoretical part which is the explicit computation of the novel logarithmically enhanced contributions[1] by, among others, specifying and evaluating the terms $d\sigma_{jk}$ mentioned above. In chapter 4 we will show and discuss the results of a numerical study performed with the newly incorporated terms. The appendix is dedicated to diverse Feynman rules and the QCD splitting functions.
We emphasize that all cross sections considered in this work are differential. We exclusively operate with natural units, i.e. it always holds $\hbar = c = 1$, [length]=[time], [energy]=[mass] and [length]=[mass]$^{-1}$.

[1] **For the reason of simplicity we include the usual delta distribution in this expression from now on.**

2. Prerequisites and fundamental calculations

2.1. Basic features of perturbative QCD

In DIS we are faced with the situation that virtual photons stemming from electrons (or positrons) scatter constituents of the proton, quarks and gluons, which are described by the theory of quantum chromodynamics (QCD). In practice, there are basically two ways today to adapt it to concrete experimental issues, QCD on the lattice or perturbative QCD (pQCD). The latter is used in the program JetVip and constitutes the basis of this thesis. In this section we will qualitatively summarize some important features of pQCD that play a role for us without raising claim to completeness. For a quantitative presentation the reader can stick to a plenty of references (e.g. [7,8,9]).
The astonishing properties of quarks and gluons have been investigated for many decades. Compared to their counterparts in quantum electrodynamics (QED), electrons and photons, it was found that not only quarks exhibit a new quantum number, the color, that commands them to live in color-neutral and compound states solely, but also the gluons which show a self-interaction for this reason. By contrast, the photon as the boson of QED is electrically neutral. On theoretical side this has the consequence that QCD relies on a non-Abelian gauge theory with SU(3)-symmetry. On practical side it means that calculations become more involved because one has to deal with an additional interaction vertex, the three-gluon-vertex. The most wide-reaching consequence, however, affects the strong coupling α_s between quarks and gluons which changes its value depending on the considered energy scale - one usually distinguishes between a long-range behaviour at small energies for which the coupling is large, and a short-range behaviour at large energies for which it is small. These characteristics of α_s become heuristically clear from the fact that quarks and gluons cannot exist as individuals, theoretically they are derived in the context of ultraviolet divergences (see below). A perturbative approach to calculate observables like (in our case) cross sections is always based on an expansion concerning the corresponding coupling leading to terms proportional to α_s^0 in lowest order (LO), α_s^1 in next-to-leading order (NLO), α_s^2 in next-to-next-to leading order (NNLO) and so on. Since the associated computations become increasingly challenging (there does not exist a full NNNLO result for any domain today) it is highly dependent on a sufficiently small coupling constant to guarantee that higher powers α_s^n tend to zero. For QCD it therefore emerges that the perturbative method is exclusively applicable to short-range energy scales. Luckily, the actual scattering process which is called 'hard scattering' is such an event including high energies and hence can be treated by pQCD; the long-range effects are expressed with the aid of global parton distribution functions (PDFs) which describe the energy-dependent deep structure of the proton in terms of quarks and gluons independently of the scattering. The observation that QCD calculations split up into these two parts finds its expression in the term 'factorization'. It is accompanied by the need to introduce a factorization scale μ_F into the calculation. In the perturbative sector of particle physics the concept of Feynman diagrams is undisputed to visualize what the physical reality behind computational prescriptions could be. The LO diagrams for QCD Compton scattering and boson gluon fusion which are

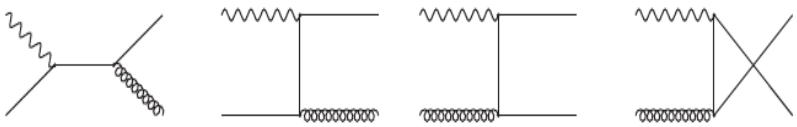

Figure 2.0: Feynman diagrams for the cross sections contributing in DIS to lowest order of perturbation theory [1].

relevant in this thesis are depicted in Figure 2.0. It is common to illustrate a photon by a wave, a gluon by a spiral and a quark by a line that is drawn through. One sometimes meets dashed lines in addition standing for so called 'ghosts' which remove redundant degrees of freedom of the gluons (see [9]). We choose the time axis to run from the left to the right. The involved particles interact at the vertices, i.e. the points where their illustrations convene. The particle that connects two vertices as a 'propagator' transfers the interaction from the initial state to the final state. In the light of this nice pictoriality one might forget that it was invented to clarify a purely mathematical procedure which will be the topic of the next section where several LO processes get evaluated. The translation prescription of Feynman diagrams into mathematic expressions are the Feynman rules which can be found in appendix A. There, as well as in chapter 2.2, the strong coupling reads g instead of α_s as it is often the case in the literature.
As it turns out the calculation of the lowest order in pQCD is a straightforward task without any conceptual problems. This is no longer true for NLO calculations. On the one hand, we have to deal with a big amount of new Feynman diagrams stemming from the adding of additional particles to the LO ones, either as virtual loops with two additional vertices, or as real objects in the initial and final state with one additional vertex (see [1] for the relevant diagrams concerning DIS). On the other hand, many of these new diagrams cause trouble when computing them in terms of different kinds of divergences. The latter become manifest by making use of dimensional regularization, i.e. the calculation of all quantities in $D = 4 - 2\varepsilon$ (or $D = 4 - \varepsilon$) dimensions. This method does not change the situation but helps to make it overseeable - since the divergences are present in the usual $D = 4$ dimensions they become arranged by it in single or double poles in ε. pQCD remains meaningful only because it is possible to get rid of these poles after performing a complete calculation properly. The origin of these so called 'mass singularities' are propagators of massless quarks and gluons if a quark collinearly emits a gluon ('collinear' divergence) or a gluon (which is massless in any case) is soft leading to $k^2 \approx 0$ for its momentum ('soft' or 'infrared' divergence). If

this happens to be independent of each other it results in a single pole, otherwise (if the emitted gluon is soft) in a double pole. The Kinoshita-Lee-Nauenberg theorem (KLN theorem) states that these singularities always appear twice, in the real contributions as well as in the virtual ones, but with opposite signs, so that they cancel each other at the end. It is not easy, however, to achieve this cancellation in the context of numerical methods; in the program JetVip a 'phase space slicing' algorithm is therefor used which is able to separate off one part of the phase space from another (see [1,10]). Moreover, some of the collinear divergences do not disappear and have to be incorporated into the parton distribution functions. So far, we have neglected one critical type of divergence that is not covered by the KLN theorem, the ultraviolet divergences. They arise due to the fact that the evaluation of loop diagrams involves the integration over unlimited momenta. This crucial problem of the virtual contributions is solved within the framework of renormalization. Its basic principle consists in absorbing the occurring infinities by a couple of renormalization constants whose amount was shown to be limited in all orders of perturbation theory. Performing this procedure one is left with solely finite quantities. The main consequence of renormalization is that the strong coupling α_s becomes scale-dependent. This fact is called the 'running of the coupling' and constitutes the theoretical explanation of the different behaviour of QCD on short and long distances. The dependence of the coupling on the renormalization scale μ_R is mostly hidden but should be kept in mind, i.e. it is always $\alpha_s = \alpha_s(\mu_R)$. The differential change of α_s with this scale is given quantitatively by the QCD beta function which can be calculated perturbatively by loop diagrams.

After this very compact presentation of the challenges in NLO of pQCD we still have to specify the outcome of the application of the KLN theorem. It is refered to as 'real corrections' and basically consists of special 'plus distributions' that will become important in chapter 2.3 and the whole progress of this thesis. It is a further characteristic of pQCD that there exist real corrections which have to be taken into account in all orders to get a reasonable result - this problem can be solved with the help of threshold resummation which will be introduced in chapter 2.3, too. The threshold resummation approach besides provides a way to gain results in approximate NNLO (aNNLO) which are computable on the level of Feynman diagrams only with tremendous effort.

Finally, we would like to mention one interesting aspect concerning the main theoretical part of this work, section 3, where we will compute real corrections including the jet radius R. The associated procedure does not represent usual perturbation theory but shows up to be strongly linked with it: There appear terms $d\sigma_{j(k)}$ and $d\sigma_{jk}$ representing the emission of real partons j and k in the final state while for the second ones parton k is assumed to be measured (to form a jet together with parton j), for the first ones not. In this sense, we are inclined to interpret the first ones as virtual, the second ones as real contributions. This idea indeed turns out to be true - using dimensional regularization one finds singularities as single and double poles in ε that, as theory maintains, cancel each other at the end. The associated calculation will be shown in detail in sections 3.2 and 3.3.

2.2. LO cross sections

In light of the effort needed to calculate QCD cross sections in higher orders of perturbation theory the computation of lowest order cross sections tends to be a quite easy task. Nevertheless, the standard LO calculations of the so called 'Born terms' also contain some algebra so that computing programs like *Form* or *FeynCalc* are partially very useful tools. In this chapter such calculations will be presented for one resolved and two direct processes concerning photoproduction in more detail. Only the squared matrix elements are given because they differ from the total cross section just by constant factors. Although these computations are basic this more in-depth presentation could be especially helpful for readers with less experience in this domain.

2.2.1. Algebraic relations

Necessarily, the intended computations make use of Dirac and Color matrices which are part of the corresponding Feynman rules. For further details concerning this aspect and, especially, the origin of Feynman rules we point to the rich literature treating these topics (e.g. [7]). Here, we only give a couple of useful relations which are employed in the following. Thereby, Einstein sum convention holds everywhere when indices occur twice in a product.
The Dirac matrices γ^μ, $(\mu = 0, ..., 3)$, originating from the Dirac equation, appear at vertices where fermions like quarks are involved. In our case their explicit representation does not matter because at the end they always show up either in a trace or in contracted form. Three important relations are

$$\begin{aligned}
&\gamma^0\gamma^0 = 1 \ , \\
&\gamma_\mu^\dagger = \gamma^0\gamma_\mu\gamma^0 \ , \\
&\gamma_\mu \not{p} \gamma^\mu = -2\not{p} \ ,
\end{aligned}$$

where Feynman slash notation ($\gamma^\mu p_\mu = \not{p}$) was used, and the definition

$$\bar{u} = u^\dagger\gamma^0 \ .$$

The spinor $u(p, s)$ which is also a part of the solution of the Dirac equation and describes the propagation of a fermion depends on its momentum and spin. It fulfills the completeness relation

$$\sum_s \bar{u}(p, s)u(p, s) = \not{p} \ ,$$

which holds in the same way for the spinor $v(p, s)$ of antiparticles while the sum involves the two possible spin configurations (up and down). The term 'Color matrices' expresses the application field of the Gell-Mann matrices in particle physics when gluons are involved. They are noted here as T^a_{ij} (or just T^a) where a ranges over the eight different

matrices which are constructed within SU(3). So N has to be replaced by 3 when it is part of equations. The same holds for the structure constants f^{abc} originating from the Lie algebra of SU(3). In our context the traces

$$\begin{aligned}
&\mathrm{Tr}(T^a T^a) = (\sum_a T^a_{ji} T^a_{ij}) \cdot (\mathrm{Tr}\mathbb{1}) = \frac{N^2-1}{2N} \cdot 3 = 4 \ , \\
&\mathrm{Tr}(T^a T^b T^b T^a) = \left(\frac{N^2-1}{2N}\right)^2 \cdot 3 = \frac{16}{3} \ , \\
&\mathrm{Tr}(T^a T^b T^c f^{abc}) = 6i = -\mathrm{Tr}(T^a T^b T^c f^{acb})
\end{aligned}$$

as well as the product of structure constants

$$f^{abc} f^{abd} = N\delta_{cd} = 3\delta_{cd}$$

play an important role. Not least, the trace of four momenta in Feynman slash notation

$$\mathrm{Tr}(\not{p}_1 \not{p}_2 \not{p}_3 \not{p}_4) = 4\left[(p_1 \cdot p_2)(p_3 \cdot p_4) - (p_1 \cdot p_3)(p_2 \cdot p_4) + (p_1 \cdot p_4)(p_2 \cdot p_3)\right]$$

is required.

2.2.2. Mandelstam variables

Scattering processes in particle physics are usually described with the aid of the three Mandelstam variables s, t and u. They contain squared sums or differences of the four-momenta p_i, corresponding to four involved particles in $2 \to 2$ processes, where the indices 1 and 2 describe the incoming, 3 and 4 the outgoing ones. Their global definition reads

$$\begin{aligned}
s &= (p_1 + p_2)^2 = (p_3 + p_4)^2 \ , \\
t &= (p_1 - p_3)^2 = (p_2 - p_4)^2 \ , \\
u &= (p_1 - p_4)^2 = (p_2 - p_3)^2 \ .
\end{aligned}$$

Applying the limit of vanishing quark masses which implies $p_i^2 = \not{p}_i^2 = m_i^2 = 0$ it passes into

$$\begin{aligned}
s &= 2p_1 p_2 = 2p_3 p_4 \ , \\
t &= -2p_1 p_3 = -2p_2 p_4 \ , \\
u &= -2p_1 p_4 = -2p_2 p_3 \ .
\end{aligned}$$

In the latter case we find the important relation $s + t + u = 0$ which will be used frequently in the following. Different scattering channels are named after these variables concerning the intermediate particle that carries the momentum squared in the related variable s, t or u. Readers should not be confused by the fact that $t-$ and $u-$channels

may often become exchanged without receiving another result. Moreover, it should be emphasized that the direction of scattering processes does not matter for the LO cross section.

2.2.3. QCD Compton scattering $\gamma q \to qg$

For QCD Compton scattering one s-channel- and one u-channel-diagram each with an intermediate quark need to be evaluated (see Figure 2.0). Applying the Feynman rules from appendix A we get the matrix element

$$iM_s = \bar{u}(p_3, s')\ (iee_q\gamma^\nu)\ \delta_{ki}\frac{\not{p}_1 + \not{p}_2}{(p_1+p_2)^2}\ (g\gamma_\mu T^a_{ij})\ u(p_1, s) \tag{2.1}$$

for the s-channel. The main piece of work constitutes the calculation of the square of (2.1) which is shown in detail now:

$$\begin{aligned}
|M_s|^2 &= \frac{1}{3}\cdot\frac{1}{4}\cdot e^2e_q^2g^2\sum_{a,s,s'}|\bar{u}(p_3,s')\gamma^\nu\frac{\not{p}_1+\not{p}_2}{(p_1+p_2)^2}\gamma_\mu T^a_{ij}u(p_1,s)|^2 \\
&= \frac{e^2e_q^2g^2}{12}\sum_{a,s,s'}\left(\bar{u}(p_3,s')\gamma^\nu\frac{\not{p}_1+\not{p}_2}{(p_1+p_2)^2}\gamma_\mu T^a_{ij}u(p_1,s)\right)^\dagger\left(\bar{u}(p_3,s')\gamma^\nu\frac{\not{p}_1+\not{p}_2}{(p_1+p_2)^2}\gamma_\mu T^a_{ij}u(p_1,s)\right) \\
&= \frac{e^2e_q^2g^2}{12}\mathrm{Tr}\left(u^\dagger T^{a\dagger}\underbrace{\gamma^{\mu\dagger}}_{\gamma^0\gamma^\mu\gamma^0}\frac{\not{p}_1+\not{p}_2}{(p_1+p_2)^2}\underbrace{\gamma^\dagger_\nu}_{\gamma^0\gamma_\nu\gamma^0}\gamma^0u'u'^\dagger\gamma^0\gamma^\nu\frac{\not{p}_1+\not{p}_2}{(p_1+p_2)^2}\gamma_\mu T^a u\right) \\
&= \frac{e^2e_q^2g^2}{12}\mathrm{Tr}\left(\underbrace{u^\dagger\gamma^0}_{\bar{u}}T^a\gamma^\mu\gamma^0\frac{\not{p}_1+\not{p}_2}{(p_1+p_2)^2}\gamma^0\gamma_\nu\underbrace{\gamma^0\gamma^0}_{1}u'\underbrace{u'^\dagger\gamma^0}_{\bar{u}'}\gamma^\nu\frac{\not{p}_1+\not{p}_2}{(p_1+p_2)^2}\gamma_\mu T^a u\right) \\
&= \frac{e^2e_q^2g^2}{12}\mathrm{Tr}\left(\bar{u}(p_1,s)u(p_1,s)T^a\gamma^\mu\frac{\not{p}_1+\not{p}_2}{(p_1+p_2)^2}\gamma_\nu u(p_3,s')\bar{u}(p_3,s')\gamma^\nu\frac{\not{p}_1+\not{p}_2}{(p_1+p_2)^2}\gamma_\mu T^a\right) \\
&= \frac{e^2e_q^2g^2}{12}\mathrm{Tr}\left(\not{p}_1\gamma^\mu\frac{\not{p}_1+\not{p}_2}{(p_1+p_2)^2}\gamma_\nu\not{p}_3\gamma^\nu\frac{\not{p}_1+\not{p}_2}{(p_1+p_2)^2}\gamma_\mu\right)\cdot\mathrm{Tr}(T^aT^a) \\
&= \frac{e^2e_q^2g^2}{3s^2}\mathrm{Tr}\left(\not{p}_1\underbrace{\gamma^\mu(\not{p}_1+\not{p}_2)\gamma_\mu}_{-2(\not{p}_1+\not{p}_2)}\underbrace{\gamma_\nu\not{p}_3\gamma^\nu}_{-2\not{p}_3}(\not{p}_1+\not{p}_2)\right) \\
&= \frac{4e^2e_q^2g^2}{3s^2}\mathrm{Tr}(\not{p}_1\not{p}_2\not{p}_3\not{p}_2) = \frac{4e^2e_q^2g^2}{3s^2}\cdot 8(p_1\cdot p_2)(p_3\cdot p_2) \\
&= \frac{8}{3}e^2e_q^2g^2\cdot\left(-\frac{u}{s}\right)
\end{aligned} \tag{2.2}$$

Here, identities from the two previous chapters were used. As usual, the sum is over

possible spins or colors of the outgoing particles, the factors 1/3 and 1/4 stem from averaging over possible flavors and spins of the incoming quark. In addition, the electromagnetic charge e, the quark charge e_q and the strong coupling strength g are involved. Most of the subsequent results will be presented briefer since they behave in exactly the same manner. For the u-channel we have the matrix element

$$iM_u = \bar{u}(p_3, s') \; (iee_q\gamma^\mu) \; \delta_{ki} \frac{\not{p}_1 - \not{p}_4}{(p_1 - p_4)^2} \; (g\gamma_\nu T^a_{ij}) \; u(p_1, s) \tag{2.3}$$

what results in

$$\begin{aligned} |M_u|^2 &= \frac{e^2 e_q^2 g^2}{3u^2} \mathrm{Tr}\left(\not{p}_1\gamma^\nu(\not{p}_1 - \not{p}_4)\gamma_\nu\gamma_\mu\not{p}_3\gamma^\mu(\not{p}_1 - \not{p}_4)\right) \\ &= \frac{4e^2 e_q^2 g^2}{3u^2} \mathrm{Tr}(\not{p}_1\not{p}_4\not{p}_3\not{p}_4) = \frac{4e^2 e_q^2 g^2}{3u^2} \cdot 8(p_1 \cdot p_4)(p_3 \cdot p_4) \\ &= \frac{8}{3} e^2 e_q^2 g^2 \cdot \left(-\frac{s}{u}\right) \; . \end{aligned} \tag{2.4}$$

The mixed matrix element yields

$$\begin{aligned} 2M_s^\dagger M_u &= 2 \cdot \frac{1}{3} \sum_{a,s,s'} \bar{u} \; (g\gamma^\mu T^a_{ij}) \; \delta_{ki} \frac{\not{p}_1 + \not{p}_2}{(p_1 + p_2)^2} \; (ee_q\gamma_\nu) \; u'\bar{u}' \; (ee_q\gamma_\mu) \; \delta_{ki} \frac{\not{p}_1 - \not{p}_4}{(p_1 - p_4)^2} \; (g\gamma^\nu T^a_{ij}) \; u \\ &\sim \mathrm{Tr}\left(\not{p}_1\gamma^\mu(\not{p}_1 + \not{p}_2)\gamma_\nu\not{p}_3\gamma_\mu(\not{p}_1 - \not{p}_4)\gamma^\nu\right) \\ &= 0 \end{aligned} \tag{2.5}$$

so that the final result for the full squared matrix element amounts to

$$|M_{\gamma q \to qg}|^2 = |M_s + M_u|^2 = |M_s|^2 + 2M_s^\dagger M_u + |M_u|^2 = \frac{8}{3} e^2 e_q^2 g^2 \cdot \left(-\frac{u}{s} - \frac{s}{u}\right) \; . \tag{2.6}$$

2.2.4. Boson gluon fusion $\gamma g \to q\bar{q}$

The process of boson gluon fusion corresponds to one t- and one u-channel-diagram (see Figure 2.0). We obtain

$$iM_t = \bar{u}(p_3, s') \; (g\gamma_\mu T^a_{ij}) \; \delta_{jk} \frac{\not{p}_1 - \not{p}_3}{(p_1 - p_3)^2} \; (iee_q\gamma^\nu) \; v(p_4, s) \tag{2.7}$$

what results in

$$
\begin{aligned}
|M_t|^2 &= \frac{e^2 e_q^2 g^2}{8t^2} \mathrm{Tr}\left(\not{p}_4 \gamma_\nu (\not{p}_1 - \not{p}_3) \gamma^\nu \gamma^\mu \not{p}_3 \gamma_\mu (\not{p}_1 - \not{p}_3) \right) \\
&= \frac{e^2 e_q^2 g^2}{2t^2} \mathrm{Tr}(\not{p}_4 \not{p}_1 \not{p}_3 \not{p}_1) = \frac{e^2 e_q^2 g^2}{2t^2} \cdot 8 (p_4 \cdot p_1)(p_3 \cdot p_1) \\
&= e^2 e_q^2 g^2 \cdot \frac{u}{t}
\end{aligned}
\tag{2.8}
$$

and

$$
iM_u = \bar{u}(p_3, s') \; (iee_q \gamma^\nu) \; \delta_{jk} \frac{\not{p}_1 - \not{p}_4}{(p_1 - p_4)^2} \; (g \gamma_\mu T^a_{ij}) \; v(p_4, s) \tag{2.9}
$$

which leads to

$$
\begin{aligned}
|M_u|^2 &= \frac{e^2 e_q^2 g^2}{8u^2} \mathrm{Tr}\left(\not{p}_4 \gamma^\mu (\not{p}_1 - \not{p}_4) \gamma_\mu \gamma_\nu \not{p}_3 \gamma^\nu (\not{p}_1 - \not{p}_4) \right) \\
&= \frac{e^2 e_q^2 g^2}{2u^2} \mathrm{Tr}(\not{p}_4 \not{p}_1 \not{p}_3 \not{p}_1) = \frac{e^2 e_q^2 g^2}{2u^2} \cdot 8 (p_4 \cdot p_1)(p_3 \cdot p_1) \\
&= e^2 e_q^2 g^2 \cdot \frac{t}{u} \; .
\end{aligned}
\tag{2.10}
$$

Here, we averaged over possible colors of the incoming gluon. For the mixed matrix element we find

$$
\begin{aligned}
2M_t^\dagger M_u &\sim \mathrm{Tr}\left(\not{p}_4 \gamma_\nu (\not{p}_1 - \not{p}_3) \gamma^\mu \not{p}_3 \gamma^\nu (\not{p}_1 - \not{p}_4) \gamma_\mu \right) \\
&= 0
\end{aligned}
\tag{2.11}
$$

so that the sum of these three results yields

$$
|M_{\gamma g \to q\bar{q}}|^2 = e^2 e_q^2 g^2 \cdot \left(\frac{u}{t} + \frac{t}{u} \right) \; . \tag{2.12}
$$

2.2.5. Quark-antiquark annihilation $q\bar{q} \to gg$

The third process which is presented here is by far the most difficult one for three reasons. First, there are three basic diagrams, again as s-, t- and u-channel, for which additionally all mixed matrix elements have to be evaluated. Secondly, the s-channel of quark-antiquark annihilation contains the three-gluon-vertex that makes calculations very elaborate. Thirdly, two ghost diagrams have to be calculated which subtract redundant non-transverse degrees of freedom of the gluons that are involved in the simplest form of the gluon polarization sum (see [9] for a precise explanation). Nonetheless, t- and u-channel are evaluated exactly as before. For

$$
iM_t = \bar{v}(p_2, s') \; (g \gamma_\mu T^a_{ij}) \; \delta_{jk} \frac{\not{p}_1 - \not{p}_3}{(p_1 - p_3)^2} \; (g \gamma_\nu T^b_{kl}) \; u(p_1, s) \tag{2.13}
$$

we get

$$
\begin{aligned}
|M_t|^2 &= \frac{1}{2!}\cdot\frac{1}{4}\cdot\frac{1}{9}\cdot\frac{g^4}{t^2}\mathrm{Tr}\left(\not p_1\gamma^\nu(\not p_1-\not p_3)\gamma_\nu\gamma^\mu\not p_2\gamma_\mu(\not p_1-\not p_3)\right)\cdot\mathrm{Tr}(T^bT^aT^aT^b)\\
&= \frac{g^4}{18t^2}\mathrm{Tr}(\not p_1\not p_3\not p_2\not p_3)\cdot\frac{16}{3} = \frac{8g^4}{27t^2}\cdot 8(p_1\cdot p_3)(p_2\cdot p_3)\\
&= \frac{16}{27}g^4\cdot\frac{u}{t}\ ,
\end{aligned}
\tag{2.14}
$$

the other one,

$$
iM_u = \bar v(p_2,s')\ (g\gamma_\nu T^b_{kl})\ \delta_{kj}\frac{\not p_1-\not p_4}{(p_1-p_4)^2}\ (g\gamma_\mu T^a_{ji})\ u(p_1,s)\quad , \tag{2.15}
$$

leads to

$$
\begin{aligned}
|M_u|^2 &= \frac{1}{72}\cdot\frac{g^4}{u^2}\mathrm{Tr}\left(\not p_1\gamma^\mu(\not p_1-\not p_4)\gamma_\mu\gamma^\nu\not p_2\gamma_\nu(\not p_1-\not p_4)\right)\cdot\mathrm{Tr}(T^aT^bT^bT^a)\\
&= \frac{g^4}{18u^2}\mathrm{Tr}(\not p_1\not p_4\not p_2\not p_4)\cdot\frac{16}{3} = \frac{8g^4}{27u^2}\cdot 8(p_1\cdot p_4)(p_2\cdot p_4)\\
&= \frac{16}{27}g^4\cdot\frac{t}{u}\ .
\end{aligned}
\tag{2.16}
$$

The new factor of $1/2!$ stems from Fermi statistics. The matrix element

$$
iM_s = (-igf^{bcd})\left[g^{\mu\nu}(k+p_3)^\lambda + g^{\nu\lambda}(p_4-p_3)^\mu + g^{\lambda\mu}(-p_4-k)^\nu\right]\varepsilon^*_\nu\varepsilon^*_\lambda\left(\frac{\delta_{ab}}{k^2}g^{\kappa\mu}\right)(g\gamma_\kappa T^a_{ij})u(p_1,s)\bar v(p_2,s') \tag{2.17}
$$

of the s-channel contains, besides two explicit gluon polarizations ε^*_ν and ε^*_λ and the abbreviation $k=p_1+p_2$, the three-gluon-vertex. Its square can be calculated by the program *Form* and reads

$$
\begin{aligned}
|M_s|^2 &= \frac{1}{72}\cdot\frac{Ng^4}{s^2}\cdot\mathrm{Tr}(T^aT^a)\cdot\mathrm{Tr}(\not p_1\gamma_\mu\not p_2\gamma^{\mu'})\cdot\left[g^{\mu\nu}(k+p_3)^\lambda + g^{\nu\lambda}(p_4-p_3)^\mu + g^{\lambda\mu}(-p_4-k)^\nu\right]\\
&\qquad\cdot\left[g^{\mu'\nu'}(k+p_3)^{\lambda'} + g^{\nu'\lambda'}(p_4-p_3)^{\mu'} + g^{\lambda'\mu'}(-p_4-k)^{\nu'}\right]g_{\nu\nu'}g_{\lambda\lambda'}\\
&= \frac{g^4}{6s^2}\cdot\mathrm{Tr}(\not p_1\gamma_\mu\not p_2\gamma^{\mu'})\cdot\left[g^{\mu\nu}(k+p_3)^\lambda + g^{\nu\lambda}(p_4-p_3)^\mu + g^{\lambda\mu}(-p_4-k)^\nu\right]\\
&\qquad\cdot\left[g^{\mu'}{}_\nu(k+p_3)_\lambda + g_{\nu\lambda}(p_4-p_3)^{\mu'} + g_\lambda{}^{\mu'}(-p_4-k)_\nu\right]\\
&= \frac{2}{3}g^4\cdot\frac{t\cdot u}{s^2} - \frac{4}{3}g^4\cdot\frac{t^2+u^2}{s^2} - \frac{4}{3}g^4
\end{aligned}
\tag{2.18}
$$

where the computation power of *Form* was employed on the contraction of the second trace in the first line with the three-gluon-vertex. The mixed matrix elements are

$$\begin{aligned}
2M_s^\dagger M_t = \frac{-2i}{72} \sum_{a,b,c,s,s'} & \bar{v}(p_2,s')\ (g\gamma_\lambda T^a_{ij})\ \frac{\not{p}_1 - \not{p}_3}{(p_1-p_3)^2}\ (g\gamma_\nu T^b_{jk})\ u(p_1,s)v(p_2,s')\bar{u}(p_1,s) \\
& \cdot(g\gamma^\kappa T^c_{kl}) \left(\frac{g_{\kappa\mu}}{k^2}\right) \left[g^{\mu\nu}(k+p_3)^\lambda + g^{\nu\lambda}(p_4-p_3)^\mu + g^{\lambda\mu}(-p_4-k)^\nu\right] g f^{cba} \\
= -\frac{ig^4}{36st} \cdot \mathrm{Tr}\Big(\not{p}_2\gamma_\lambda(\not{p}_1 - \not{p}_3)\gamma_\nu \not{p}_1 \gamma_\mu \cdot \left[g^{\mu\nu}(k+p_3)^\lambda + g^{\nu\lambda}(p_4-p_3)^\mu + g^{\lambda\mu}(-p_4-k)^\nu\right]\Big) \\
\cdot \mathrm{Tr}(T^a T^b T^c f^{acb}) \\
= -\frac{4}{3} g^4 \cdot \frac{t}{s}\ ,
\end{aligned} \tag{2.19}$$

$$\begin{aligned}
2M_s^\dagger M_u = -\frac{ig^4}{36su} \cdot \mathrm{Tr}\Big(\not{p}_2\gamma_\nu(\not{p}_1 - \not{p}_4)\gamma_\lambda \not{p}_1 \gamma_\mu \cdot \left[g^{\mu\nu}(k+p_3)^\lambda + g^{\nu\lambda}(p_4-p_3)^\mu + g^{\lambda\mu}(-p_4-k)^\nu\right]\Big) \\
\cdot \mathrm{Tr}(T^b T^a T^c f^{bac}) \\
= -\frac{4}{3} g^4 \cdot \frac{u}{s}
\end{aligned} \tag{2.20}$$

which add up to

$$2M_s^\dagger M_t + 2M_s^\dagger M_u = -\frac{4}{3} g^4 \cdot \frac{t+u}{s} = -\frac{4}{3} g^4 \cdot \frac{(-s)}{s} = \frac{4}{3} g^4\ , \tag{2.21}$$

and lastly

$$\begin{aligned}
2M_t^\dagger M_u &\sim \mathrm{Tr}\left(\not{p}_1 \gamma^\nu (\not{p}_1 - \not{p}_3)\gamma^\mu \not{p}_2 \gamma_\nu (\not{p}_1 - \not{p}_4)\gamma_\mu\right) \\
&= 0\ .
\end{aligned} \tag{2.22}$$

Finally, the ghost diagrams are constructed by replacing the two outgoing gluons by ghost lines which carry a momentum p_3 in the first and p_4 in the second version. Using the corresponding Feynman rules for gluon-ghost-vertex and ghost propagator we arrive at the matrix elements

$$iM_{ghost,1} = \bar{v}(p_2,s')\ (-igf^{bcd}p_3) \left(\frac{\delta_{ab}}{k^2} g^{\mu\nu}\right) (g\gamma_\mu T^a_{ij})\ u(p_1,s) \tag{2.23}$$

and

$$iM_{ghost,2} = \bar{v}(p_2, s')\ (-igf^{bcd}p_4)\left(\frac{\delta_{ab}}{k^2}g^{\mu\nu}\right)(g\gamma_\mu T^a_{ij})\ u(p_1, s) \tag{2.24}$$

which read

$$\begin{aligned} |M_{ghost,1}|^2 &= \frac{1}{72}\cdot\frac{Ng^4}{s^2}\cdot \mathrm{Tr}(T^aT^a)\cdot \mathrm{Tr}(\not{p}_1\not{p}_3\not{p}_2\not{p}_3) \\ &= \frac{g^4}{6s^2}\cdot 8(p_1\cdot p_3)(p_2\cdot p_3) \\ &= \frac{1}{3}g^4\cdot\frac{t\cdot u}{s^2} \end{aligned} \tag{2.25}$$

and

$$\begin{aligned} |M_{ghost,2}|^2 &= \frac{1}{72}\cdot\frac{Ng^4}{s^2}\cdot \mathrm{Tr}(T^aT^a)\cdot \mathrm{Tr}(\not{p}_1\not{p}_4\not{p}_2\not{p}_4) \\ &= \frac{g^4}{6s^2}\cdot 8(p_1\cdot p_4)(p_2\cdot p_4) \\ &= \frac{1}{3}g^4\cdot\frac{u\cdot t}{s^2} \end{aligned} \tag{2.26}$$

in their squared shape.
The desired final result is now again achieved by adding up all so far indicated contributions to

$$\begin{aligned} |M_{q\bar{q}\to gg}|^2 &= |M_s|^2 + |M_t|^2 + |M_u|^2 + 2M_s^\dagger M_t + 2M_s^\dagger M_u + 2M_t^\dagger M_u - |M_{ghost,1}|^2 - |M_{ghost,2}|^2 \\ &= \frac{4}{3}g^4\cdot\left[\frac{4}{9}\left(\frac{t}{u}+\frac{u}{t}\right) - \frac{t^2+u^2}{s^2}\right]\ . \end{aligned} \tag{2.27}$$

2.3. Threshold resummation approach to aNNLO

Although there has been a lot of effort concerning perturbative calculations in NNLO, many processes in particle physics are still only known to full NLO or, ideally, to aNNLO. This term can refer to the usual perturbative approach, illustrated by Feynman diagrams, thereby neglecting several contributions, but also to a threshold resummation formalism as presented by Kidonakis [4]. The latter has not less then two advantages: First of all, it becomes apparent that the threshold resummation can be formulated in a 'unified' form meaning that the same formulas can more or less be applied to a couple of processes. Secondly, the results are based on an expansion, too, so that it is comparatively easy to produce outcomes in still higher orders (see e.g. [11]). This second aspect also reveals that the approximate character - unlike within the usual approach where it arises by just neglecting contributing Feynman diagrams - is a generic feature of the threshold resummation.
Concerning QCD the idea for this approach is motivated by the observation that at threshold $z \to 1$, where gluons with very small momenta are emitted from a parental particle, there exist logarithmic terms of the form

$$\mathcal{D}_l = \left[\frac{\ln^l(1-z)}{1-z}\right]_+ \tag{2.28}$$

with $l \leq 2n-1$ at nth order of perturbation theory which have to be summed up to all orders even if the whole computation is limited to NLO or NNLO. z here means the fraction of the total momenta of parental and emitted particle which is often employed in pair-invariant-mass kinematics (PIM kinematics). The procedure resulting from this issue is possible due to factorization theorems and is termed 'resummation'. At the end of it one gets a 'resummed cross section' in the unphysical Mellin space that cannot be used directly - a difficult transformation back to physical space is required whereby the appearance of Landau poles constitutes a severe problem. This difficulty can be solved, yielding outcomes in nth perturbative order that are, however, only approximately correct. Nonetheless, beyond NLO they can be extremely worthwile, of course. Details on this approach can be found in numerous references, for example [12]. We will now solely focus on issues that are relevant for this thesis.
The lengthy NNLO master formula of Kidonakis will not be shown here, it was discussed in detail in the work [1] on which this thesis is based on. The corresponding NLO formula containing soft and virtual corrections is - as well as the NNLO master formula - needed for simple color flow because we have to deal with one photon in the initial state. In the $\overline{\text{MS}}$ scheme it reads

$$\sigma^{(1)} = \sigma^B \frac{\alpha_s}{\pi}\left[c_3 \cdot \left(\frac{\ln(1-z)}{1-z}\right)_+ + c_2 \cdot \left(\frac{1}{1-z}\right)_+ + c_1 \cdot \delta(1-z)\right] \tag{2.29}$$

including the Born cross section σ^B and the strong coupling α_s. This expression is of greater interest since it involves the coefficients c_3, c_2 and c_1 which are an essential part

of the NNLO master formula, too, and besides the main focus of this thesis. Their global $\overline{\text{MS}}$ calculation prescription of Kidonakis reads

$$c_3 = \sum_i 2C_i - \sum_j C_j \quad , \tag{2.30}$$

$$\begin{aligned} c_2 = 2\ \text{Re}\Gamma_S^{\prime(1)} &- \sum_i \left[C_i + 2C_i\ \delta_K\ \ln\left(\frac{-t_i}{M^2}\right) + C_i\ \ln\left(\frac{\mu_F^2}{s}\right)\right] \\ &- \sum_j \left[B_j^{\prime(1)} + C_j + C_j\ \delta_K\ \ln\left(\frac{M^2}{s}\right)\right] \qquad \text{and} \end{aligned} \tag{2.31}$$

$$c_1 = \sum_i \left[C_i\ \delta_K\ \ln\left(\frac{-t_i}{M^2}\right) - \gamma_i^{(1)}\right] \ln\left(\frac{\mu_F^2}{s}\right) + d_{\alpha_s}\frac{\beta_0}{4}\ln\left(\frac{\mu_R^2}{s}\right) + T_1 \tag{2.32}$$

wherein one can find Mandelstam variables s and t, factorization, renormalization and hard scales μ_F, μ_R and M^2, respectively, the Casimir invariants of SU(3), $C_A = 3$ and $C_F = \frac{4}{3}$, the QCD beta function β_0, powers of the coupling d_{α_s}, and terms $B^{\prime(1)}$, $\gamma^{(1)}$ which are different for quarks and gluons, namely $B_{q,\bar{q}}^{\prime(1)} = \gamma_{q,\bar{q}}^{(1)} = \frac{3C_F}{4}$, $B_g^{\prime(1)} = \gamma_g^{(1)} = \frac{\beta_0}{4}$. The term T_1 contains scale-independent virtual corrections that are not predicted by the threshold resummation approach. The factor δ_K equals 0 for PIM kinematics. The sum over i applies to initial-state, the sum over j to final-state partons - therefore it can be applied to any desired partonic process. Additionally, the coefficient c_2 contains the one-loop soft anomalous dimensions $\Gamma_S^{\prime(1)}$ which will be discussed extensively in chapter 2.5. We will close this section by giving the explicit results for the three coefficients for boson gluon fusion and QCD Compton scattering. For later use we already replace here every s by M^2 (and s^2 by M^4) as it was done in [1].
For boson gluon fusion $\boldsymbol{\gamma g \to q\bar{q}}$ the one-loop soft anomalous dimension
$\text{Re}(\Gamma_S^{\prime(1)}) = C_F + \frac{C_A}{2}\ \ln\left(\frac{tu}{M^4}\right) + \frac{C_A}{2}$ can be read off our result (2.49) by neglecting the gauge-dependent and imaginary parts (and performing $s^2 \to M^4$). Consequently, we obtain by making use of (2.30), (2.31) and (2.32)

$$c_3 = 2C_A - 2C_F \quad , \tag{2.33}$$

$$c_2 = C_A\ \ln\left(\frac{tu}{M^4}\right) - C_A\ \ln\left(\frac{\mu_F^2}{M^2}\right) - \frac{3}{2}C_F \qquad \text{and} \tag{2.34}$$

$$c_1^{\mu} = -\frac{\beta_0}{4}\ \ln\left(\frac{\mu_F^2}{M^2}\right) + \frac{\beta_0}{4}\ \ln\left(\frac{\mu_R^2}{M^2}\right) \tag{2.35}$$

whereby c_1^{μ} only includes the gauge-dependent terms of c_1, i.e. $c_1^{\mu} = c_1 - T_1$.
Proceeding in the same way with QCD Compton scattering $\boldsymbol{\gamma q \to qg}$ we get while employing $\text{Re}(\Gamma_S^{\prime(1)}) = C_F\ \ln\left(-\frac{u}{M^2}\right) + C_F + \frac{C_A}{2}\ \ln\left(\frac{t}{u}\right) + \frac{C_A}{2}$ (from (2.54) after exchanging t- and u-channel)

$$c_3 = C_F - C_A \quad , \tag{2.36}$$

$$c_2 = 2C_F \ln\left(-\frac{u}{M^2}\right) + C_A \ln\left(\frac{t}{u}\right) - C_F \ln\left(\frac{\mu_F^2}{M^2}\right) - \frac{3}{4}C_F - \frac{\beta_0}{4} \qquad \text{and} \tag{2.37}$$

$$c_1^\mu = -\frac{3}{4}C_F \ln\left(\frac{\mu_F^2}{M^2}\right) + \frac{\beta_0}{4} \ln\left(\frac{\mu_R^2}{M^2}\right) \tag{2.38}$$

as results.

2.4. JetVip with aNNLO contributions

In this section we will present a short qualitative summary of the results that were achieved in the thesis [1] on which our current work is based on. A summary including quantitative aspects is available in [2].
In [1] the NNLO master formula of Kidonakis which includes the coefficients presented before has been implemented into the Fortran program JetVip [3] that originally provided a full NLO calculation of the inclusive jet production cross section in DIS. Two analyses were performed with JetVip, firstly, a pure NLO calculation to compare its predictions with data for collisions of electrons (positrons) and protons at the HERA collider in Hamburg, secondly, a calculation additionally including the aNNLO contributions to compare it with the same data set. The outcomes of this second computation were quite satisfying since, on the one hand, the total cross section was shown to become significantly reduced by the NNLO terms what lead to better agreement with the p_T-distributed data, and, on the other hand, the scale dependence could be reduced in the regime of very high photon virtuality Q^2, as expected, but was surprisingly found to be enhanced inside all other bins of Q^2 and p_T. Finally, a determination of the strong coupling α_s has been performed by using a special set of parton densities which did not yield a quantitative improvement.
On the theoretical side, two interesting aspects were found in [1] which arised due to the fact that, in principal, all terms emerging in the NLO ansatz of Kidonakis (2.29) should be present in the full NLO calculation of the program JetVip, too. This was not confirmed totally: differences of a factor 2 concerning some scale-dependent terms that, within the Kidonakis approach, basically arise due to the terms $2\mathrm{Re}(\Gamma_S^{\prime(1)})$ became manifest. Moreover, the final-state contributions of Kidonakis were shown to lack in JetVip. This last point, however, can be understood by considering that the program JetVip makes use of a 'phase space slicing' algorithm to cancel mass singularities stemming from virtual and real contributions. This algorithm introduces a 'cutoff parameter' leading to analytical expressions which are not factors in front of the distributions $\mathcal{D}_1$ and $\mathcal{D}_0$.
In the further process of this work the program JetVip will get modifications starting from the status that has just been presented.

2.5. One-loop soft anomalous dimensions

The approach of Kidonakis [4] to calculate NLO and NNLO corrections to QCD cross sections is grounded on the re-expansion of resummed cross sections from Mellin space to physical space. Hereof, the topic of soft-gluon resummation is of special importance considering the computation of the one-loop soft anomalous dimensions $\Gamma_S^{\prime(1)}$ that are part of the coefficients c_2 for simple color flow (e.g. direct photon production) and the terms A^c for complex color flow (e.g. resolved photon production). This chapter will concentrate on the explicit calculation of these anomalous dimensions for the two processes of direct photon production to verify the results for them given in [4]. Moreover, one example for the simplest case of complex color flow (which can still be done by hand) will be presented.
The wide concept of soft-gluon resummation is introduced in a great number of references (see for example [12,13]) and will therefore not been repeated here in detail. We only give a short review of the required framework.

2.5.1. The one-loop eikonal integral

In this section we give a brief review of chapter 5.4 in [12].
As explained there in more detail the one-loop anomalous dimensions for soft gluon emission are given by the contraction of a color part C and a kinematic part ω. For complex color flow they are determined by

$$\Gamma_{IJ}^{ij\to kl} = -\sum_{ab} C_{IJ}^{ab} \cdot (\mathrm{Res}_{\varepsilon\to 0}\ \omega^{ab}) \tag{2.39}$$

which reduces to

$$\Gamma^{ij\to kl} = -\sum_{ab} C^{ab} \cdot (\mathrm{Res}_{\varepsilon\to 0}\ \omega^{ab}) \tag{2.40}$$

in the case of simple color flow [14]. As it is reflected in these formulas, the color part is just a number for simple color flow but a matrix (at least 2×2) for complex color flow. The kinematic part is determined in terms of the UV-divergent part (as $\mathrm{Res}_{\varepsilon\to 0}$) of one-loop vertex corrections in the eikonal approximation. This approximation reflects the point that we deal with gluons with very small momenta k. Considering a quark with momentum p that has emitted a gluon with (very small) momentum k its propagator undergoes the simplification $\frac{(\not{p}-\not{k})}{(p-k)^2+i\epsilon} \to \frac{\not{p}}{-2p\cdot k+i\epsilon}$. The corrections are calculated by using the corresponding eikonal Feynman rules shown in appendix B. The corresponding diagrams are of the form as displayed in Figure 2.1: The incoming and outgoing Wilson lines stand for the incoming and outgoing particles of the considered process for which all possible gluon exchange channels, denoted by (ab) in the equations, have to be taken into account. For massive particles the self-energies have to be added. Fortunately, this computation reduces to the solution of only one integral if one introduces the variables Δ and δ to absorb the different signs. Regarding the eikonal Feynman rules they can be

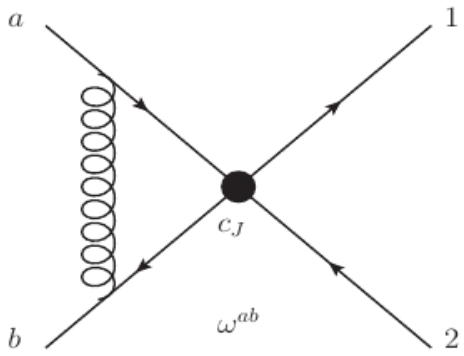

Figure 2.1: Example for the depiction of one-loop vertex corrections in the eikonal approximation [14]. In our case the gluon can couple to every Wilson line except that one representing the photon (e.g. line '1' or '2').

defined as $\Delta = -1$ for antiquarks, $\Delta = 1$ for all other partons, $\delta = -1$ for all incoming partons emitting gluons and $\delta = 1$ for all outgoing partons emitting gluons. When gluons are absorbed the sign of δ must be inverted.
The resulting eikonal integral reads

$$\Omega^{ab} = g^2 \int \frac{d^d k}{(2\pi)^d} \frac{-i}{k^2 + i\epsilon} \frac{\Delta_a v_a^\mu}{\delta_a v_a \cdot k + i\epsilon} \frac{\Delta_b v_b^\nu}{\delta_b v_b \cdot k + i\epsilon} N^{\mu\nu}(k) \tag{2.41}$$

where the gluon propagator

$$D^{\mu\nu}(k) = \frac{-i}{k^2 + i\epsilon} N^{\mu\nu}(k) \tag{2.42}$$

is defined in axial gauge by

$$N^{\mu\nu}(k) = g^{\mu\nu} - \frac{n^\mu k^\nu + k^\mu n^\nu}{n \cdot k} + n^2 \frac{k^\mu k^\nu}{(n \cdot k)^2} \tag{2.43}$$

with a gauge vector n. The labeling Ω^{ab} instead of ω^{ab} denotes the full kinematic part (which vanishes in usual dimensional regularization) instead of only its UV-divergent part. The dimensionless vectors v are normalized momentum vectors of the corresponding particles and given by $v^\mu = \sqrt{2/s}\, p^\mu$ with s being the classical center-of-mass energy squared. The index a stands for the incoming, b for the outgoing particle by convention. If both particles are incoming or outgoing, a denotes that one emitting the gluon, b that one absorbing the gluon.
After extracting the UV-divergence from (2.41) the quantity ω^{ab} can be calculated step by step for all possible gluon exchange channels concerning massless ($v^2 = 0$) and massive ($v^2 \neq 0$) particles as well as self-energies for the latter. This computation is also

done explicitly in chapter 5.4 of [12] and in chapter 7.3 of [15]. For our purposes we only need the expression for exclusively massless particles ($v_a^2 = v_b^2 = 0$). It reads

$$\omega^{ab} = S_{ab}\frac{\alpha_s}{\pi\varepsilon}\left[-\ln\left(\frac{v_{ab}}{2}\right) + \frac{1}{2}\ln(\nu_a\nu_b) + i\pi - 1\right] \tag{2.44}$$

and contains the sign factor $S_{ab} = \Delta_a\Delta_b\delta_a\delta_b$, the product $v_{ab} = v_a \cdot v_b$ and the gauge-dependent term $\nu_a = \frac{(v_a\cdot n)^2}{|n|^2}$. Latter terms always cancel in full calculations of cross sections. In [4] the dash on $\Gamma_S^{\prime(1)}$ indicates that only gauge-independent terms are considered. The scalar product of normalized momentum vectors, v_{ab}, can be expressed in terms of Mandelstam variables. Using the numbers 1 and 2 for incoming, 3 and 4 for outgoing particles and keeping in mind that the latter are all massless we obtain

$$v_{12} = 1 \quad , \quad v_{13} = v_{24} = -\frac{t}{s} \quad \text{and} \quad v_{14} = v_{23} = -\frac{u}{s} \quad . \tag{2.45}$$

With these ingredients we are now able to perform the intended calculations of one-loop soft anomalous dimensions.

2.5.2. Boson gluon fusion $\gamma g \to q\bar{q}$

The process of boson gluon fusion includes a photon, i.e. represents an example of simple color flow which has to be treated by the prescription (2.40). We start with the inverse process $q\bar{q} \to \gamma g$ to reproduce the result given in chapter 3.7 of [4] and will easily see that the outcome must be the same for both directions. The inverse process is closely related to that of gaugino-gluino production discussed in chapter 6.3 of [14] while the associated color factors C^{ab} are exactly the same. As illustrated there they consist of the color part stemming from the corresponding loop diagram which has to be normalized by the color tensor stemming from the single colored particle in the final state. For the reason of unambiguity we replace the indices a and b by the particle symbols q, $\bar{q}$ and g from now on. Following [14] we accordingly determine

$$\begin{aligned} C^{q\bar{q}} &= \frac{\mathrm{Tr}(T^iT^jT^iT^j)}{\mathrm{Tr}(T^iT^i)} = C_F - \frac{C_A}{2} \quad , \\ C^{qg} &= \frac{\mathrm{Tr}(T^iT^jT^k)(-if^{kij})}{\mathrm{Tr}(T^iT^i)} = \frac{C_A}{2} \quad \text{and} \\ C^{\bar{q}g} &= \frac{\mathrm{Tr}(T^iT^jT^k)(-if^{kji})}{\mathrm{Tr}(T^iT^i)} = -\frac{C_A}{2} \end{aligned} \tag{2.46}$$

whereby we do not need the self-energy color factor since we are invariably working with massless particles. As a last step we have to consider the sign factors S_{ab} appearing in the term (2.44) for ω^{ab} which are quickly computed to be

$$
\begin{aligned}
S_{q\bar{q}} &= \Delta_q \Delta_{\bar{q}} \delta_q \delta_{\bar{q}} = 1 \cdot (-1) \cdot (-1) \cdot 1 = 1 \qquad , \\
S_{qg} &= \Delta_q \Delta_g \delta_q \delta_g = 1 \cdot 1 \cdot (-1) \cdot (-1) = 1 \qquad \text{and} \\
S_{\bar{q}g} &= \Delta_{\bar{q}} \Delta_g \delta_{\bar{q}} \delta_g = (-1) \cdot 1 \cdot (-1) \cdot (-1) = -1
\end{aligned}
\tag{2.47}
$$

where the explanation at the top of page 18 was used. According to (2.40), (2.44), (2.45), (2.46) and (2.47) we subsequently find the one-loop soft anomalous dimension

$$
\begin{aligned}
\Gamma^{q\bar{q}\to\gamma g} &= -\sum_{ab} C^{ab} \cdot (\mathrm{Res}_{\varepsilon\to 0}\ \omega^{ab}) = -\mathrm{Res}_{\varepsilon\to 0}(C^{q\bar{q}} \cdot \omega^{q\bar{q}} + C^{qg} \cdot \omega^{qg} + C^{\bar{q}g} \cdot \omega^{\bar{q}g}) \\
&= -\frac{\alpha_s}{\pi}\left(C_F - \frac{C_A}{2}\right) \cdot \left(-\ln\left(\frac{1}{2}\right) + \frac{1}{2}\ln(\nu_q\nu_{\bar{q}}) + i\pi - 1\right) \\
&\quad - \frac{\alpha_s}{\pi} \cdot \frac{C_A}{2} \cdot \left(-\ln\left(-\frac{t}{2s}\right) + \frac{1}{2}\ln(\nu_q\nu_g) + i\pi - 1\right) \\
&\quad + \frac{\alpha_s}{\pi} \cdot \frac{C_A}{2} \cdot \left(\ln\left(-\frac{u}{2s}\right) - \frac{1}{2}\ln(\nu_{\bar{q}}\nu_g) - i\pi + 1\right) \\
&= -\frac{\alpha_s}{\pi} \cdot C_F \cdot \left(\ln 2 + \frac{1}{2}\ln(\nu_q\nu_{\bar{q}}) + i\pi - 1\right) \\
&\quad - \frac{\alpha_s}{\pi} \cdot \frac{C_A}{2} \cdot \left(-\ln 2 - \ln\left(\frac{tu}{4s^2}\right) - \frac{1}{2}\ln(\nu_q\nu_{\bar{q}}) + \frac{1}{2}\ln(\nu_q\nu_{\bar{q}}) + \frac{1}{2}\ln(\nu_g\nu_g) + i\pi - 1\right) \\
&= \frac{\alpha_s}{2\pi}\left[C_F \cdot (-2\ln 2 - \ln(\nu_q\nu_{\bar{q}}) - 2i\pi + 2) + C_A \cdot \left(\ln 2 - 2\ln 2 + \ln\left(\frac{tu}{s^2}\right) - \ln(\nu_g) - i\pi + 1\right)\right] \\
&= \frac{\alpha_s}{2\pi}\left[C_F \cdot (-\ln(4\nu_q\nu_{\bar{q}}) + 2 - 2i\pi) + C_A \cdot \left(\ln\left(\frac{tu}{s^2}\right) - \ln(2\nu_g) + 1 - i\pi\right)\right]
\end{aligned}
\tag{2.48}
$$

which is exactly the result presented in [16]. (The different sign on the second factor of $(i\pi)$ is probably not intended there. In most practical calculations, however, the imaginary part does not matter.) Moreover, taking only the real part of (2.48) and neglecting the gauge-dependent terms as well as the common prefactor of $\frac{\alpha_s}{\pi}$ we reproduce the quantity $\mathrm{Re}\Gamma_S^{\prime(1)} = C_F + \frac{C_A}{2}\ln\left(\frac{tu}{s^2}\right) + \frac{C_A}{2}$ that is presented in chapter 3.7 of [4] for the inverse boson gluon fusion.

Finally, we can treat the correct process of boson gluon fusion, namely $\gamma g \to q\bar{q}$, without much effort: Taking into account all of our previous knowledge we see that only two quantities could be sensitive to the direction of the process, the color factors C^{ab} and the signs S_{ab}. Indeed, the color factors, as seen above, stem from loops which are generally at most sensitive to the direction they are passed through which for its part is again independent of the process direction. Accordingly, only the sign factors S_{ab} remain. To see that they do not change as well we look at their computation in (2.47) again. $S_{q\bar{q}}$ does not depend on the process direction anyway. Since factors of Δ (as defined at the beginning of page 18) just depend on the parton type they stay the same, too. Factors

of δ actually change depending on whether a particle comes in or goes out but this does not matter for S_{qg} and $S_{\bar{q}g}$ which are symmetric in incoming and outgoing particles. Summarizing all these observations (2.47) passes into

$$\begin{aligned} S_{q\bar{q}} &= \Delta_q \Delta_{\bar{q}} \delta_q \delta_{\bar{q}} = 1 \cdot (-1) \cdot (-1) \cdot 1 = 1 \quad , \\ S_{qg} &= \Delta_q \Delta_g \delta_q \delta_g = 1 \cdot 1 \cdot 1 \cdot 1 = 1 \qquad\qquad \text{and} \\ S_{\bar{q}g} &= \Delta_{\bar{q}} \Delta_g \delta_{\bar{q}} \delta_g = (-1) \cdot 1 \cdot 1 \cdot 1 = -1 \end{aligned}$$

which exactly constitutes the same outcome.
According to this conclusion we state the one-loop soft anomalous dimension

$$\Gamma^{\gamma g \to q\bar{q}} = \Gamma^{q\bar{q} \to \gamma g} = \frac{\alpha_s}{2\pi} \left[C_F \cdot (-\ln(4\nu_q \nu_{\bar{q}}) + 2 - 2i\pi) + C_A \cdot \left(\ln\left(\frac{tu}{s^2}\right) + 1 - \ln(2\nu_g) - i\pi \right) \right] \tag{2.49}$$

for boson gluon fusion and its inverse.

2.5.3. QCD Compton scattering $\gamma q \to qg$

QCD Compton scattering represents the second example of simple color flow in the context of photoproduction. The calculation of its one-loop soft anomalous dimension is performed in the same way as for boson gluon fusion in the previous chapter. Again, we present the computation for its inverse $qg \to \gamma q$ from which the equality concerning the original direction results from the same arguments as before. The indices a and b are replaced by the particle symbols q, $\bar{q}$ and g as before, too. The required color factors C_{ab} read

$$\begin{aligned} C^{qq'} &= \frac{\mathrm{Tr}(T^i T^j T^i T^j)}{\mathrm{Tr}(T^i T^i)} = C_F - \frac{C_A}{2} \quad , \\ C^{qg} &= \frac{\mathrm{Tr}(T^i T^j T^k)(-if^{kji})}{\mathrm{Tr}(T^i T^i)} = -\frac{C_A}{2} \qquad \text{and} \\ C^{gq'} &= \frac{\mathrm{Tr}(T^i T^j T^k)(-if^{kij})}{\mathrm{Tr}(T^i T^i)} = \frac{C_A}{2} \end{aligned} \tag{2.50}$$

where we denote the outgoing quark as q' to distinguish it from the incoming one, q. Obviously, we recover the results from last section. The signs S_{ab} are given by

$$\begin{aligned} S_{qq'} &= \Delta_q \Delta_{q'} \delta_q \delta_{q'} = 1 \cdot 1 \cdot (-1) \cdot (-1) = 1 \quad , \\ S_{qg} &= \Delta_q \Delta_g \delta_q \delta_g = 1 \cdot 1 \cdot (-1) \cdot 1 = -1 \qquad \text{and} \\ S_{gq'} &= \Delta_g \Delta_{q'} \delta_g \delta_{q'} = 1 \cdot 1 \cdot (-1) \cdot (-1) = 1 \ . \end{aligned} \tag{2.51}$$

Using (2.40), (2.44), (2.45), (2.50) and (2.51) we hence obtain the one-loop soft anomalous dimension

$$
\begin{aligned}
\Gamma^{qg\to\gamma q'} &= -\sum_{ab} C^{ab}\cdot(\mathrm{Res}_{\varepsilon\to 0}\,\omega^{ab}) = -\mathrm{Res}_{\varepsilon\to 0}(C^{qq'}\cdot\omega^{qq'} + C^{qg}\cdot\omega^{qg} + C^{gq'}\cdot\omega^{gq'}) \\
&= -\frac{\alpha_s}{\pi}\left(C_F - \frac{C_A}{2}\right)\cdot\left(-\ln\left(-\frac{t}{2s}\right) + \frac{1}{2}\,\ln(\nu_q\nu_{q'}) + i\pi - 1\right) \\
&\qquad + \frac{\alpha_s}{\pi}\cdot\frac{C_A}{2}\cdot\left(\ln\left(\frac{1}{2}\right) - \frac{1}{2}\,\ln(\nu_q\nu_g) - i\pi + 1\right) \\
&\qquad - \frac{\alpha_s}{\pi}\cdot\frac{C_A}{2}\cdot\left(-\ln\left(-\frac{u}{2s}\right) + \frac{1}{2}\,\ln(\nu_g\nu_{q'}) + i\pi - 1\right) \\
&= -\frac{\alpha_s}{\pi}\cdot C_F\cdot\left(\ln 2 - \ln\left(-\frac{t}{s}\right) + \frac{1}{2}\,\ln(\nu_q\nu_{q'}) + i\pi - 1\right) \\
&\quad - \frac{\alpha_s}{\pi}\cdot\frac{C_A}{2}\cdot\left(\ln 2 + \ln\left(\frac{t}{2s}\cdot\frac{2s}{u}\right) - \frac{1}{2}\,\ln(\nu_q\nu_{q'}) + \frac{1}{2}\,\ln(\nu_{q'}\nu_q) + \frac{1}{2}\,\ln(\nu_g\nu_g) + i\pi - 1\right) \\
&= \frac{\alpha_s}{2\pi}\left[C_F\cdot\left(2\,\ln\left(-\frac{t}{s}\right) - \ln(4\nu_q\nu_{q'}) + 2 - 2i\pi\right) + C_A\cdot\left(\ln\left(\frac{u}{t}\right) - \ln(2\nu_g) + 1 - i\pi\right)\right]
\end{aligned}
\tag{2.52}
$$

which corresponds to the result in [16] except for the imaginary part in the first bracket and the definition of t- and u-channel which is reverse there. Also, the result given in chapter 3.7 of [4], $\mathrm{Re}\Gamma_S^{\prime(1)} = C_F\,\ln\left(-\frac{t}{s}\right) + C_F + \frac{C_A}{2}\,\ln\left(\frac{u}{t}\right) + \frac{C_A}{2}$, can be read off (2.52) again where the variables t and u are interchanged as well.
The same one-loop soft anomalous dimension belongs to the original QCD compton scattering $\gamma q \to qg$ for the reasons discussed in the previous section. We obtain the signs S_{ab} as

$$
\begin{aligned}
S_{q'q} &= \Delta_{q'}\Delta_q\delta_{q'}\delta_q = 1\cdot 1\cdot(-1)\cdot(-1) = 1 \quad , \\
S_{q'g} &= \Delta_{q'}\Delta_g\delta_{q'}\delta_g = 1\cdot 1\cdot(-1)\cdot(-1) = 1 \qquad \text{and} \\
S_{qg} &= \Delta_q\Delta_g\delta_q\delta_g = 1\cdot 1\cdot 1\cdot(-1) = -1
\end{aligned}
\tag{2.53}
$$

where q' now denotes the incoming quark. They totally correspond to (2.51) because of $S_{ab} = S_{ba}$.
We therefore state the one-loop soft anomalous dimension

$$
\Gamma^{\gamma q\to qg} = \Gamma^{qg\to\gamma q} = \frac{\alpha_s}{2\pi}\left[C_F\cdot\left(2\,\ln\left(-\frac{t}{s}\right) - \ln(4\nu_q\nu_{q'}) + 2 - 2i\pi\right) + C_A\cdot\left(\ln\left(\frac{u}{t}\right) - \ln(2\nu_g) + 1 - i\pi\right)\right]
\tag{2.54}
$$

for QCD Compton scattering and its inverse.

2.5.4. Light quark production $q\bar{q} \to q\bar{q}$

The calculation of one-loop soft anomalous dimensions for processes involving complex color flow, i.e. all particles are partons, is considerably more tedious, especially if more than one gluon is part of them. The example presented in the following is the simplest one which can partly still be done in an intuitive way. Again, we follow chapter 5.4 in [12] where more in-depth explanations concerning the theoretical framework can be found.
As depicted in (2.39), in contrast to the processes just treated, we now need a matrix C_{IJ}^{ab} to perform our computation. It is often referred to as *color mixing matrix*. Starting from the appearing color structure C_J^{ab} it can be found in the following way: Defining the quantity η_{IJ}^{ab} as

$$\eta_{IJ}^{ab} = c_I^\dagger C_J^{ab} = c_I^\dagger c_K C_{KJ}^{ab} = S_{IK}^{(0)} C_{KJ}^{ab} \tag{2.55}$$

where $c_{I,K}$ are tensors expressing the chosen color basis and $c_I^\dagger c_K = S_{IK}^{(0)}$ is the leading-order soft function we obtain the color mixing matrix by carrying out the prescription

$$C_{KJ}^{ab} = (S^{(0)})_{KI}^{-1} \eta_{IJ}^{ab} \tag{2.56}$$

which is just the reversal of the previous definition. The color basis can be adopted in different ways. Often, it is aimed for a basis that leads to a diagonal one-loop soft anomalous dimension matrix. We will make use of the most intuitive way which finally leads to the results presented in [13]. This is the non-orthogonal singlet-basis

$$c_I = \begin{pmatrix} \delta_{a_2 a_1}\delta_{a_3 a_4} \\ \delta_{a_1 a_3}\delta_{a_2 a_4} \end{pmatrix} \tag{2.57}$$

which is also used in [12]. The numbers 1 and 2 stand for incoming quarks or antiquarks, 3 and 4 for the outgoing ones, as before. Color indices are denoted by a. Taking this into account a term like $\delta_{a_2 a_1}$ just wants to express that two (incoming) particles have the same color. Regarding the whole line $\delta_{a_2 a_1}\delta_{a_3 a_4}$ it becomes obvious that there can solely be a gluon exchange between incoming and outgoing particles, i.e. the line characterises an s-channel. Correspondingly, the second line in (2.57) expresses a t-channel. With this basis we obtain

$$\begin{aligned} S_{IJ}^{(0)} = c_I^\dagger c_J &= \begin{pmatrix} \delta_{a_2 a_1}\delta_{a_3 a_4} & \delta_{a_1 a_3}\delta_{a_2 a_4} \end{pmatrix} \begin{pmatrix} \delta_{a_2 a_1}\delta_{a_3 a_4} \\ \delta_{a_1 a_3}\delta_{a_2 a_4} \end{pmatrix} = \begin{pmatrix} (\delta_{a_2 a_1}\delta_{a_3 a_4})^2 & \delta_{a_3 a_2}\delta_{a_2 a_3} \\ \delta_{a_2 a_3}\delta_{a_3 a_2} & (\delta_{a_1 a_3}\delta_{a_2 a_4})^2 \end{pmatrix} \\ &= \begin{pmatrix} (\delta_{a_2 a_1})^2(\delta_{a_3 a_4})^2 & (\delta_{a_3 a_2})^2 \\ (\delta_{a_2 a_3})^2 & (\delta_{a_1 a_3})^2(\delta_{a_2 a_4})^2 \end{pmatrix} = \begin{pmatrix} N^2 & N \\ N & N^2 \end{pmatrix} = \begin{pmatrix} 9 & 3 \\ 3 & 9 \end{pmatrix} \end{aligned} \tag{2.58}$$

as the leading-order soft function. Its inverse is easily obtained by demanding

$$(S^{(0)})^{-1}_{KI} S^{(0)}_{IJ} := \begin{pmatrix} s_{11} & s_{12} \\ s_{21} & s_{22} \end{pmatrix} \begin{pmatrix} N^2 & N \\ N & N^2 \end{pmatrix} \overset{!}{=} \mathbb{1}_{2\times 2} = \begin{pmatrix} 1 & 0 \\ 0 & 1 \end{pmatrix}$$

which leads to the simultaneous equations

$$\begin{aligned} s_{11}N^2 + s_{12}N = 1 \quad , \\ s_{11}N + s_{12}N^2 = 0 \quad , \\ s_{21}N^2 + s_{22}N = 0 \quad , \\ s_{21}N + s_{22}N^2 = 1 \end{aligned}$$

that for their part are solved quickly by hand. They yield

$$(S^{(0)})^{-1}_{KI} = \begin{pmatrix} \frac{1}{N^2-1} & \frac{1}{N(1-N^2)} \\ \frac{1}{N(1-N^2)} & \frac{1}{N^2-1} \end{pmatrix} = \begin{pmatrix} \frac{1}{8} & -\frac{1}{24} \\ -\frac{1}{24} & \frac{1}{8} \end{pmatrix} \tag{2.59}$$

for the inverse soft function in leading order. Here, $N = 3$ because of the fundamental representation SU(3) was employed.
As a last step before the actual calculations we have to figure out the color structure C_J^{ab} which can be slightly different depending on the particles a and b between those the gluon is exchanged. Here, we will use the numbers 1 and 2 for incoming, 3 and 4 for outgoing particles again to be able to compare our final result with that from [13].
The case $a = 1$, $b = 2$ (which is identical with $a = 3$, $b = 4$) is presented in [12] where

$$C_J^{12} = T^d_{a_2 b_2} c_J T^d_{b_1 a_1} \delta_{a_3 b_3} \delta_{b_4 a_4} \tag{2.60}$$

can be found as the corresponding color structure. The index b_i has been defined to divide the color of the Wilson lines into two parts so that a gluon can be attached between them. According to this, the color factor C_J^{12} expresses a gluon exchange between the two incoming lines which is controlled by the overall color basis c_J. Proceeding from this expression the color mixing matrix

$$C^{12}_{KJ} = C^{34}_{KJ} = \begin{pmatrix} C_F & \frac{1}{2} \\ 0 & -\frac{1}{2N} \end{pmatrix} \tag{2.61}$$

was calculated in [12]. Using the previous explanations we will now perform the computation for the two remaining cases and start with $a = 1$, $b = 3$. Since the indices b_i are connected with the vertex in this notation the replacement $a \to b$ has to be performed in (2.57) concerning the color factor. Taking this into account we get

$$C_J^{13} = T^d_{a_1b_1} c_J T^d_{b_3a_3} \delta_{a_2b_2}\delta_{b_4a_4} = T^d_{a_1b_1} \begin{pmatrix} \delta_{b_2b_1}\delta_{b_3b_4} \\ \delta_{b_1b_3}\delta_{b_2b_4} \end{pmatrix} T^d_{b_3a_3}\delta_{a_2b_2}\delta_{b_4a_4} = \begin{pmatrix} T^d_{a_1b_2}T^d_{b_4a_3} \\ T^d_{a_1b_3}T^d_{b_3a_3}\delta_{b_2b_4} \end{pmatrix} \delta_{a_2b_2}\delta_{b_4a_4}$$
$$= \begin{pmatrix} T^d_{a_1a_2}T^d_{a_4a_3} \\ T^d_{a_1b_3}T^d_{b_3a_3}\delta_{a_4a_2} \end{pmatrix} \tag{2.62}$$

analogously to (2.60). Inserting this into (2.55) yields

$$\eta^{13}_{IJ} = c_I^\dagger C_J^{13} = \begin{pmatrix} \delta_{a_2a_1}\delta_{a_3a_4} & \delta_{a_1a_3}\delta_{a_2a_4} \end{pmatrix} \begin{pmatrix} T^d_{a_1a_2}T^d_{a_4a_3} \\ T^d_{a_1b_3}T^d_{b_3a_3}\delta_{a_4a_2} \end{pmatrix} = \begin{pmatrix} 0 & NC_F \\ NC_F & N^2C_F \end{pmatrix}$$

which, according to (2.56), leads to the color mixing matrix

$$C^{13}_{KJ} = (S^{(0)})^{-1}_{KI}\eta^{13}_{IJ} = \begin{pmatrix} \frac{1}{8} & -\frac{1}{24} \\ -\frac{1}{24} & \frac{1}{8} \end{pmatrix} \begin{pmatrix} 0 & NC_F \\ NC_F & N^2C_F \end{pmatrix} = \begin{pmatrix} \frac{1}{8} & -\frac{1}{24} \\ -\frac{1}{24} & \frac{1}{8} \end{pmatrix} \begin{pmatrix} 0 & 4 \\ 4 & 12 \end{pmatrix} = \begin{pmatrix} -\frac{1}{6} & 0 \\ \frac{1}{2} & \frac{4}{3} \end{pmatrix}$$

where $N = 3$ and $C_F = \frac{4}{3}$ was inserted. Writing this result in terms of N and C_F again and observing that (2.62) is invariant under the replacements $1 \to 2$ and $3 \to 4$ we obtain

$$C^{13}_{KJ} = C^{24}_{KJ} = \begin{pmatrix} -\frac{1}{2N} & 0 \\ \frac{1}{2} & C_F \end{pmatrix} \tag{2.63}$$

as final outcome.
The calculation for $a = 1$, $b = 4$ behaves in exactly the same way: From the color factor

$$C_J^{14} = T^d_{a_1b_1} c_J T^d_{b_4a_4}\delta_{a_2b_2}\delta_{b_3a_3} = T^d_{a_1b_1} \begin{pmatrix} \delta_{b_2b_1}\delta_{b_3b_4} \\ \delta_{b_1b_3}\delta_{b_2b_4} \end{pmatrix} T^d_{b_4a_4}\delta_{a_2b_2}\delta_{b_3a_3} = \begin{pmatrix} T^d_{a_1a_2}T^d_{a_3a_4} \\ T^d_{a_1a_3}T^d_{a_2a_4} \end{pmatrix} \tag{2.64}$$

we deduce

$$\eta^{14}_{IJ} = c_I^\dagger C_J^{14} = \begin{pmatrix} \delta_{a_2a_1}\delta_{a_3a_4} & \delta_{a_1a_3}\delta_{a_2a_4} \end{pmatrix} \begin{pmatrix} T^d_{a_1a_2}T^d_{a_3a_4} \\ T^d_{a_1a_3}T^d_{a_2a_4} \end{pmatrix} = \begin{pmatrix} 0 & NC_F \\ NC_F & 0 \end{pmatrix}$$

which causes

$$C^{14}_{KJ} = (S^{(0)})^{-1}_{KI}\eta^{14}_{IJ} = \begin{pmatrix} \frac{1}{8} & -\frac{1}{24} \\ -\frac{1}{24} & \frac{1}{8} \end{pmatrix} \begin{pmatrix} 0 & 4 \\ 4 & 0 \end{pmatrix} = \begin{pmatrix} -\frac{1}{6} & \frac{1}{2} \\ \frac{1}{2} & -\frac{1}{6} \end{pmatrix}$$

as color mixing matrix. Since (2.64) is invariant under $1 \to 2$ and $4 \to 3$ we can write

$$C_{KJ}^{14} = C_{KJ}^{23} = \begin{pmatrix} -\frac{1}{2N} & \frac{1}{2} \\ \frac{1}{2} & -\frac{1}{2N} \end{pmatrix} \tag{2.65}$$

as final result. The case $a = b$ for the outgoing particles which also plays a role in [12] is irrelevant for our purposes because we do not treat the production of any massive particles. The associated calculation is, however, simple because its color structure corresponds to that one of a quark self-energy.
For the actual process we use numbers for a and b in ω^{ab} again. To this, we define the numbers 1 and 3 to belong to a quark, 2 and 4 to an antiquark. The signs $S_{ab} = \Delta_a \Delta_b \delta_a \delta_b$ are accordingly computed to be

$$\begin{aligned} &S_{12} = 1 \cdot (-1) \cdot (-1) \cdot 1 = S_{34} = 1 \cdot (-1) \cdot 1 \cdot (-1) = 1 \quad , \\ &S_{13} = 1 \cdot 1 \cdot (-1) \cdot (-1) = S_{24} = (-1) \cdot (-1) \cdot (-1) \cdot (-1) = 1 \quad \text{and} \\ &S_{14} = 1 \cdot (-1) \cdot (-1) \cdot (-1) = S_{23} = (-1) \cdot 1 \cdot (-1) \cdot (-1) = -1 \quad . \end{aligned} \tag{2.66}$$

Now, we are able to perform the last step of the calculation of the one-loop soft anomalous dimension matrix for $q\bar{q} \to q\bar{q}$. It is given in the shape

$$\Gamma_{IJ}^{q\bar{q}\to q\bar{q}} = \begin{pmatrix} \Gamma_{11}^{q\bar{q}\to q\bar{q}} & \Gamma_{12}^{q\bar{q}\to q\bar{q}} \\ \Gamma_{21}^{q\bar{q}\to q\bar{q}} & \Gamma_{22}^{q\bar{q}\to q\bar{q}} \end{pmatrix} \tag{2.67}$$

where, according to (2.39), (2.44), (2.45), (2.61), (2.63), (2.65) and (2.66), we calculate

$$\begin{aligned} \Gamma_{11}^{q\bar{q}\to q\bar{q}} &= -\sum_{ab} C_{11}^{ab} \cdot (\mathrm{Res}_{\varepsilon\to 0}\ \omega^{ab}) = -\mathrm{Res}_{\varepsilon\to 0}(C_{11}^{12}\omega^{12} + C_{11}^{34}\omega^{34} + C_{11}^{13}\omega^{13} + C_{11}^{24}\omega^{24} + C_{11}^{14}\omega^{14} + C_{11}^{23}\omega^{23}) \\ &= -\mathrm{Res}_{\varepsilon\to 0}\left(C_F \cdot (\omega^{12} + \omega^{34}) - \frac{1}{2N} \cdot (\omega^{13} + \omega^{24} + \omega^{14} + \omega^{23})\right) \\ &= -\frac{\alpha_s}{\pi} \cdot C_F \cdot \left(-\ln\left(\frac{v_{12}}{2}\right) - \ln\left(\frac{v_{34}}{2}\right) + \frac{1}{2}\ln(\nu_1\nu_2) + \frac{1}{2}\ln(\nu_3\nu_4) + 2i\pi - 2\right) - \frac{\alpha_s}{\pi} \cdot \frac{1}{2N} \cdot \\ &\quad \left(\ln\left(\frac{v_{13}}{2}\right) + \ln\left(\frac{v_{24}}{2}\right) - \ln\left(\frac{v_{14}}{2}\right) - \ln\left(\frac{v_{23}}{2}\right) - \frac{1}{2}\ln(\nu_1\nu_3) - \frac{1}{2}\ln(\nu_2\nu_4) + \frac{1}{2}\ln(\nu_1\nu_4) + \frac{1}{2}\ln(\nu_2\nu_3)\right) \\ &= -\frac{\alpha_s}{\pi} \cdot C_F \cdot \left(-\ln\left(\frac{v_{12}v_{34}}{4}\right) + \frac{1}{2}\ \ln(\nu_1\nu_2\nu_3\nu_4) + 2i\pi - 2\right) \\ &\quad + \frac{\alpha_s}{\pi} \cdot \frac{1}{2N} \cdot \left(\ln\left(\frac{v_{14}v_{23}}{v_{13}v_{24}}\right) + \frac{1}{2}\ \ln(\nu_1\nu_3\nu_2\nu_4) - \frac{1}{2}\ \ln(\nu_1\nu_4\nu_2\nu_3)\right) \\ &= \frac{\alpha_s}{\pi} \cdot C_F \cdot \left(\ln\left(\frac{v_{12}v_{34}}{4}\right) - \frac{1}{2}\ \ln(\nu_1\nu_2\nu_3\nu_4) + 2 - 2i\pi\right) - \frac{\alpha_s}{2\pi} \cdot \frac{1}{N} \cdot \ln\left(\frac{v_{13}v_{24}}{v_{14}v_{23}}\right) \quad , \end{aligned}$$

$$\begin{aligned}\Gamma_{12}^{q\bar{q}\to q\bar{q}} &= -\sum_{ab} C_{12}^{ab}\cdot(\mathrm{Res}_{\varepsilon\to 0}\ \omega^{ab}) = -\mathrm{Res}_{\varepsilon\to 0}\left(\frac{1}{2}\cdot(\omega^{12}+\omega^{34}+\omega^{14}+\omega^{23})\right)\\ &= -\frac{\alpha_s}{2\pi}\cdot\left(-\ln\left(\frac{v_{12}v_{34}}{4}\right)+\frac{1}{2}\ln(\nu_1\nu_2\nu_3\nu_4)+2i\pi-2+\ln\left(\frac{v_{14}v_{23}}{4}\right)-\frac{1}{2}\ln(\nu_1\nu_4\nu_2\nu_3)-2i\pi+2\right)\\ &= \frac{\alpha_s}{2\pi}\ln\left(\frac{v_{12}v_{34}}{v_{14}v_{23}}\right)\quad ,\end{aligned}$$

$$\begin{aligned}\Gamma_{21}^{q\bar{q}\to q\bar{q}} &= -\sum_{ab} C_{21}^{ab}\cdot(\mathrm{Res}_{\varepsilon\to 0}\ \omega^{ab}) = -\mathrm{Res}_{\varepsilon\to 0}\left(\frac{1}{2}\cdot(\omega^{13}+\omega^{24}+\omega^{14}+\omega^{23})\right)\\ &= \frac{\alpha_s}{2\pi}\ln\left(\frac{v_{13}v_{24}}{v_{14}v_{23}}\right)\end{aligned}$$

and

$$\begin{aligned}\Gamma_{22}^{q\bar{q}\to q\bar{q}} &= -\sum_{ab} C_{22}^{ab}\cdot(\mathrm{Res}_{\varepsilon\to 0}\ \omega^{ab}) = -\mathrm{Res}_{\varepsilon\to 0}\left(C_F\cdot(\omega^{13}+\omega^{24})-\frac{1}{2N}\cdot(\omega^{12}+\omega^{34}+\omega^{14}+\omega^{23})\right)\\ &= \frac{\alpha_s}{\pi}\cdot C_F\cdot\left(\ln\left(\frac{v_{13}v_{24}}{4}\right)-\frac{1}{2}\ln(\nu_1\nu_2\nu_3\nu_4)+2-2i\pi\right)-\frac{\alpha_s}{2\pi}\cdot\frac{1}{N}\cdot\ln\left(\frac{v_{12}v_{34}}{v_{14}v_{23}}\right)\end{aligned}$$

as expressions for its four components. This result precisely coincides with that one presented in [13], despite the interchange of t- and u-channel and one differing imaginary part.

3. Dependence on the jet radius

Most numerical NLO calculations as provided in the program JetVip do not contain a dependence on the jet radius R. Though, it has been developed a method which allows to add it directly to the corresponding former NLO terms. The outcome of this procedure is called a 'jet cross section' in the following. As mentioned before we are not interested in a modification of our full NLO calculation since we would not expect considerable improvements. The crucial point is that we are able by this ansatz to find additional contributions to the coefficients c_3, c_2 and c_1 of the presented threshold resummation approach which for their part affect the aNNLO corrections.
In general, independently of the employed jet algorithm, the radius R constitutes a measure for the spatial distance of particles that come out of a scattering process. Therefore, it is obvious that it should be more or less exclusively determined by processes of real emission. This is exactly what has been revealed in reference [17] on which many of the following considerations up to chapter 3.3 are based on. The basic idea can be explained as follows.
Considering a QCD scattering process in NLO there exist real contributions in which a parton j emits a parton k both stiring out of the place of the hard scattering. Such events are usually integrated over the full available phase space meaning that all (physically and experimentally) relevant directions of motion of particle k are taken into account. We now want to constrain these directions of motion by requiring a stable jet size by choosing an explicit cone opening δ (or, equivalently, radius R defined by $R = \delta \cdot \cosh(\eta)$ with η denoting the pseudorapidity) in whose area parton k is allowed to stay. Technically, this demand requires to replace those terms in the original NLO calculation in which parton k is located within the cone opening by such contributions that allow to form the jet by both partons j and k. Denoting the first terms by $d\sigma_{j(k)}$, the second ones by $d\sigma_{jk}$, and the inclusive NLO cross section that produces parton j by $d\sigma_j$, we accordingly have to compute the combination $d\sigma_j - d\sigma_{j(k)} + d\sigma_{jk}$. Of course, this cannot yet be the full result for an underlying scattering process which in LO produces one particle more than just j. In NLO, the jet can either be formed by one or by two particles (see Figure 3.1) while three particles are produced in total. For the total cross section all of these have to be treated as equal. For the case of two partons j and k forming the jet one additionally has to differentiate the cases where j emits k and where k emits j. Taking care of these aspects the final inclusive jet cross section for a process $a + b \to \text{jet} + X$ (X being any possible particle) can be written as

$$\begin{aligned} d\sigma_{a+b\to\text{jet}+X} =& (d\sigma_j - d\sigma_{j(k)} - d\sigma_{j(l)}) + (d\sigma_k - d\sigma_{k(j)} - d\sigma_{k(l)}) \\ &+ (d\sigma_l - d\sigma_{l(j)} - d\sigma_{l(k)}) + d\sigma_{jk} + d\sigma_{jl} + d\sigma_{kl} \end{aligned} \tag{3.1}$$

where the ordinary (LO plus) NLO parts $d\sigma_j$, $d\sigma_k$ and $d\sigma_l$ are inclusive ones as well, i.e. the cross section $d\sigma_j$ has the underlying LO process $a + b \to j + X$. The inclusiveness of all objects in [17] can be understood by the fact that it treats collisions of protons so that there are exclusively partons (and never photons) in the initial state. For one photon as particle a (or b) there does not exist such an inclusiveness because, if all other

involved particles are known, X is fixed due to a limited amount of reaction channels. Having a closer look on prescription (3.1) one sees that it focuses on a specific final-state configuration (j, k, l) no matter which partons a, b concretely produced it. Due to this point it is forced to change slightly for our purposes:
For boson gluon fusion $\boldsymbol{\gamma g \to q\bar{q}}$ it passes into

$$d\sigma_{\gamma+g\to\text{jet}+X} = (d\sigma_q - d\sigma_{q(g)} - d\sigma_{g(q)}) + (d\sigma_{\bar{q}} - d\sigma_{\bar{q}(g)} - d\sigma_{g(\bar{q})}) + d\sigma_{qg} + d\sigma_{\bar{q}g} \tag{3.2}$$

whereby in fact, as it will turn out later, not all of these contributions are different.
For QCD Compton scattering $\boldsymbol{\gamma q \to qg}$ we state

$$d\sigma_{\gamma+q\to\text{jet}+X} = (d\sigma_q - d\sigma_{q(\bar{q})} - d\sigma_{q(g)}) + (d\sigma_g - d\sigma_{g(q)} - d\sigma_{g(g)}) + d\sigma_{q\bar{q}} + d\sigma_{qg} + d\sigma_{gg} \tag{3.3}$$

as the appropriate expression. All associated computations have analytic character what is due to the fact that they may be performed in the 'narrow-jet approximation' (NJA); sometimes one meets the principally identical label 'small-cone approximation' (SCA) which is only used if the employed jet algorithm is a cone algorithm. The NJA is formally identical to the limiting case $R \to 0$, so it might be useless. By numerical studies, however, it was found that the corresponding results can be applied to a wide range of R that is relevant in experiment (normally $R \leq 0.7$). The NJA allows an analytical treatment of our project because it limits the angular dependence to the propagator of particles j and k that are supposed to move collinearly. Within this collinear approximation, writing for now the terms $d\sigma_{j(k)}$ and $d\sigma_{jk}$ generally as $d\sigma_{a+b\to j+k+l}$ and skipping the necessary phase space integration, one can formulate a factorization of the form

$$d\sigma_{a+b\to j+k+l} \propto \frac{1}{2p_j \cdot p_k} d\sigma_{a+b\to I+l} \times P^{<}_{j\leftarrow I}(z) \tag{3.4}$$

with the first factor being the propagator mentioned before. $P^{<}_{j\leftarrow I}(z)$ denotes a D-dimensional QCD splitting function with z being the relative amount of energy that is kept by particle I undergoing the splitting; the sign '$<$' denotes that potential contributions of delta functions have to be dropped since $z < 1$. The QCD splitting functions are derived in appendix C. The term $d\sigma_{a+b\to I+l}$ obviously plays the role of a LO cross section for the process $a + b \to I + l$ with I being the particle that, after a splitting, shapes the jet (see Figure 3.1).
In the subsequent chapters we will motivate and give several calculational details how to get the still unknown terms (3.4) appearing in (3.1), (3.2) and (3.3). Unfortunately, it turns out at the end that the achieved results are not optimal to combine them to the desired jet cross sections $d\sigma_{\gamma+g\to\text{jet}+X}$ and $d\sigma_{\gamma+q\to\text{jet}+X}$. Hence, we will introduce the recently developed jet functions in chapter 3.4 which finally give us the correct result. Regardless of this the method presented up to now and deepened afterwards is essential to understand the terms appearing in these jet functions as well as the way how the jet radius R enters the coefficients c_i of the threshold resummation approach.

3.1. Phase space in the collinear approximation

Considering a $2 \to 3$ process in jet production we denote - as before - the two incoming particles by the letters a and b, the three outgoing ones by j,k and l while partons j and k are supposed to form the jet. To calculate the crucial terms $d\sigma_{j(k)}$ and $d\sigma_{jk}$ starting from (3.4) the propagator $\frac{1}{2p_j \cdot p_k}$ must be weighted in the usual and reduced $2 \to 3$ phase space, respectively. The computation is performed in D dimensions to be able to regularize collinear singularities at the end. Following [17] we write the denominator of the propagator as

$$2p_j \cdot p_k = 2E_j^2 \frac{v(1-w)}{1-v+vw}(1-\cos(\theta_{jk}))$$

with θ_{jk} being the angle between partons j and k what is equivalent to

$$E_k = E_j \frac{v(1-w)}{1-v+vw}$$

as the relation of the energies. During the computation we will step by step make use of the notation in terms of v and w instead of pure Mandelstam variables, namely

$$v = 1 + \frac{t}{s} \quad , \quad w = -\frac{u}{s+t} \quad , \quad z = 1 - v + vw \quad \text{and} \quad v' = \frac{vw}{1-v+vw} \quad ,$$

that is applied in [17]. As usual, the calculation will be performed in the center-of-mass system of one particle, in this case particle l, denoted by l^*. Expressing kinematic variables in terms of Mandelstam variables we are able to write the involved energies concretely as

$$E_j = E_l = \sqrt{z}E_j^* = \sqrt{z}E_l^* = \sqrt{z}E_b^* = \frac{\sqrt{sz}}{2} = \frac{\sqrt{s(1-v+vw)}}{2} \quad , \quad E_k = \frac{\sqrt{s}}{2\sqrt{z}}(1-z)$$

while the prescription for E_k is equivalent to that one above.
The remain of this approach basically consists of exploiting properties of the delta distribution, replacing factors of E_k by E_j as expressed above and finally plugging in the dimensional regularization prescription $D = 4 - 2\varepsilon$. Moreover, the part of the angular integrations which can be carried out directly,

$$\int \sin^{D-4}\phi \; d\phi \; d\phi_l^* \quad ,$$

will be combined with the common factors of the $(D-2)$-sphere to $\frac{4\pi^{D-2}}{\Gamma^2\left(\frac{D-2}{2}\right)}$. The symbol δ in the upper limit of the only remaining angular integral means the cone opening of the jet formed by particles j and k. Taking all remarks of this page into account we get

$$
\begin{aligned}
\int \frac{dPS^{(3)}}{dvdw}\frac{1}{(2p_j\cdot p_k)} &= \int vs\frac{dPS^{(3)}}{dt\ dz}\frac{1}{(2p_j\cdot p_k)} = \int \frac{dp_j^{D-1}dp_k^{D-1}dp_l^{D-1}}{(2\pi)^{2D-3}(2E_j)(2E_k)(2E_l)}\frac{vs}{(2E_jE_k)(1-\cos(\theta_{jk}))} \\
&\qquad \cdot \delta^{(D)}(p_a+p_b-p_j-p_k-p_l)\ \delta(t+s+(p_b-p_l)^2)\ \delta\left(z-\frac{4E_j^2}{s}\right) \\
&= \int \frac{dp_k^{D-1}dp_l^{D-1}}{(2\pi)^{2D-3}8E_jE_kE_l}\frac{vs}{2E_j^2}\frac{1-v+vw}{v(1-w)}\frac{1}{1-\cos(\theta_{jk})}\delta(E_a+E_b-E_j-E_k-E_l) \\
&\qquad \cdot \delta(t+s+(p_b-p_l)^2)\ \delta\left(z-\frac{4E_j^2}{s}\right) \\
&= \int \frac{vs}{(2\pi)^{2D-3}}\frac{1}{16E_j^3}\frac{1-v+vw}{v(1-w)}\frac{1}{1-\cos(\theta_{jk})}E_k^{D-3}dE_k\ \sin^{D-3}(\theta_{jk})\ d\theta_{jk} \\
&\quad \cdot \frac{4\pi^{D-2}}{\Gamma^2\left(\frac{D-2}{2}\right)}\cdot E_l^{*D-3}dE_l^*\ \sin^{D-3}(\theta_l^*)\ d\theta_l^*\ \delta(E_a+E_b-E_j-E_k-E_l) \\
&\qquad \cdot \delta(t+s-2E_b^*E_l^*(1-\cos(\theta_l^*)))\ \delta\left(z-\frac{4E_j^2}{s}\right) \\
&= \int \frac{vs}{(2\pi)^{5-4\varepsilon}}\frac{1}{16E_j^2}\frac{1-v+vw}{v(1-w)}\frac{4\pi^{2-2\varepsilon}}{\Gamma^2(1-\varepsilon)}E_j^{-2\varepsilon}\left(\frac{v(1-w)}{1-v+vw}\right)^{1-2\varepsilon}\frac{\sqrt{s}}{2}\left(\frac{\sqrt{s}}{2}\right)^{1-2\varepsilon} \\
&\quad \cdot (1-\cos^2(\theta_l^*))^{-\varepsilon}\ d\cos(\theta_l^*)\ \delta\left(\cos(\theta_l^*)-1+\frac{2u}{s}\right)\frac{2}{s}\cdot\int_0^\delta \frac{\sin^{1-2\varepsilon}(\theta_{jk})}{1-\cos(\theta_{jk})}\ d\theta_{jk} \\
&= \frac{vs}{2^{8-4\varepsilon}\pi^{3-2\varepsilon}\Gamma^2(1-\varepsilon)}\frac{4}{s(1-v+vw)}\left(\frac{E_jv(1-w)}{1-v+vw}\right)^{-2\varepsilon}\left(\frac{\sqrt{s}}{2}\right)^{-2\varepsilon}\left(\frac{4ut}{s^2}\right)^{-\varepsilon} \\
&\qquad \cdot \int_0^\delta \frac{\sin^{1-2\varepsilon}(\theta_{jk})}{1-\cos(\theta_{jk})}\ d\theta_{jk} \\
&= \frac{(16\pi^2)^\varepsilon}{64\pi^3\Gamma^2(1-\varepsilon)}\frac{v}{1-v+vw}\left(\frac{E_jv(1-w)}{1-v+vw}\right)^{-2\varepsilon}(vw(1-v))^{-\varepsilon}\int_0^\delta \frac{\sin^{1-2\varepsilon}(\theta_{jk})}{1-\cos(\theta_{jk})}\ d\theta_{jk} \\
&= \frac{(16\pi^2)^\varepsilon}{64\pi^3\Gamma^2(1-\varepsilon)}\cdot\left(\frac{vw(1-v)}{(1-v+vw)^2}\right)^{-\varepsilon}\cdot\frac{v}{1-v+vw}\cdot(E_j^2v^2(1-w)^2)^{-\varepsilon} \\
&\qquad \cdot \int_0^\delta \frac{\sin^{1-2\varepsilon}(\theta_{jk})}{1-\cos(\theta_{jk})}\ d\theta_{jk} \\
&= \left[\frac{1}{8\pi}\left(\frac{4\pi}{s}\right)^\varepsilon\frac{1}{\Gamma(1-\varepsilon)}[v'(1-v')]^{-\varepsilon}\right]\cdot\frac{1}{8\pi^2}\left(\frac{4\pi}{s}\right)^\varepsilon\frac{1}{\Gamma(1-\varepsilon)}\frac{v}{1-v+vw} \\
&\qquad \cdot\left(\frac{E_j^2v^2(1-w)^2}{s}\right)^{-\varepsilon}\cdot\int_0^\delta \frac{\sin^{1-2\varepsilon}(\theta_{jk})}{1-\cos(\theta_{jk})}\ d\theta_{jk}
\end{aligned}
\tag{3.5}
$$

which constitutes the outcome (13) in [17] and will especially be needed to compute $d\sigma_{j(k)}$.

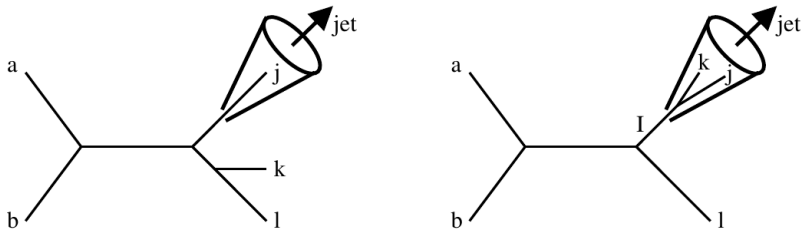

Figure 3.1: Contributions to the jet cross section in NLO with a jet formed by one ($d\sigma_j$) or two partons ($d\sigma_{j(k)}$, $d\sigma_{jk}$) [17].

For the calculation of $d\sigma_{jk}$ the momenta p_j and p_k are combined to one jet momentum $P_{\text{jet}} = p_j + p_k$ expressing the jointly formation of the jet. The desired result can be obtained in the same manner presented before just multiplying with the factor $\frac{1}{sv}\frac{E_{\text{jet}}}{E_k}$ used in (19) of [17] at the end as well as taking the limit $w \to 1$ which effectively reduces the $2 \to 3$ to a $2 \to 2$ phase space.
The only crucial difference concerning the previous computation affects the energy integrations dE_j and dE_k: Using the delta distributions as before the integration over dE_j instead of dE_k is retained but not performed, and factors of E_k are not replaced by E_j. Furthermore, the angle θ_{jk} of the pure phase space integration (not the factor $(1-\cos(\theta_{jk}))$ in the propagator) has to change over to θ_j which now denotes the angle between the momenta p_j and P_{jet}. Paying attention to these details one can avoid to use the strongly modified phase space proposed in equation (19) of [17]. The final outcome of this procedure reads

$$\int \frac{dPS^{(3)}}{dvdw}\frac{1}{(2p_j\cdot p_k)} = \left[\frac{1}{8\pi}\left(\frac{4\pi}{s}\right)^{\varepsilon}\frac{1}{\Gamma(1-\varepsilon)}[v(1-v)]^{-\varepsilon}\right]\cdot\frac{1}{8\pi^2}\left(\frac{4\pi}{s}\right)^{\varepsilon}\frac{1}{\Gamma(1-\varepsilon)}\,\delta(1-w) \cdot\int_0^{E_{\text{jet}}}\frac{E_{\text{jet}}}{E_k^2}\left(\frac{E_j^2}{s}\right)^{-\varepsilon}dE_j\cdot\int_0^{\theta_{\max}}\frac{\sin^{1-2\varepsilon}(\theta_j)}{1-\cos(\theta_{jk})}\,d\theta_j \tag{3.6}$$

and has to be employed for the calculation of $d\sigma_{jk}$ in the next section. There, we will rewrite the angular integration as an integral over the invariant mass of the jet, so we do not need to specify a concrete value of $\theta_{\max}$ here.
Comparing (3.5) and (3.6) there appear some factors in both equations (the difference $v' \to v$ between them is only due to the $\delta(1-w)$ in (3.6)) while that ones in cornered brackets belong to the underlying $2 \to 2$ process. They will be omitted in all succeeding considerations.

3.2. Jet algorithm and calculation of $d\sigma_{jk}$

The crucial difference between the calculation of $d\sigma_{j(k)}$ and $d\sigma_{jk}$ is that for the latter ones an integration over the splitting functions $P^{<}_{j\leftarrow I}(z)$ must be performed according to (3.4). This fact arises because, unlike (3.5), there remains an energy integration in the corresponding phase space expression (3.6). Because the splitting functions always depend on the energy fraction z it is useful to write it as an integral over z. At the same time, it is common to write the θ_j-integration in (3.6) as an integration over the invariant mass $m^2 = P^2_{\text{jet}} = 2p_j \cdot p_k$ of the jet which we assume to be greater than zero even at partonic threshold. To do so, the choice of a specific jet algorithm is required first of all.
Jet algorithms are an ingredient of all modern computer codes that treat partonic scattering since they serve to define a jet out of the final-state particles. We will make use of a k_T-algorithm as it is most common nowadays [18]. This kind of algorithm defines a distance

$$d_{jk} = \min(k^2_{T_j}, k^2_{T_k})\frac{R^2_{jk}}{R^2}$$

between two final-state partons j and k with k_{T_j}, k_{T_k} being their transverse momenta, R the jet radius, and the quantity R_{jk} given by

$$R_{jk} = \sqrt{(\eta_j - \eta_k)^2 + (\phi_j - \phi_k)^2} \tag{3.7}$$

wherein η_j, η_k are their pseudorapidities and ϕ_j, ϕ_k their azimuthal angles. The algorithm compares the distance d_{jk} between the particles with the distances

$$d_{j,\text{beam}} = k^2_{T_j} \quad \text{and} \quad d_{k,\text{beam}} = k^2_{T_k}$$

which constitute a measure for the distance between partons j, k and the beam axis of the colliding particles, respectively. Now, a jet is formed by the algorithm if one or both of the latter distances is smaller than d_{jk}, i.e. a parton is called a jet in the framework of a k_T-algorithm if it is closer to the beam axis than to any other (final-state) parton of the event. In the reversed case the partons j and k formally become a single object by (most commonly) adding their four-momenta ('E recombination scheme'). The algorithm is repeated until exclusively jets are left over in the final state.
To continue the calculation of $d\sigma_{jk}$ we need explicit expressions for the momenta of the partons. According to [18] they can be written as

$$p_j = E_j\left(1, \frac{\cos(\phi_j)}{\cosh(\eta_j)}, \frac{\sin(\phi_j)}{\cosh(\eta_j)}, \tanh(\eta_j)\right) \quad , \quad p_k = E_k\left(1, \frac{\cos(\phi_k)}{\cosh(\eta_k)}, \frac{\sin(\phi_k)}{\cosh(\eta_k)}, \tanh(\eta_k)\right)$$

with E_j, E_k being their associated energies as before. Making use of the fact that m^2 is very small in the NJA, and rapidities may be added as $\eta_j + \eta_k = \eta_{\text{jet}}$, one obtains

$$m^2 = 2p_j \cdot p_k \approx \frac{E_j E_k}{\cosh^2(\eta_{\text{jet}})}((\eta_j - \eta_k)^2 + (\phi_j - \phi_k)^2)$$

what is with (3.7) equivalent to

$$m^2 \approx \frac{E_j E_k}{\cosh^2(\eta_{\text{jet}})} R_{jk}^2$$

so that a connection to the k_T-algorithm is established. What we actually need is a maximum value of m^2 to replace the $\theta_{\max}$ in (3.6). Recognizing that for $d\sigma_{jk}$ partons j and k always form a jet together we can state the requirement $R_{jk}^2 \leq R^2$ which is implicitely included in the definition of d_{jk}. So we get

$$m_{\max}^2 = \frac{E_j E_k}{\cosh^2(\eta_{\text{jet}})} R^2 = \frac{E_{\text{jet}}^2 R^2}{\cosh^2(\eta_{\text{jet}})} z(1-z) \tag{3.8}$$

as maximum value of the invariant jet mass where $z = E_j/E_{\text{jet}}$ and $E_j + E_k = E_{\text{jet}}$ was employed.
Now, we are able to return to the two integrals

$$\int_0^{E_{\text{jet}}} \frac{E_{\text{jet}}}{E_k^2} \left(\frac{E_j^2}{s}\right)^{-\varepsilon} dE_j \cdot \int_0^{\theta_{\max}} \frac{\sin^{1-2\varepsilon}(\theta_j)}{1-\cos(\theta_{jk})}\, d\theta_j$$

from (3.6) that we are going to rewrite. Therefor, we still need the dependences of the angles on the invariant jet mass which have been found to be

$$\cos(\theta_j) = \frac{2E_j E_{\text{jet}} - m^2}{2E_j\sqrt{E_{\text{jet}}^2 - m^2}} \qquad \text{and} \qquad \cos(\theta_{jk}) = 1 - \frac{m^2}{2E_j E_k} \tag{3.9}$$

in [18]. The rest of the calculation is quite straightforward. In the course of this, all terms in m^2 will finally be set to zero since $m^2 << 1$. Beginning with the angular integral we first of all need

$$
\begin{aligned}
\frac{d\theta_j}{dm^2} &= \frac{d}{dm^2}\,\arccos\left(\frac{2E_jE_{\text{jet}}-m^2}{2E_j\sqrt{E_{\text{jet}}^2-m^2}}\right)\\
&= \frac{2E_j\sqrt{E_{\text{jet}}^2-m^2}-(2E_jE_{\text{jet}}-m^2)E_j(E_{\text{jet}}^2-m^2)^{-\frac{1}{2}}}{4E_j^2(E_{\text{jet}}^2-m^2)}\cdot\frac{1}{\sqrt{1-\left(\frac{2E_jE_{\text{jet}}-m^2}{2E_j\sqrt{E_{\text{jet}}^2-m^2}}\right)^2}}\\
&= \left(\frac{(E_{\text{jet}}^2-m^2)^{-\frac{1}{2}}}{2E_j}-\frac{E_{\text{jet}}(E_{\text{jet}}^2-m^2)^{-\frac{3}{2}}}{2}\right)\cdot\frac{1}{\sqrt{1-\left(\frac{2E_jE_{\text{jet}}-m^2}{2E_j\sqrt{E_{\text{jet}}^2-m^2}}\right)^2}}\\
&\approx \left(\frac{1}{2E_{\text{jet}}E_j}-\frac{1}{2E_{\text{jet}}^2}\right)\cdot\frac{1}{\sqrt{1-\left(\frac{2E_jE_{\text{jet}}-m^2}{2E_j\sqrt{E_{\text{jet}}^2-m^2}}\right)^2}}\\
&= \frac{1}{2}\frac{E_k}{E_jE_{\text{jet}}^2}\cdot\frac{1}{\sqrt{1-\left(\frac{2E_jE_{\text{jet}}-m^2}{2E_j\sqrt{E_{\text{jet}}^2-m^2}}\right)^2}}
\end{aligned}
$$

whereby the square root factor and the term $\sin(\theta_j)=\sqrt{1-\cos^2(\theta_j)}$ in the integral cancel each other when substituting $d\theta_j$ by dm^2. For the term $\sin^{-2\varepsilon}(\theta_j)=(\sin^2(\theta_j))^{-\varepsilon}$ we compute

$$
\begin{aligned}
(\sin^2(\theta_j))^{-\varepsilon} = (1-\cos^2(\theta_j))^{-\varepsilon} &= \left(1-\frac{4E_j^2E_{\text{jet}}^2-4E_jE_{\text{jet}}m^2+m^4}{4E_j^2(E_{\text{jet}}^2-m^2)}\right)^{-\varepsilon}\\
&= \left(\frac{4E_j^2E_{\text{jet}}^2-4E_j^2m^2-4E_j^2E_{\text{jet}}^2+4E_jE_{\text{jet}}m^2-m^4}{4E_j^2E_{\text{jet}}^2\left(1-\frac{m^2}{E_{\text{jet}}^2}\right)}\right)^{-\varepsilon}\\
&= \left(\frac{4E_jm^2(E_{\text{jet}}-E_j)-m^4}{4E_j^2E_{\text{jet}}^2\left(1-\frac{m^2}{E_{\text{jet}}^2}\right)}\right)^{-\varepsilon} \approx \left(\frac{E_km^2\left(1+\frac{m^2}{E_{\text{jet}}^2}\right)}{E_jE_{\text{jet}}^2}\right)^{-\varepsilon}\\
&\approx \left(\frac{E_km^2}{E_jE_{\text{jet}}^2}\right)^{-\varepsilon}
\end{aligned}
$$

so that, after taking $1-\cos(\theta_{jk})=\frac{m^2}{2E_jE_k}$ from (3.9), we obtain

$$
\int_0^{\theta_{\max}}\frac{\sin^{1-2\varepsilon}(\theta_j)}{1-\cos(\theta_{jk})}\,d\theta_j \;\to\; \int_0^{m^2_{\max}}\frac{E_k^2}{E_{\text{jet}}^2m^2}\left(\frac{E_km^2}{E_jE_{\text{jet}}^2}\right)^{-\varepsilon}dm^2
$$

from the substitution. Merging this result with the E_j-integral that has been transformed to a z-integral with the help of the simple relation $\frac{dE_j}{dz} = E_{\text{jet}}$ yields

$$\int_0^1 \int_0^{m^2_{\max}} \frac{E^2_{\text{jet}}}{E^2_k} \left(\frac{E^2_j}{s}\right)^{-\varepsilon} \cdot \frac{E^2_k}{E^2_{\text{jet}} m^2} \left(\frac{E_k m^2}{E_j E^2_{\text{jet}}}\right)^{-\varepsilon} dz\; dm^2 = \int_0^1 \int_0^{m^2_{\max}} \left(\frac{E_j E_k}{E^2_{\text{jet}} s}\right)^{-\varepsilon} \cdot \frac{m^{-2\varepsilon}}{m^2}\; dz\; dm^2$$
$$= \int_0^1 \left(\frac{z(1-z)}{s}\right)^{-\varepsilon} dz \int_0^{m^2_{\max}} \frac{m^{-2\varepsilon}}{m^2}\; dm^2 \quad .$$

By performing the dm^2-integration with the maximum value $m^2_{\max}$ from (3.8) as

$$\int_0^{m^2_{\max}} \frac{m^{-2\varepsilon}}{m^2}\, dm^2 = \int_0^{m^2_{\max}} (m^2)^{-1-\varepsilon}\, dm^2 = -\frac{1}{\varepsilon}(m^2_{\max})^{-\varepsilon} = -\frac{1}{\varepsilon}\left(\frac{E^2_{\text{jet}} R^2}{\cosh^2(\eta_{\text{jet}})}\right)^{-\varepsilon} (z(1-z))^{-\varepsilon}$$

we ultimately arrive, summarizing the previous steps, at

$$\int_0^{E_{\text{jet}}} \frac{E_{\text{jet}}}{E^2_k} \left(\frac{E^2_j}{s}\right)^{-\varepsilon} dE_j \int_0^{m^2_{\max}} \frac{E^2_k}{E^2_{\text{jet}} m^2} \left(\frac{E_k m^2}{E_j E^2_{\text{jet}}}\right)^{-\varepsilon} dm^2 = \int_0^1 \left(\frac{z(1-z)}{s}\right)^{-\varepsilon} dz \int_0^{m^2_{\max}} \frac{m^{-2\varepsilon}}{m^2}\; dm^2$$
$$= -\frac{1}{\varepsilon}\left(\frac{E^2_{\text{jet}} R^2}{\cosh^2(\eta_{\text{jet}}) s}\right)^{-\varepsilon} \int_0^1 (z(1-z))^{-2\varepsilon}\; dz \tag{3.10}$$

for the phase space integration. Due to the factorization depicted in (3.4) a splitting function $P^{<}_{j\leftarrow I}(z)$ has to be attached to the z-integral. So we are left with performing

$$I_{j\leftarrow I} = \int_0^1 (z(1-z))^{-2\varepsilon} P^{<}_{j\leftarrow I}(z)\; dz$$

whereby the splitting functions $P^{<}_{j\leftarrow I}(z)$ exactly have the shape that can be found in appendix C. Since we are still general at this point all four possible combinations of j and I must be considered. $I_{j\leftarrow I}$ can be computed with standard computational software like *Mathematica*, in doing so expanding the result up to the second order in ε.
By this procedure

$$\begin{aligned} I_{q\leftarrow q} &= I_{g\leftarrow q} = C_F \left[-\frac{1}{\varepsilon} - \frac{3}{2} + \varepsilon\left(-\frac{13}{2} + \frac{2\pi^2}{3}\right)\right] \quad , \\ I_{q\leftarrow g} &= \frac{1}{2}\left(\frac{2}{3} + \frac{23}{9}\varepsilon\right) \qquad\qquad \text{and} \\ I_{g\leftarrow g} &= 2C_A \left[-\frac{1}{\varepsilon} - \frac{11}{6} + \varepsilon\left(-\frac{67}{9} + \frac{2\pi^2}{3}\right)\right] \end{aligned} \tag{3.11}$$

are found to be the solutions wherefrom the symmetry property of $d\sigma_{jk}$ for $j \neq k$, namely $d\sigma_{jk} = d\sigma_{kj}$, can be directly realized (remember that a gluon $\rightarrow$ quark splitting creates a quark-antiquark pair and not a quark and a gluon).
They enable us to state our final result

$$d\sigma_{jk} = -\frac{1}{\varepsilon}\left(\frac{E_{\text{jet}}^2\delta^2}{s}\right)^{-\varepsilon}\delta(1-w)\cdot d\sigma_{a+b\rightarrow I+l}\cdot I_{j\leftarrow I} \tag{3.12}$$

provided that the 'intermediate' parton I gives not just rise to parton j but also k. The relation $R = \delta\cdot\cosh(\eta_{\text{jet}})$ was used here to replace the jet radius momentarily by the cone opening for further calculations in the subsequent chapter.
From (3.12) we clearly see that our final expression is singular due to - at least - one pole in ε and hence pointless so long as it is not combined with further contributions stemming from the $d\sigma_{j(k)}$. An interesting and valuable observation affects the integral $I_{q\leftarrow g}$ which is the only one in (3.11) not including a further $\frac{1}{\varepsilon}$-term. The reason for this becomes clear from the fact that it stems from the decay of a gluon into a quark-antiquark pair, i.e. it is the only integral not treating the splitting into a gluon. The collinear emission of soft gluons in classical perturbation theory is in turn well known to produce double poles in dimensional regularization - we discover them by inserting the other integrals from (3.11) into (3.12). It provides a good check of our former calculation procedure that such double poles arise in the $d\sigma_{jk}$ if a gluon takes part of the final state, and only a single pole if there are exclusively quarks and antiquarks. How to get rid of these single and double poles will be discussed in the next chapter.

3.3. Calculation of $d\sigma_{j(k)}$, factorization and removal of singularities

To compute the contributions $d\sigma_{j(k)}$ we go back to the phase space equation (3.5). The NJA supposes a small jet cone opening $\delta << 1$ so that the only remained integration in (3.5) yields the approximate solution

$$\int_0^\delta \frac{\sin^{1-2\varepsilon}(\theta_{jk})}{1-\cos(\theta_{jk})}\,d\theta_{jk} \approx \int_0^\delta \frac{(\theta_{jk})^{1-2\varepsilon}}{\frac{(\theta_{jk})^2}{2}}\,d\theta_{jk} = \int_0^\delta 2(\theta_{jk})^{1-2\varepsilon}\,d\theta_{jk} = -\frac{1}{\varepsilon}\delta^{-2\varepsilon}$$

which shows the same single collinear pole as the outcome (3.12) for $d\sigma_{jk}$. According to (3.4) we have, as before, to multiply by a splitting function so that

$$d\sigma_{a+b\rightarrow j+k+l} = \frac{\alpha_s}{2\pi}\frac{v}{1-v+vw}\cdot\left(-\frac{1}{\varepsilon}\right)\cdot\left(\frac{E_j^2\delta^2v^2(1-w)^2}{s}\right)^{-\varepsilon}\cdot d\sigma_{a+b\rightarrow I+l}\cdot P_{j\leftarrow I}^{<}(z) \tag{3.13}$$

constitutes the expression of interest in what follows. In contrast to the calculation of $d\sigma_{jk}$ in the previous section, there is no integration left over the argument z of $P_{j\leftarrow I}^{<}$.

Nonetheless, there arise double poles in ε again when a diagonal splitting function with $j = I$ occurs because the latter is singular in the threshold limit $z \to 1$. The main reason for the consistency of this whole approach is that they are cancelled by corresponding terms in the $d\sigma_{jk}$.
We will now start with the easier case $j \neq I$. It is treated by a standard factorization procedure (not to be confused with that one in (3.4)) to remove the single pole what is achieved by adding an appropriate 'factorization cross section' to (3.13). Following [17] such a term can be written as

$$d\sigma_{\text{fact}} = -\frac{\alpha_s}{2\pi}\frac{v}{1-v+vw}\cdot\left(-\frac{1}{\varepsilon}\right)\cdot\left(\frac{\mu_F^2}{s}\right)^{-\varepsilon}\cdot d\sigma_{a+b\to I+l}\cdot P_{j\leftarrow I}^{<(4)}(z) \tag{3.14}$$

with $P_{j\leftarrow I}^{<(4)}(z)$ being a splitting function as presented in appendix C in strictly $D = 4$ dimensions, i.e. $P_{j\leftarrow I}^{<(4)}(z) = P_{j\leftarrow I}^{<}(z) - \varepsilon P_{j\leftarrow I}^{(\varepsilon)}(z)$. By making use of the ordinary expansion $x^{-\varepsilon} = 1 - \varepsilon\cdot\ln(x) + ...$ the addition of the differing terms in (3.13) and (3.14) is then performed as

$$\begin{aligned} d\sigma_{a+b\to j+k+l} + d\sigma_{\text{fact}} \propto{}& \left(-\frac{1}{\varepsilon}\right)\cdot\left(P_{j\leftarrow I}^{<(4)} + \varepsilon P_{j\leftarrow I}^{(\varepsilon)}\right)\cdot\left(1-\varepsilon\cdot\ln\left(\frac{E_j^2\delta^2v^2(1-w)^2}{s}\right)\right) \\ &+\frac{1}{\varepsilon}\cdot P_{j\leftarrow I}^{<(4)}\cdot\left(1-\varepsilon\cdot\ln\left(\frac{\mu_F^2}{s}\right)\right) \\ ={}& -\frac{1}{\varepsilon}P_{j\leftarrow I}^{<(4)} - P_{j\leftarrow I}^{(\varepsilon)} + P_{j\leftarrow I}^{<(4)}\ln\left(\frac{E_j^2\delta^2v^2(1-w)^2}{s}\right) + \varepsilon P_{j\leftarrow I}^{(\varepsilon)}\cdot \\ &\ln\left(\frac{E_j^2\delta^2v^2(1-w)^2}{s}\right) + \frac{1}{\varepsilon}P_{j\leftarrow I}^{<(4)} - P_{j\leftarrow I}^{<(4)}\ln\left(\frac{\mu_F^2}{s}\right) \end{aligned}$$

what after taking the limit $\varepsilon \to 0$ gives the desired result

$$d\sigma_{j(k)} = \frac{\alpha_s}{2\pi}\frac{v}{1-v+vw}\cdot d\sigma_{a+b\to I+l}\cdot\left(P_{j\leftarrow I}^{<(4)}\ln\left(\frac{E_j^2\delta^2v^2(1-w)^2}{\mu_F^2}\right) - P_{j\leftarrow I}^{(\varepsilon)}\right) \tag{3.15}$$

for $j \neq I$ while parton I has to fulfil the requirement $I \to j + k$ as in (3.12).
Before proceeding with the computation it is reasonable to specify the terms we still need. In (3.2) and (3.3) we had already stated them, namely $d\sigma_{q(g)}$, $d\sigma_{\bar{q}(g)}$, $d\sigma_{g(q)}$, $d\sigma_{g(\bar{q})}$, $d\sigma_{q(\bar{q})}$ and $d\sigma_{g(g)}$ for $d\sigma_{j(k)}$ on the one hand, $d\sigma_{qg}$, $d\sigma_{\bar{q}g}$, $d\sigma_{q\bar{q}}$ and $d\sigma_{gg}$ for $d\sigma_{jk}$ on the other hand. Besides the observation that $d\sigma_{q(g)} = d\sigma_{\bar{q}(g)}$ and $d\sigma_{g(q)} = d\sigma_{g(\bar{q})}$ due to properties of the splitting functions it is obvious in light of the former discussion that $d\sigma_{g(q)}$ and $d\sigma_{q(\bar{q})}$ are determined by (3.15), i.e. the situation with $I \neq j$. The remaining ones can be ordered in two groups depending on whether parton I is a quark (antiquark) or a gluon. The 'quark group' is formed by $d\sigma_{q(g)}$ and $d\sigma_{qg}$, the 'gluon group' by $d\sigma_{g(g)}$, $d\sigma_{q(\bar{q})}$ and $d\sigma_{gg}$. This kind of categorization can be considered as a late justification of

(3.2) and (3.3) where $I = q, \bar{q}$ and $I = q, g$, respectively.
We will now present a sketch of the procedure that arranges the different terms appearing in those two groups to a meaningful final result. For all $d\sigma_{jk}$ we already have the global results (3.11) and (3.12). The remaining $d\sigma_{j(k)}$ which belong to the more difficult case $I = j$ are treated with the aid of the factor $(1-w)^{-2\varepsilon}$ in (3.13) that can be expressed as

$$(1-w)^{-1-2\varepsilon} = -\frac{1}{2\varepsilon}\delta(1-w) + \frac{1}{(1-w)_+} - 2\varepsilon \left(\frac{\ln(1-w)}{1-w}\right)_+ + \mathcal{O}(\varepsilon^2) \tag{3.16}$$

with the plus distribution defined as

$$\int_0^1 f(w)\ [g(w)]_+\ dw = \int_0^1 [f(w) - f(1)]\ g(w)\ dw$$

using any smooth test function f [19]. The distributions in (3.16) have exactly the same meaning as the terms $\mathcal{D}_1$, $\mathcal{D}_0$ and $\delta(1-z)$ of the threshold resummation approach, cf. (2.28) and (2.29), since the limit $w \to 1$ is identical to $z \to 1$. Indeed, we can ignore any integration prescription at this point because we are computing differential cross sections. This implies that the two types of cancellations

$$\frac{1-w}{(1-w)_+} = 1 \qquad \text{and} \qquad (1-w)\cdot\left(\frac{\ln(1-w)}{1-w}\right)_+ = \ln(1-w)\ ,$$

are possible where the factor $(1-w)$ compensates the $(1-w)^{-1}$ that was needed to obtain (3.16). Of course, the explicit splitting functions (see appendix C) entering the calculation are also needed in terms of v and w instead of z (remember that $z = 1 - v + vw$).
To get the quark part $d\sigma_{q(g)} - d\sigma_{qg}$ we need the quark-to-quark splitting function in terms of v and w for $d\sigma_{q(g)}$. From (C.3) we deduce

$$\begin{aligned} P^{<(4)}_{q\leftarrow q} - P^{(\varepsilon)}_{q\leftarrow q} &= C_F\left(\frac{2}{v(1-w)_+} + v(1-w)\right) \qquad \text{and} \\ P^{<(4)}_{q\leftarrow q} - P^{(4)}_{q\leftarrow q} &= -\frac{3}{2}C_F\frac{\delta(1-w)}{v} \end{aligned}$$

with $P^{(4)}_{q\leftarrow q}$ indicating the full four-dimensional splitting function that includes the case $w = 1$ ($z = 1$) in the factor $\delta(1-w)$. Its appearance stems, as well as the replacement of s by μ_F^2 that already showed up in (3.15), and that one of E_j^2 by E^2_{jet} in (3.13), from the factorization and is essential to remove the double pole in $d\sigma_{qg}$.
According to (3.11), (3.12), (3.13) and (3.16) we have to evaluate

$$
\begin{aligned}
d\sigma_{q(g)} - d\sigma_{qg} \propto & \left(-\frac{1}{\varepsilon}\right) \cdot \frac{v(1-w)}{1-v(1-w)} \cdot \left(\frac{E_{\text{jet}}^2\delta^2}{\mu_F^2}\right)^{-\varepsilon} v^{-2\varepsilon} \cdot \left(P_{q\leftarrow q}^{<(4)} - P_{q\leftarrow q}^{(\varepsilon)}\right) \cdot (1-w)^{-1-2\varepsilon} \\
& - \frac{v}{\varepsilon^2}\left(P_{q\leftarrow q}^{<(4)} - P_{q\leftarrow q}^{(4)}\right) + \frac{1}{\varepsilon}\left(\frac{E_{\text{jet}}^2\delta^2}{\mu_F^2}\right)^{-\varepsilon} \delta(1-w) \cdot I_{q\leftarrow q} \\
= & \left(-\frac{1}{\varepsilon}\right) C_F \frac{v(1-w)}{1-v(1-w)} \left(1 - \varepsilon \cdot \ln\left(\frac{E_{\text{jet}}^2\delta^2}{\mu_F^2}\right)\right) (1 - 2\varepsilon \ln(v) + 2\varepsilon^2 \ln^2(v)) \cdot \\
& \left(\frac{2}{v(1-w)_+} + v(1-w)\right) \cdot \left(-\frac{1}{2\varepsilon}\delta(1-w) + \frac{1}{(1-w)_+} - 2\varepsilon\left(\frac{\ln(1-w)}{1-w}\right)_+\right) + \\
& \frac{1}{\varepsilon^2}\frac{3}{2}\delta(1-w) + \frac{1}{\varepsilon} C_F \left(1 - \varepsilon \cdot \ln\left(\frac{E_{\text{jet}}^2\delta^2}{\mu_F^2}\right)\right) \delta(1-w) \cdot \left[-\frac{1}{\varepsilon} - \frac{3}{2} + \varepsilon\left(-\frac{13}{2} + \frac{2\pi^2}{3}\right)\right]
\end{aligned}
\tag{3.17}
$$

for the quark group. To keep the lengthy final expression as clear as possible, all combinations leading to powers of ε^1 or ε^2 will directly be dropped, and the limit $w \to 1$ will be executed in all prefactors of distributions in $(1-w)$. The two poles in ε that remain after multiplying out the expressions get subtracted in the $\overline{\text{MS}}$ scheme as suggested in [17].
Taking all these remarks into account one finds

$$
\begin{aligned}
d\sigma_{q(g)} - d\sigma_{qg} = & \frac{\alpha_s}{2\pi} C_F \left\{ 4\left(\frac{\ln(1-w)}{1-w}\right)_+ + \left(4\,\ln(v) + 2\,\ln\left(\frac{E_{\text{jet}}^2\delta^2}{\mu_F^2}\right)\right) \cdot \frac{1}{(1-w)_+} \; + \right. \\
& \left(\left(2\,\ln(v) + \frac{3}{2}\right) \ln\left(\frac{E_{\text{jet}}^2\delta^2}{\mu_F^2}\right) + 2\,\ln^2(v) - \frac{13}{2} + \frac{2\pi^2}{3} \right) \cdot \delta(1-w) \\
& \left. + \; \frac{v^2(1-w)}{1-v(1-w)} \; \left(1 + \ln\left(\frac{E_{\text{jet}}^2\delta^2 v^2 (1-w)^2}{\mu_F^2}\right)\right) \right\} \cdot d\sigma_{a+b\to I+l}
\end{aligned}
\tag{3.18}
$$

as finite result.
The procedure to compute the gluon part $d\sigma_{g(g)} - N_f d\sigma_{q\bar{q}} - 1/2 d\sigma_{gg}$ behaves in the same manner. It explicitly depends on the number of active flavors N_f and, concerning $d\sigma_{g(g)}$, on the gluon-to-gluon splitting function. Finding the latter in (C.8) we have

$$
\begin{aligned}
P_{g\leftarrow g}^{<} &= 2C_A \left(\frac{1}{v(1-w)_+} + \frac{v(1-w)}{1-v(1-w)} + v(1-w)(1-v(1-w))\right) \quad \text{and} \\
P_{g\leftarrow g}^{<} - P_{g\leftarrow g} &= -\frac{\beta_0}{2}\frac{\delta(1-w)}{v}
\end{aligned}
$$

and find the expression

$$
\begin{aligned}
d\sigma_{g(g)} - N_f d\sigma_{q\bar{q}} - \frac{1}{2} d\sigma_{gg} \propto \; & \left(-\frac{1}{\varepsilon}\right) \cdot \frac{v(1-w)}{1-v(1-w)} \cdot \left(\frac{E_{\text{jet}}^2 \delta^2}{\mu_F^2}\right)^{-\varepsilon} v^{-2\varepsilon} \cdot P_{g\leftarrow g}^{<} \cdot (1-w)^{-1-2\varepsilon} - \\
& \frac{v}{\varepsilon^2}\left(P_{g\leftarrow g}^{<} - P_{g\leftarrow g}\right) + \frac{1}{\varepsilon}\left(\frac{E_{\text{jet}}^2 \delta^2}{\mu_F^2}\right)^{-\varepsilon} \delta(1-w) \cdot \left(N_f \cdot I_{q\leftarrow g} + \frac{1}{2} I_{g\leftarrow g}\right) \\
= \; & \left(-\frac{1}{\varepsilon}\right) 2C_A \frac{v(1-w)}{1-v(1-w)} \left(1 - \varepsilon \cdot \ln\left(\frac{E_{\text{jet}}^2 \delta^2}{\mu_F^2}\right)\right) (1 - 2\varepsilon \ln(v) + 2\varepsilon^2 \ln^2(v)) \cdot \\
& \left(\frac{1}{v(1-w)_+} + \frac{v(1-w)}{1-v(1-w)} + v(1-w)(1-v(1-w))\right) \cdot \\
& \left(-\frac{1}{2\varepsilon}\delta(1-w) + \frac{1}{(1-w)_+} - 2\varepsilon \left(\frac{\ln(1-w)}{1-w}\right)_+\right) + \frac{1}{\varepsilon^2}\frac{\beta_0}{2}\delta(1-w) \\
& + \frac{1}{\varepsilon} N_f \left(1 - \varepsilon \cdot \ln\left(\frac{E_{\text{jet}}^2 \delta^2}{\mu_F^2}\right)\right) \delta(1-w) \cdot \frac{1}{2}\left(\frac{2}{3} + \frac{23}{9}\varepsilon\right) \\
& + \frac{1}{\varepsilon} C_A \left(1 - \varepsilon \cdot \ln\left(\frac{E_{\text{jet}}^2 \delta^2}{\mu_F^2}\right)\right) \delta(1-w) \cdot \left[-\frac{1}{\varepsilon} - \frac{11}{6} + \varepsilon\left(-\frac{67}{9} + \frac{2\pi^2}{3}\right)\right]
\end{aligned}
\tag{3.19}
$$

for the gluon group. Evaluating it in the same manner as before we get the final outcome

$$
\begin{aligned}
d\sigma_{g(g)} - N_f d\sigma_{q\bar{q}} - \frac{1}{2} d\sigma_{gg} = \frac{\alpha_s}{2\pi} C_A \Bigg\{ & 4\left(\frac{\ln(1-w)}{1-w}\right)_+ + \left(4\ln(v) + 2\ln\left(\frac{E_{\text{jet}}^2 \delta^2}{\mu_F^2}\right)\right) \cdot \frac{1}{(1-w)_+} + \\
& \left(\left(2\ln(v) + \frac{\beta_0}{2C_A}\right)\ln\left(\frac{E_{\text{jet}}^2 \delta^2}{\mu_F^2}\right) + 2\ln^2(v) + \frac{23}{18}\frac{N_f}{C_A} - \frac{67}{9} + \frac{2\pi^2}{3}\right) \cdot \delta(1-w) \\
& + \frac{2v^2(1-w)}{(1-v(1-w))^2}(1 + (1-v)^2 + vw(2-2v+vw))\ln\left(\frac{E_{\text{jet}}^2 \delta^2 v^2 (1-w)^2}{\mu_F^2}\right)\Bigg\} \\
& \cdot d\sigma_{a+b\to I+l}
\end{aligned}
\tag{3.20}
$$

with the LO QCD beta function $\beta_0 = \frac{11}{3}C_A - \frac{2}{3}N_f$. It likewise depends on the characteristic distributions in (1-w) as (3.18).
With (3.18) and (3.20) we now have the complete overview concerning the terms we need for (3.2) and (3.3). We are left, however, with the problem that they are so far written in terms of v and w instead of z which is used in the threshold resummation approach. Having a closer look at them it is not totally clear how to deal with the terms $\ln(v)$ and $\ln^2(v)$ when rewriting (3.18) and (3.20). Luckily, there has been found another ansatz to calculate the contributions we are interested in only depending on z in the context of soft-collinear effective theories (SCET). The results obtained within this framework additionally constitute a rough check of the computations of the last three chapters.

3.4. Reformulation with jet functions

In the former section we found two different expressions depending on whether the intermediate parton I of the NLO splitting process is a quark or a gluon. After adding the terms $d\sigma_{g(q)}$ (which equals $d\sigma_{g(\bar{q})}$) and $d\sigma_{q(\bar{q})}$ to them, respectively, they have universal character meaning that they are correct for every scattering process that, in LO, produces a quark or a gluon. In particle physics such an universality often manifests itself in a factorization. That this is indeed true in our case was shown in [20] and partly already earlier by making use of SCET. Coming back to the details of our interest this insight has the consequence that the summations in (3.2) and (3.3) turn into the sum of products of the NLO terms $d\sigma_i$ and jet functions J_i, namely

$$d\sigma_{\gamma+g\to\text{jet}+X} = \sum_{i=q,\bar{q}} d\sigma_i \times J_i = d\sigma_q \cdot J_q + d\sigma_{\bar{q}} \cdot J_{\bar{q}} = 2d\sigma_q \cdot J_q \tag{3.21}$$

and

$$d\sigma_{\gamma+q\to\text{jet}+X} = \sum_{i=q,g} d\sigma_i \times J_i = d\sigma_q \cdot J_q + d\sigma_g \cdot J_g \quad , \tag{3.22}$$

with J_q and J_g containing the desired expressions depending on z. To understand this procedure it is crucial to bear in mind that $d\sigma_i$ contain a sum of the associated Born term $d\sigma_i^{(0)}$ and the NLO corrections $d\sigma_i^{(1)}$, i.e. $d\sigma_i = d\sigma_i^{(0)} + \frac{\alpha_s}{\pi} \cdot d\sigma_i^{(1)}$. The jet functions J_i introduced above have a similar shape, $J_i = \delta(1-z) - \frac{\alpha_s}{\pi} \cdot ...$ (see below). Multiplying out these sums up to order α_s^1 again yields the sum of two parts, the product of $d\sigma_i$ with $\delta(1-z)$ that just reproduces $d\sigma_i$, and the product of the Born term $d\sigma_i^{(0)}$ with the terms proportional to α_s^1 in J_i. The latter should provide us with all necessary combinations of $d\sigma_{j(k)}$ and $d\sigma_{jk}$ which we tediously derived before. Although it is of no significance for this approach, the reader should keep in mind the following: Due to the fact that we deal with a photon in the initial state our terms $d\sigma_i$ are not inclusive as they are in other related works (see the discussion on page 28). This simply means that we do not know $d\sigma_q$, $d\sigma_{\bar{q}}$ and $d\sigma_g$ as individuals but only the combinations $d\sigma_q + d\sigma_{\bar{q}}$ in (3.2) and $d\sigma_q + d\sigma_g$ in (3.3) which correspond to the full NLO terms for the LO processes $\gamma + g \to q + \bar{q}$ and $\gamma + q \to q + g$, respectively.
As we would already expect at this step the jet functions J_q and J_g consist of expressions proportional to distributions in $(1-z)$ as well as expressions containing (parts of) splitting functions. We will present them here as a whole - aside from the fact that we take the threshold limit $z \to 1$ of prefactors of the distributions in $(1-z)$ - although we finally just need the former distributed terms, but already insert here the choice for the squared transverse momentum suggested for the threshold resummation approach in [4], $p_T^2 = \frac{tu}{M^2}$, with the Mandelstam variables t and u and any hard scale M^2 of the process. This at the back of one's mind the jet functions read

$$J_q\left(\mu_F,\mu_R,p_T^2,R,z\right)=\delta(1-z)-\frac{\alpha_s}{\pi}C_F\left\{2\left(\frac{\ln(1-z)}{1-z}\right)_+ +\left(2\,\ln(R)+\ln\left(\frac{tu}{\mu_F^2M^2}\right)\right)\cdot\frac{1}{(1-z)_+}\right.$$
$$+\left(\frac{3}{2}\,\ln(R)+\frac{3}{4}\,\ln\left(\frac{tu}{\mu_F^2M^2}\right)+\frac{1}{2}\left(-\frac{13}{2}+\frac{2\pi^2}{3}\right)\right)\cdot\delta(1-z)$$
$$\left.+\frac{1+(1-z)^2}{z}\left(\ln(1-z)+\ln(R)+\frac{1}{2}\,\ln\left(\frac{tu}{\mu_F^2M^2}\right)\right)+\frac{1}{2}\right\} \tag{3.23}$$

and

$$J_g\left(\mu_F,\mu_R,p_T^2,R,z\right)=\delta(1-z)-\frac{\alpha_s}{\pi}C_A\left\{2\left(\frac{\ln(1-z)}{1-z}\right)_+ +\left(2\,\ln(R)+\ln\left(\frac{tu}{\mu_F^2M^2}\right)\right)\cdot\frac{1}{(1-z)_+}\right.$$
$$+\left(\frac{\beta_0}{2C_A}\left(\ln(R)+\frac{1}{2}\,\ln\left(\frac{tu}{\mu_F^2M^2}\right)\right)+\frac{1}{2}\left(-\frac{67}{9}+\frac{2\pi^2}{3}\right)+\frac{23}{36}\frac{N_f}{C_A}\right)\cdot$$
$$\delta(1-z)+\left(2\left(\frac{1}{z}+z(1-z)-2\right)+\frac{N_f}{C_A}(z^2+(1-z)^2)\right)\cdot$$
$$\left.\left(\ln(R)+\frac{1}{2}\,\ln\left(\frac{tu}{\mu_F^2M^2}\right)\right)+\frac{N_f}{C_A}(z^2+(1-z)^2)\cdot\ln(1-z)+\frac{N_f}{C_A}z\,(1-z)\right\} \tag{3.24}$$

where the strong coupling α_s is implicitly understood to depend on the renormalization scale μ_R. Noticing that $R=\delta\cdot\cosh(\eta_{\text{jet}})$ and $E_{\text{jet}}=p_T\cdot\cosh(\eta_{\text{jet}})$ we can directly compare them with our results for the quark group (3.18) and the gluon group (3.20), respectively, and recognize all characteristics that show up there. We particularly find the terms $d\sigma_{g(q)}$ and $d\sigma_{q(\bar{q})}$ in J_q and J_g, respectively, that are treated by prescription (3.15) within our previous approach whereby $d\sigma_{q(\bar{q})}$ gets an additional factor of N_f analogously to $d\sigma_{q\bar{q}}$ inside the gluon group expression.
With (3.21)-(3.24) we are now able to proceed to the very last theoretical step of this thesis, namely determining the modifications of the coefficients c_3, c_2 and c_1 of the threshold resummation approach in (2.33)-(2.38). Since we have exclusively calculated final-state contributions it should most likely be correct to replace the terms produced by the sum over j in (2.30) and (2.31) by our results although we are not able to prove it. This procedure does not affect the coefficient c_1^μ which therefore just gets the new terms from J_q and J_g in addition. One important point was found in the underlying calculations of [17,18] concerning the coefficient c_3 for the case of a non-vanishing invariant mass of the produced jet at threshold - while computing the final-state corrections in NLO one gets the former contributions ($-C_F$ for a quark, $-C_A$ for a gluon) only for partons which are not part of the jet, but exactly the same contributions for fragmenting partons in the jet as for an initial-state particle ($+2C_F$ for a quark, $+2C_A$ for a gluon). Regarding the example of boson gluon fusion they compute the coefficient $c_3=2C_A-C_F$ whereby

the $+2C_F$ for the final-state jet producing quark is cancelled by the jet function J_q. We will adopt the coefficient c_3 for boson gluon fusion and its analogue for QCD Compton scattering in this shape.
Taking this into account and beyond that combining (3.23) and (3.24) with (2.34), (2.35), (2.37) and (2.38) as explained before we find the new coefficients

$$c_3 = 2C_A - C_F \quad , \tag{3.25}$$

$$c_2 = (C_A - 2C_F)\,\ln\left(\frac{tu}{M^4}\right) - (C_A - 2C_F)\,\ln\left(\frac{\mu_F^2}{M^2}\right) - 4C_F\,\ln(R) \qquad \text{and} \tag{3.26}$$

$$\begin{aligned} c_1^\mu = &\left(\frac{3}{2}C_F - \frac{\beta_0}{4}\right)\,\ln\left(\frac{\mu_F^2}{M^2}\right) + \frac{\beta_0}{4}\,\ln\left(\frac{\mu_R^2}{M^2}\right) - \frac{3}{2}C_F\,\ln\left(\frac{tu}{M^4}\right) \\ &-3C_F\,\ln(R) + \left(\frac{13}{2} - \frac{2\pi^2}{3}\right)C_F \end{aligned} \tag{3.27}$$

for boson gluon fusion $\boldsymbol{\gamma g \to q\bar{q}}$, and

$$c_3 = \frac{3}{2}C_F - \frac{1}{2}C_A \quad , \tag{3.28}$$

$$\begin{aligned} c_2 =&2C_F\,\ln\left(-\frac{u}{M^2}\right) + C_A\,\ln\left(\frac{t}{u}\right) + C_A\,\ln\left(\frac{\mu_F^2}{M^2}\right) \\ &- (C_F + C_A)\,\ln\left(\frac{tu}{M^4}\right) - 2(C_F + C_A)\,\ln(R) \qquad \text{and} \end{aligned} \tag{3.29}$$

$$\begin{aligned} c_1^\mu = &\frac{\beta_0}{4}\,\ln\left(\frac{\mu_F^2}{M^2}\right) + \frac{\beta_0}{4}\,\ln\left(\frac{\mu_R^2}{M^2}\right) - \left(\frac{3}{4}C_F + \frac{\beta_0}{4}\right)\,\ln\left(\frac{tu}{M^4}\right) \\ &- \left(\frac{3}{2}C_F + \frac{\beta_0}{2}\right)\,\ln(R) + \left(\frac{13}{4} - \frac{\pi^2}{3}\right)C_F + \left(\frac{67}{18} - \frac{\pi^2}{3}\right)C_A - \frac{23}{36}N_f \end{aligned} \tag{3.30}$$

for QCD Compton scattering $\boldsymbol{\gamma q \to qg}$. Here, we did not keep up the former separation of scale-dependent and scale-independent terms.

4. Numerical results

In this chapter we repeat the numerical analysis of data from the HERA collider that has been carried out in [1,2], now making use of the code modified with respect to the supplemented coefficients from the threshold resummation approach, (3.25)-(3.30). The collision of electrons/positrons with 27.6 GeV and protons with 920 GeV happened under the kinematic restrictions

$$150 \text{ GeV}^2 < Q^2 < 15000 \text{ GeV}^2 \quad ,$$
$$7 \text{ GeV} < p_T < 50 \text{ GeV} \quad \text{and}$$
$$-1.0 < \eta_{lab} < 2.5$$

for the photon virtuality Q^2, the transverse momentum p_T and the pseudorapidity η_{lab} in the laboratory frame, respectively, with $\mathcal{L} = 357.6 \pm 8.9\text{pb}^{-1}$ being the integrated luminosity (see [21] for more details). The jet radius was explicitly given as $R = 1$.
The experimental data was published as bin-wise and double differential cross sections of single jets in the shape $d\sigma/(dp_T dQ^2)$ in [21]; they have been converted into single differential ones already in [1] to be comparable to the numerical predictions and are shown in Table 1. For the latter we use the scale choice

$$\mu_R = \sqrt{p_T^2 + Q^2} \quad , \quad \mu_F = \sqrt{Q^2} \tag{4.1}$$

and establish an error estimation by varying these scales by a factor of 2 up and down simultaneously as in [1,2]. According to these references we choose the MSTW2008 grids with the strong coupling fixed to $\alpha_s = 0.118$ but now within the newest version of LHAPDF [22]. We extended the steering file used in [1,2] by adding R as the 'jet radius parameter' and established a connection to the employed k_T-algorithm which was originally fixed to $R = 1$. In the following study all results obtained with the original scales (4.1) will be called 'central'. The attribute 'old' denotes predictions that were calculated based on the old version of the code as used in [1,2].
In Figure 4.1 we compare results obtained by both versions while the new one is fixed to $R = 1$, i.e. the jet radius employed in the experiment. Concerning the reproduction of the former study in the upper diagram we surprisingly observe that the theoretical aNNLO prediction and the data do not coincide any more in the highest Q^2-bin despite the included errors although the only obvious change in the numerical treatment was the usage of the new LHAPDF6.2.1 set instead of LHAPDF5.9.1. In the lower diagram generated by our modified code with R-dependence we see a slight but significant change of the theoretical results whereby the reduction of the error which means a reduction of the scale dependence is very remarkable. They remain being a suitable description of the data in all bins, now also the highest one again. The tendency of a slight underestimation of the data persists, too, and is even a bit more pronounced in the middle and higher bins. This aspect also becomes visible in Figure 4.2 where the latter diagrams are

Q^2-bins [GeV^2]	$d\sigma/dQ^2$ [pb/GeV^2]	p_T-bins [GeV]	$d\sigma/dp_T$ [pb/GeV]
$150 < Q^2 < 200$	2.1791200 ± 0.0675894	$7 < p_T < 11$	67.142500 ± 1.335675
$200 \leq Q^2 < 270$	1.2538143 ± 0.0431575	$11 \leq p_T < 18$	20.137143 ± 0.512620
$270 \leq Q^2 < 400$	0.6685462 ± 0.0225371	$18 \leq p_T < 30$	3.3698333 ± 0.118470
$400 \leq Q^2 < 700$	0.2775700 ± 0.0093049	$30 \leq p_T < 50$	0.2795000 ± 0.019181
$700 \leq Q^2 < 5000$	0.0194116 ± 0.0005877		
$5000 \leq Q^2 < 15000$	0.0005183 ± 0.0000529		

Table 1: Single differential DIS cross sections distributed in Q^2 (left) and p_T (right) from the HERA experiment. The conversion by multiplying with the respectively other bin-width and summation is based on data presented double differentially in Q^2 and p_T in [21].

normalized to the aNNLO result with central scale choice of the old code version. This kind of depiction additionally manifests the far smaller scale dependence of the novel results, particularly from the middle to the lowest bin. Despite the fact that this generally constitutes an important theoretical achievement it is an interesting discovery because in [1,2] the transition from NLO to aNNLO was found to reduce the scale dependence only in the highest Q^2-bin where our new results for the error alter least of all. In Figure 4.3 we present the analogous comparison as in Figure 4.1 for the p_T-distribution. The upper diagram reveals a good reproduction of the corresponding former results. The lower diagram shows a distinct failure of the new aNNLO results for $R = 1$ between middle and high values of p_T. It is clear, of course, that a collinear approximation as we used it to calculate the new R-dependent contributions cannot be unreservedly applicable to high transverse momenta. But, nevertheless, it is an exceptional finding that we get this result although those terms just contribute in NNLO and not in NLO in our case. Since this behaviour for p_T was also present for $R < 1$ we will focus on the Q^2-distribution from now on. From Figure 4.4 to 4.8 we show a combination of pure and normalized diagrams for gradually decreasing values of R up to $R = 0.7$ which is already far away from the actual experimental conditions. Nonetheless, we observe no qualitatively significant modifications of our aNNLO prediction except for the fact that the scale dependence starts to increase slightly but unsystematically again. Because of this observation we investigated the situations $R = 0.6$ and $R = 0.5$ as well in Figure 4.9 which further on lead to very similar outcomes as the previous ones. This finding might be a direct consequence of our approach to consider the R-dependent and associated novel terms just in NNLO and leaving the full NLO calculation untouched. In this context we additionally have to stress the following: All former studies (see e.g. [17,18,20]) employing those contributions had a setup with $R \leq 0.7$ thereby respecting the fact that they are computed within the narrow-jet approximation (NJA) for which $R = 0.7$ is already an extremely large number. It turned out, however, that the NJA even provides reasonable results for the latter. Our study, with $R = 1$ given by experiment, is in fact a large range away from $R = 0.7$. Now, one could imagine two scenarios as the most probable explanations for our findings. The positive one states that our

appropriate results for $R = 1$ in Figure 4.1 and 4.2 might be a hint that the NJA is, in practice, still usable for such a large jet radius. The negative and much more plausible one states that this is not the case and that our investigation was successful just because we did not implement the new terms into the NLO part of our program. If this is true our good outcomes would be arised by accident. In light of the impact of those terms in NNLO one could expect that their usage in NLO would considerably enhance the underestimation of the data by theory, thereby distinctly worsening our results. The compensation for this mismatch would then come from a calculation beyond the NJA which should definitely increase the total cross section because, from a heuristical point of view, it is clear that a larger jet radius corresponds to a larger amount of final-state particles. Such a calculation does not exist so far to our knowledge. Fortunately, we were able to study these correlations in greater detail by computing the associated cross sections in approximate NLO. This option within our programm was implemented in [1] where it was called kNLO with the 'k' denoting the threshold resummation approach by Kidonakis. It accordingly consists of its NLO contributions (2.29), completed by the global LO terms and that ones depending on the phase space slicing cutoff parameter within the code, and therefore offers a possibility to estimate the significance of the distributions in z of the jet functions in NLO. In Figure 4.10 we present kNLO cross sections of the old and the new version of the code for the Q^2-distribution. As it already turned out in [1] they are not appropriate for higher Q^2 what seems to be valid for both versions. It is, however, a decisive result that we find, within the other bins, a distinct reduction of the old kNLO predictions for small R (we have chosen the example $R = 0.7$ in Figure 4.10), but just a very slight one for $R = 1$. This constitutes a strong evidence that the new terms are actually dominated by the R-dependent ones, i.e. $\ln(R)$, whose magnitude grows larger when R diverges from 1, of course. Taking this point into account our upper results for $R = 1$ appreciate in value considerably although we still cannot assess the impact of a computation beyond the NJA.

After discussing the problems of our study we should emphasize the strongly reduced scale dependence again. It constitutes a very favourable and indisputable outcome because there is no reason why it could be happened accidentally: The scale dependence is primarily determined by the coefficients of the threshold resummation approach, (3.25)-(3.30), which are part of the NNLO master formula as well as of the NLO calculation. Taking this into account one would expect that their yet absent implementation in NLO could decrease the scale dependence even further. In this respect, a corresponding tendency can already be seen in our kNLO results in Figure 4.10.

Finally, we want to mention another remarkable aspect discussed in [18], namely that there can arise negative cross sections for small values of R although the NJA is formally valid for them. The reason for this consists of logarithmic terms $\alpha_s^n \ln^n(R)$ in higher orders of perturbation theory that become sizeable in this case and have to be resummed. Interestingly, we could verify the appearance of some negative cross sections even within our pure aNNLO approach for $R \leq 0.1$. Considering this order of R our results generally failed reproducing the data, of course.

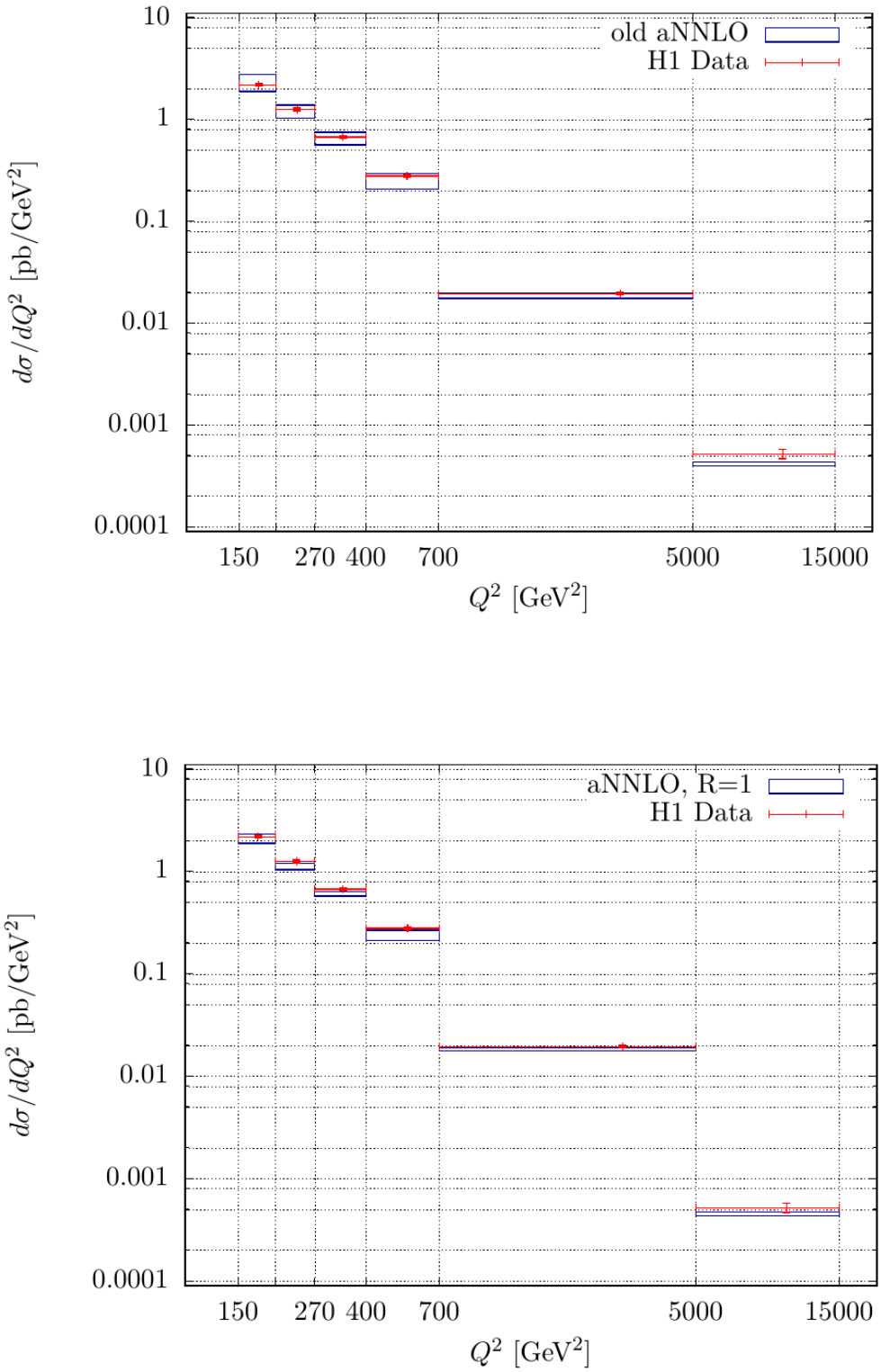

Figure 4.1: aNNLO results for the Q^2-distribution from the native code (top) and with R=1 from the modified code (bottom). The error bands have been obtained by scale variation.

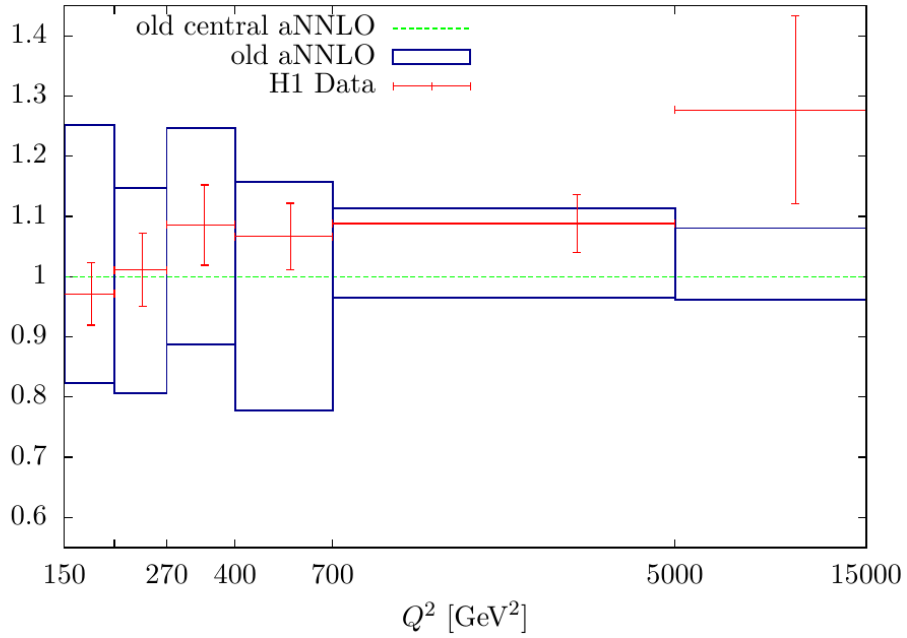

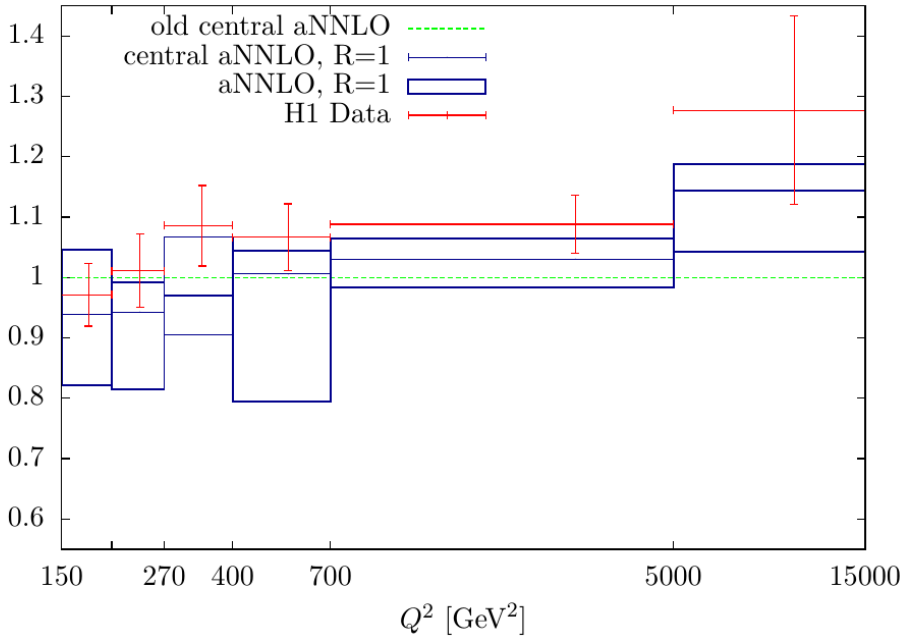

Figure 4.2: aNNLO results for the Q^2-distribution from the native code (top) and with R=1 from the modified code (bottom) normalized to the central aNNLO prediction from the native code. The error bands have been obtained by scale variation.

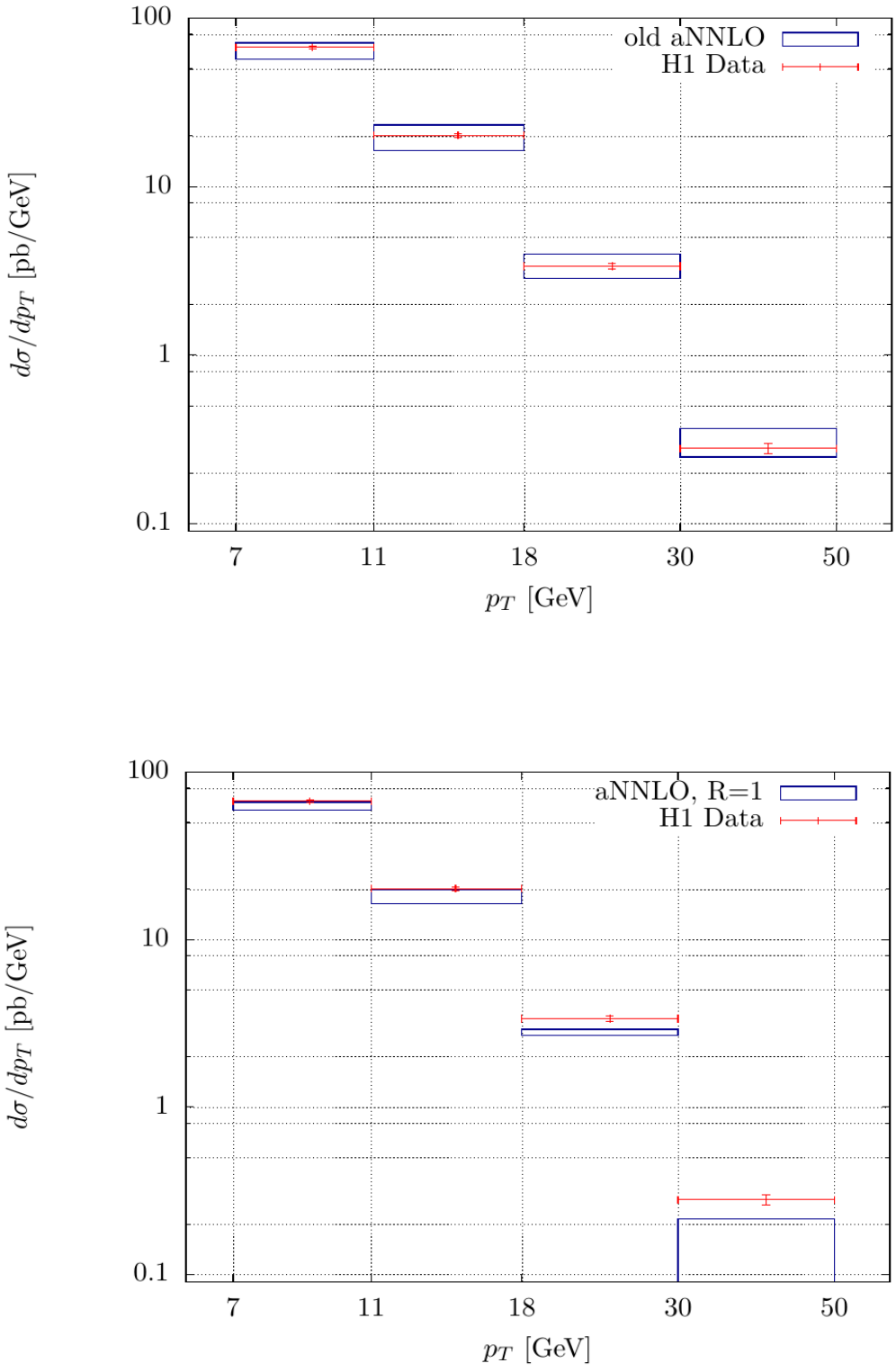

Figure 4.3: aNNLO results for the p_T-distribution from the native code (top) and with R=1 from the modified code (bottom). The error bands have been obtained by scale variation.

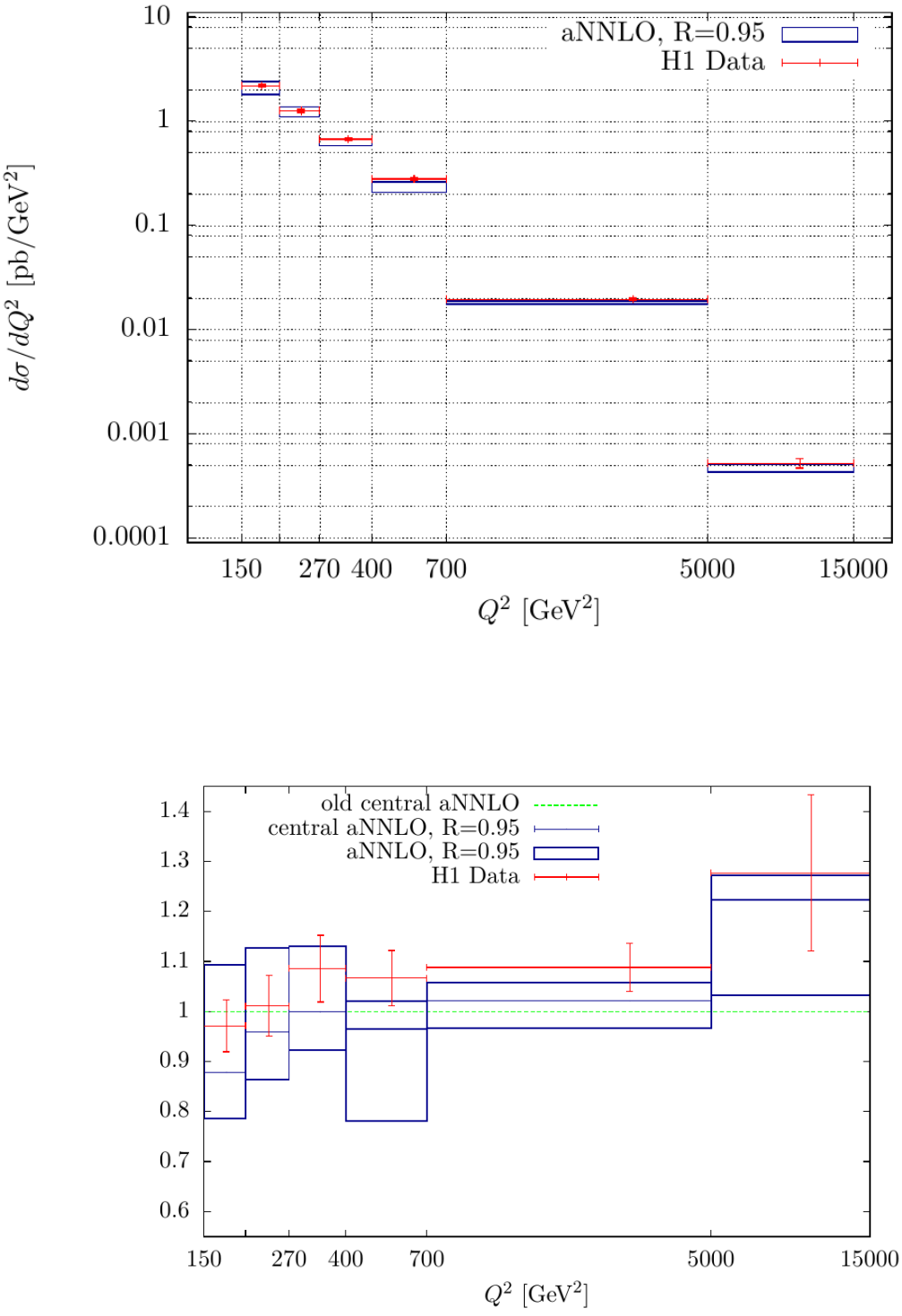

Figure 4.4: aNNLO results with R=0.95 for the Q^2-distribution in the original (top) and normalized to the central aNNLO prediction from the native code (bottom). The error bands have been obtained by scale variation.

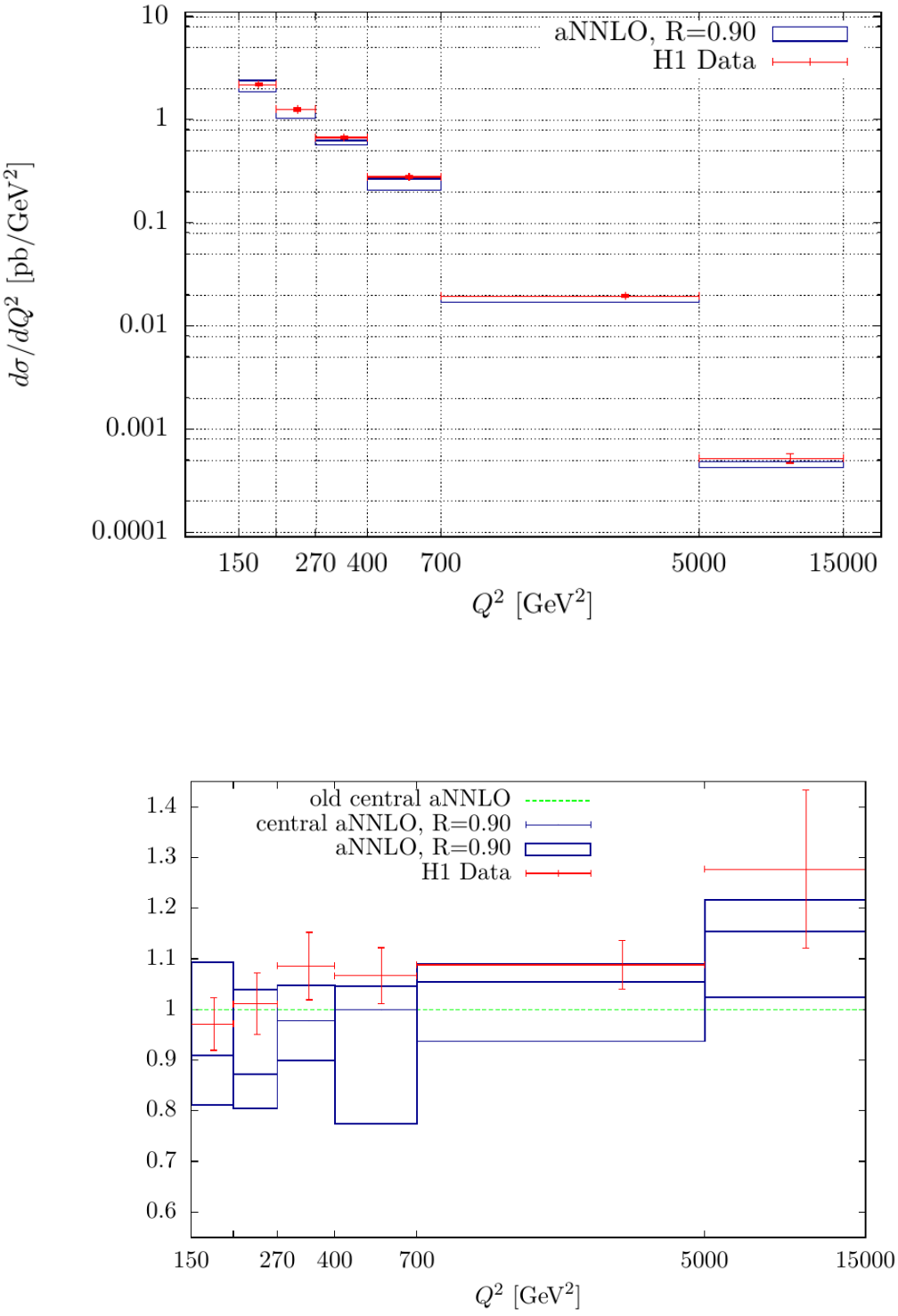

Figure 4.5: aNNLO results with R=0.90 for the Q^2-distribution in the original (top) and normalized to the central aNNLO prediction from the native code (bottom). The error bands have been obtained by scale variation.

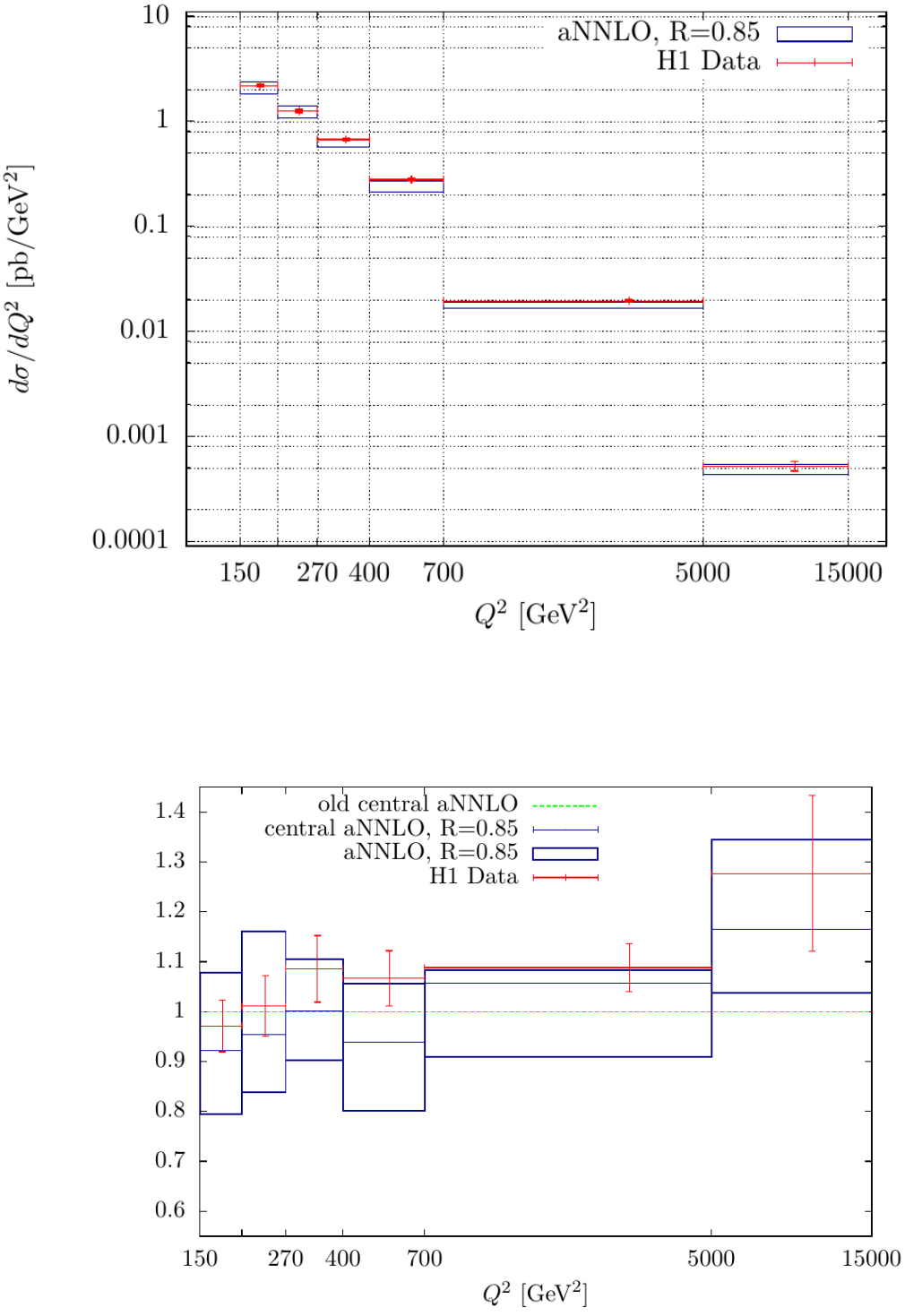

Figure 4.6: aNNLO results with R=0.85 for the Q^2-distribution in the original (top) and normalized to the central aNNLO prediction from the native code (bottom). The error bands have been obtained by scale variation.

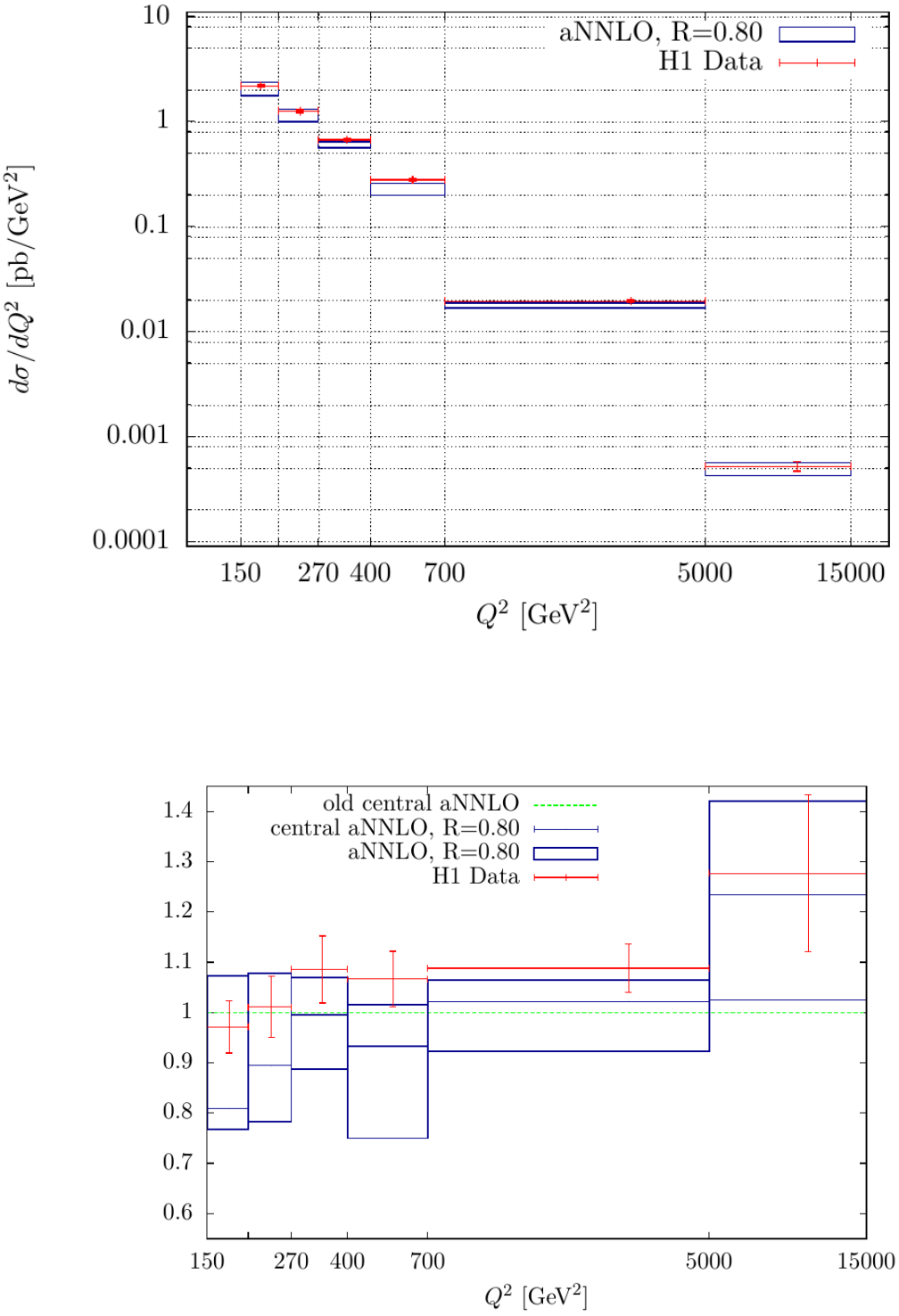

Figure 4.7: aNNLO results with R=0.80 for the Q^2-distribution in the original (top) and normalized to the central aNNLO prediction from the native code (bottom). The error bands have been obtained by scale variation.

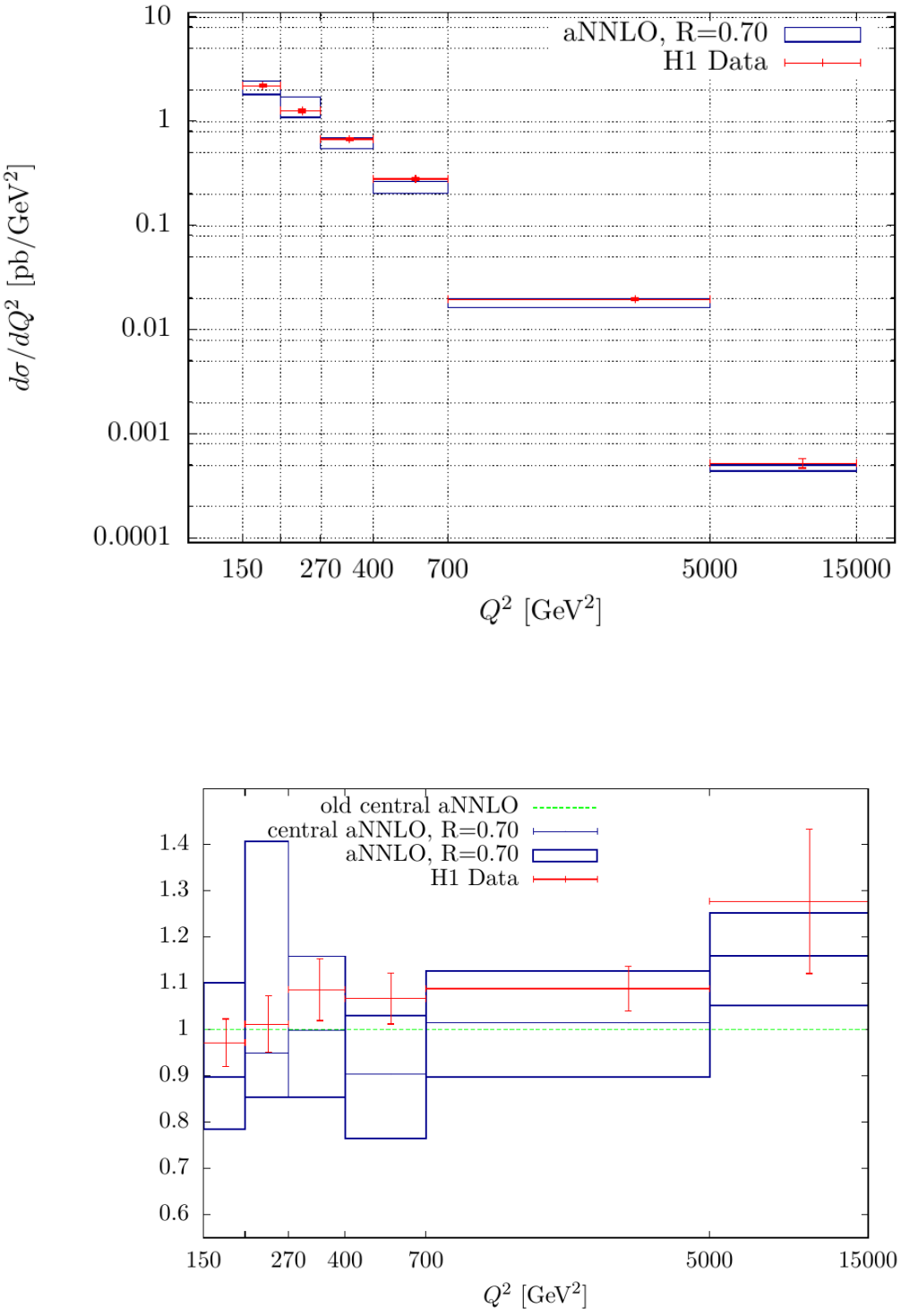

Figure 4.8: aNNLO results with R=0.70 for the Q^2-distribution in the original (top) and normalized to the central aNNLO prediction from the native code (bottom). The error bands have been obtained by scale variation.

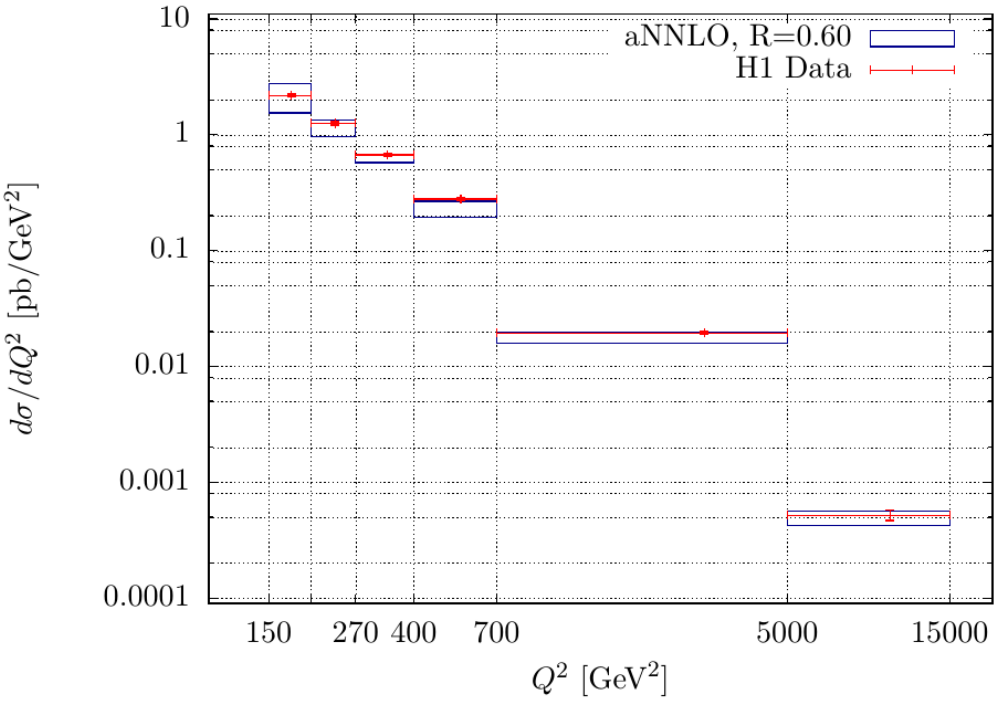

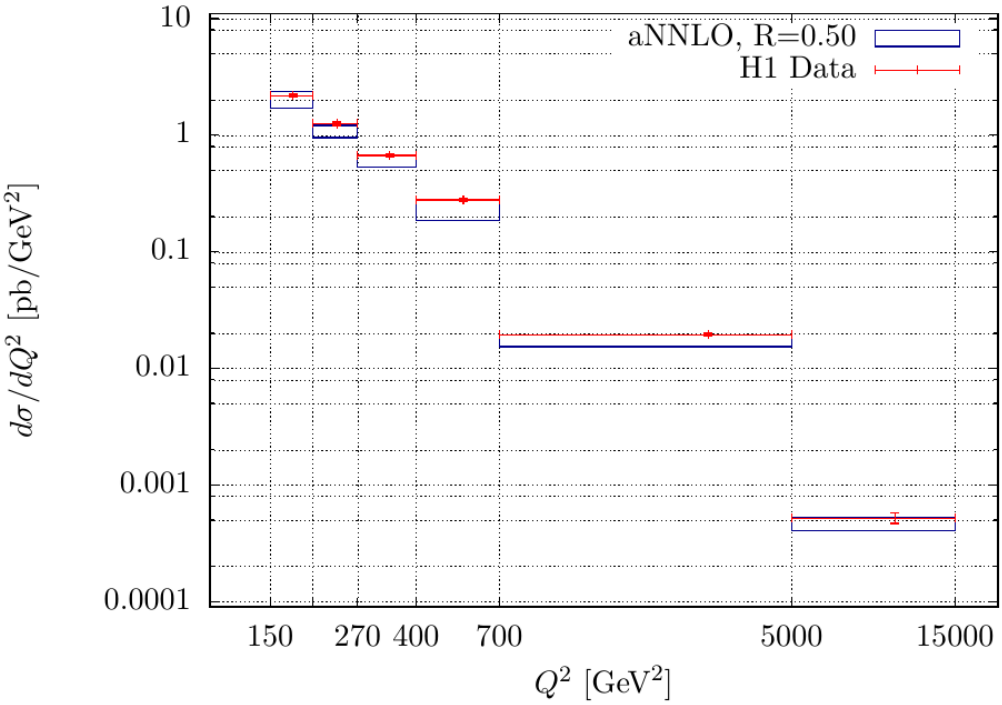

Figure 4.9: aNNLO results with R=0.60 (top) and R=0.50 (bottom) for the Q^2-distribution. The error bands have been obtained by scale variation.

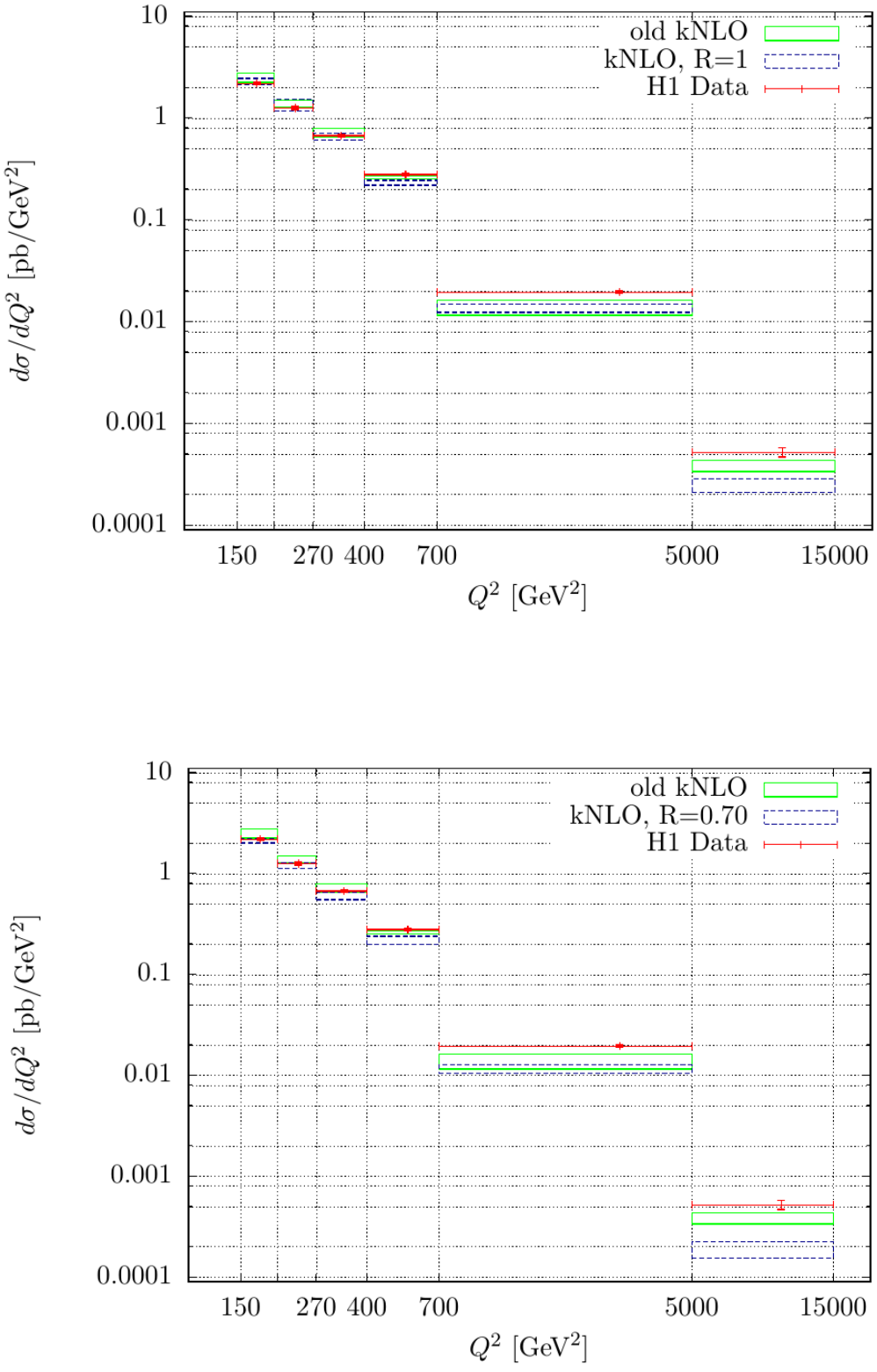

Figure 4.10: Approximate NLO results ('kNLO') for the Q^2-distribution from the native code compared to that ones with R=1 (top) and R=0.70 (bottom) from the modified code. The error bands have been obtained by scale variation.

5. Conclusions

In this work we numerically investigated inclusive jet production in deep-inelastic scattering on the basis of an approximate next-to-next-to-leading order (aNNLO) approach stemming from a unified threshold resummation formalism. The implementation of the latter into the program JetVip, providing a full NLO calculation of DIS cross sections, had been carried out within an earlier thesis. Assuming a non-vanishing invariant mass of the jets at partonic threshold we were able to find new logarithmically enhanced NLO contributions partly dependending on the jet radius R in the literature which are an ingredient of recently discovered jet functions. Motivated by them we reconstructed one method of their derivation, namely by computing special real and virtual final-state contributions to partonic jet production in NLO analytically within the narrow-jet approximation (NJA) and removing all appearing soft and collinear singularitites. Instead of using the whole jet functions within the NLO calculation of JetVip we settled for just taking the novel logarithmically enhanced terms and substituting similar ones occurring within the threshold resummation aNNLO approach by them. After performing the necessary changes to the former code we repeated the analysis of data from the HERA collider done in the earlier work. We found a remarkably reduced dependence on the renormalization and factorization scales corresponding to an improved theoretical accuracy. The data was shown to be reproduced properly for $R = 1$ given by the experiment, despite a slight tendency of underestimation. The finding of an extremely small change of our results when inserting considerably smaller values of R evokes, however, the suspicion that the satisfactory outcomes for the total cross section for $R = 1$ might be an interplay of the two aspects that, on the one hand, we did not consider the full jet functions in NLO and, on the other hand, the NJA was shown to be accurate only for $R \leq 0.7$ within earlier studies. The latter point would make it presently impossible to improve the coherence of our results due to the necessity to perform the above calculation beyond the NJA what has not been carried out so far in the literature to our knowledge. Moreover, it would mean that the NLO implementation could be worthwhile only if there exists data with $R \leq 0.7$ to compare with. We could, however, mainly rehabilitate our predictions for $R = 1$ in the context of an approximate NLO calculation, involving all distributions in z of the jet functions, by demonstrating that the latter are controlled predominantly by the terms $\ln(R)$ that vanish for $R = 1$. Nevertheless, the question whether - in light of this finding - the NJA can be applied generally for the case $R = 1$ remains open.

A. Applied QCD Feynman rules

Quark, incoming	$u(p,s)$
Quark, outgoing	$\bar{u}(p,s)$
Antiquark, incoming	$\bar{v}(p,s)$
Antiquark, outgoing	$v(p,s)$
Quark propagator	$\delta_{ij}\ \dfrac{\not{p}+m}{p^2-m^2}$
Gluon propagator	$\dfrac{\delta_{ab}}{p^2}\ g^{\mu\nu}$
Photon-quark-vertex	$iee_q\gamma^\mu$
Quark-gluon-vertex	$g\gamma_\mu T^a_{ij}$
Gluon-ghost-vertex	$-igf^{abc}p$
Three-gluon-vertex	$-igf^{abc}\left[g^{\mu\nu}(p_1-p_2)^\lambda + g^{\nu\lambda}(p_2-p_3)^\mu + g^{\lambda\mu}(p_3-p_1)^\nu\right]$

B. Eikonal Feynman rules for QCD

Incoming quark, emitting a gluon	$gT^a_{ij}\dfrac{v^\mu}{-v\cdot k+i\epsilon}$
Incoming antiquark, emitting a gluon	$-gT^a_{ij}\dfrac{v^\mu}{-v\cdot k+i\epsilon}$
Incoming gluon, emitting a gluon	$-igf^{abc}\dfrac{v^\mu}{-v\cdot k+i\epsilon}$
Outgoing quark, emitting a gluon	$gT^a_{ij}\dfrac{v^\mu}{v\cdot k+i\epsilon}$
Outgoing antiquark, emitting a gluon	$-gT^a_{ij}\dfrac{v^\mu}{v\cdot k+i\epsilon}$
Outgoing gluon, emitting a gluon	$-igf^{abc}\dfrac{v^\mu}{v\cdot k+i\epsilon}$
Incoming quark, absorbing a gluon	$gT^a_{ij}\dfrac{v^\mu}{v\cdot k+i\epsilon}$
Incoming antiquark, absorbing a gluon	$-gT^a_{ij}\dfrac{v^\mu}{v\cdot k+i\epsilon}$
Incoming gluon, absorbing a gluon	$-igf^{abc}\dfrac{v^\mu}{v\cdot k+i\epsilon}$
Outgoing quark, absorbing a gluon	$gT^a_{ij}\dfrac{v^\mu}{-v\cdot k+i\epsilon}$
Outgoing antiquark, absorbing a gluon	$-gT^a_{ij}\dfrac{v^\mu}{-v\cdot k+i\epsilon}$
Outgoing gluon, absorbing a gluon	$-igf^{abc}\dfrac{v^\mu}{-v\cdot k+i\epsilon}$

C. Splitting functions

The derivation of QCD splitting functions, which play an essential role in the Altarelli-Parisi equations as well as in calculations of cross sections, can be performed in different ways (see for example [7,23]). In this thesis it will be done in a quite intuitive manner as motivated in [7]. We will therefore concentrate on a more in-depth presentation of the calculation which is suggested there - for further explanations of the particular ingredients we refer the reader to chapter 17.5 of [7]. The computations are done here in D dimensions using the prescription $D = 4 - 2\epsilon$ at the end to obtain the shape of the splitting functions that is employed in [18] and chapter 3 of this thesis. For the same reason the contributions of delta functions are omitted what is denoted by '$<$', standing for $z < 1$.
One small blemish affects the procedure in higher dimensions because the latter enter the calculations through the Dirac matrices γ^μ which fulfill equations like

$$\gamma^\alpha \gamma^\mu \gamma_\alpha = (D-2)\gamma^\mu \ .$$

in D dimensions. In the following calculations, however, the Dirac matrices appear in terms of Pauli matrices for the reason of clarity concerning the details of their contractions with spinors. Because of this, factors of $\sqrt{D-2}$ seem to enter through the back door already in the not-yet-squared matrix elements although the contraction of Dirac matrices formally takes place during squaring first.
Another crucial point is the negligence of constant terms in ϵ what appears to be arbitrary and to be done only for the reason of obtaining the splitting functions as they occur in [18]. Here, the decisive argument constitutes the observation that these terms would keep their power in ϵ even after performing the integrals $I_{j \leftarrow I}$ in chapter 3.2 of this thesis and therefore would drop out anyway in the limit $\epsilon \to 0$.
The computation requires the following steps: The Feynman rules for the emission vertex of the corresponding process have to be applied, thereby taking into account all possible states which are allowed by helicity conservation. Finally, all these contributions are squared, added up and averaged over spin, flavor or color of the splitting (incoming) particle. Without loss of generality the momentum of the particle that splits will be supposed to lie in x-direction while after splitting the (outgoing) particles will move in the x-z-plane, additionally carrying a transverse momentum $p_\perp$ that is small due to the collinear limit. With these considerations the four-momenta of the involved particles can become parametrized by

$$\begin{aligned} p^\mu &= (p, 0, 0, p) \ , \\ q^\mu &= \left(zp, p_\perp, 0, zp - \frac{p_\perp^2}{2zp} \right) \ , \\ k^\mu &= \left((1-z)p, -p_\perp, 0, (1-z)p + \frac{p_\perp^2}{2zp} \right) \ , \end{aligned}$$

where p^μ obviously represents the incoming, q^μ and k^μ the outgoing ones (the index μ will be omitted below).

C.1. Quark $\rightarrow$ gluon splitting $P^<_{g\leftarrow q}$

In the case of a quark emitting a gluon we assign the four-momentum q to the gluon and k to the remaining quark, z means the energy fraction of the incoming quark which is carried away by the gluon. Then, for the left-handed spinors the expressions

$$u_L(p) = \sqrt{2p^0}\begin{pmatrix} \xi(p) \\ 0 \end{pmatrix} \ , \ u_L(k) = \sqrt{2k^0}\begin{pmatrix} \xi(k) \\ 0 \end{pmatrix}$$

hold, respectively, where

$$\xi(p) = \begin{pmatrix} 0 \\ 1 \end{pmatrix} \ , \ \xi(k) = \begin{pmatrix} \frac{p_\perp}{2(1-z)p} \\ 1 \end{pmatrix} \ .$$

The gluon polarizations can be expressed by

$$\varepsilon_L(q) = \frac{1}{\sqrt{2}}\begin{pmatrix} 1 \\ -i \\ -\frac{p_\perp}{zp} \end{pmatrix} \ , \ \varepsilon_R(q) = \frac{1}{\sqrt{2}}\begin{pmatrix} 1 \\ i \\ -\frac{p_\perp}{zp} \end{pmatrix}$$

for the left- and right-handed case. Helicity conservation now permits four different channels while two of them are achieved by a global helicity flip whereby the corresponding matrix element keeps its previous value due to parity invariance. Hence, only two channels have to be computed explicitly. We choose the two channels with a left-handed incoming quark. So we get

$$\begin{aligned}
iM(q_L \rightarrow q_L\ g_R) &= \bar{u}_L(k)\ (g\gamma_\mu T^a_{ij})\ u_L(p)\ \varepsilon^{*\mu}_R(q) = \frac{\sqrt{2}gT^a_{ij}}{\sqrt{D-2}}\ \sqrt{2(1-z)p}\sqrt{2p}\ \xi^\dagger(k)\sigma^i\varepsilon^{*i}_R\xi(p) \\
&= \frac{2gT^a_{ij}}{\sqrt{D-2}}\ p\sqrt{1-z}\ \xi^\dagger(k)\ \left(\sigma_1\cdot 1 - \sigma_2\cdot i - \sigma_3\cdot\frac{p_\perp}{zp}\right)\ \xi(p) \\
&= \frac{2gT^a_{ij}\ p\sqrt{1-z}\ \xi^\dagger(k)}{\sqrt{D-2}}\left[\begin{pmatrix} 0 & 1 \\ 1 & 0 \end{pmatrix}\cdot 1 - \begin{pmatrix} 0 & -i \\ i & 0 \end{pmatrix}\cdot i - \begin{pmatrix} 1 & 0 \\ 0 & -1 \end{pmatrix}\cdot\frac{p_\perp}{zp}\right]\ \xi(p) \\
&= \frac{2gT^a_{ij}\ p\sqrt{1-z}}{\sqrt{D-2}}\begin{pmatrix} \frac{p_\perp}{2(1-z)p} & 1 \end{pmatrix}\left[\begin{pmatrix} 0 & 0 \\ 2 & 0 \end{pmatrix} - \begin{pmatrix} \frac{p_\perp}{zp} & 0 \\ 0 & -\frac{p_\perp}{zp} \end{pmatrix}\right]\begin{pmatrix} 0 \\ 1 \end{pmatrix} \\
&= \frac{2gT^a_{ij}\ p\sqrt{1-z}}{\sqrt{D-2}}\ \frac{D-2}{2}\begin{pmatrix} \frac{p_\perp}{2(1-z)p} & 1 \end{pmatrix}\begin{pmatrix} 0 \\ \frac{p_\perp}{zp} \end{pmatrix} \\
&= gT^a_{ij}\frac{\sqrt{(D-2)(1-z)}}{z}p_\perp
\end{aligned}$$

and

$$
\begin{aligned}
iM(q_L \to q_L\ g_L) &= \bar{u}_L(k)\ (g\gamma_\mu T^a_{ij})\ u_L(p)\ \varepsilon^{*\mu}_L(q) = \frac{\sqrt{2}gT^a_{ij}}{\sqrt{D-2}}\ \sqrt{2(1-z)p}\sqrt{2p}\ \xi^\dagger(k)\ \sigma^i \varepsilon^{*i}_L\ \xi(p) \\
&= \frac{2gT^a_{ij}\ p\sqrt{1-z}}{\sqrt{D-2}}\ \xi^\dagger(k) \left[\begin{pmatrix} 0 & 1 \\ 1 & 0 \end{pmatrix} \cdot 1 + \begin{pmatrix} 0 & -i \\ i & 0 \end{pmatrix} \cdot i - \begin{pmatrix} 1 & 0 \\ 0 & -1 \end{pmatrix} \cdot \frac{p_\perp}{zp} \right] \xi(p) \\
&= \frac{2gT^a_{ij}\ p\sqrt{1-z}}{\sqrt{D-2}} \begin{pmatrix} \frac{p_\perp}{2(1-z)p} & 1 \end{pmatrix} \left[\begin{pmatrix} 0 & 2 \\ 0 & 0 \end{pmatrix} - \begin{pmatrix} \frac{p_\perp}{zp} & 0 \\ 0 & -\frac{p_\perp}{zp} \end{pmatrix} \right] \begin{pmatrix} 0 \\ 1 \end{pmatrix} \\
&= \frac{2gT^a_{ij}\ p\sqrt{1-z}}{\sqrt{D-2}} \begin{pmatrix} \frac{p_\perp}{2(1-z)p} & 1 \end{pmatrix} \begin{pmatrix} 2 \\ \frac{p_\perp}{zp} \end{pmatrix} \\
&= \frac{2gT^a_{ij}\ p\sqrt{1-z}}{\sqrt{D-2}} \left(\frac{p_\perp}{(1-z)p} + \frac{p_\perp}{zp} \right) \\
&= \frac{2gT^a_{ij}}{\sqrt{D-2}}\ \frac{\sqrt{1-z}}{z(1-z)}\ p_\perp
\end{aligned}
$$

where the additional factor of $\frac{D-2}{2}$ in the fifth line of the first matrix element arises from the vanishing contraction between Pauli matrices and the spinor $\xi(p)$ in the fourth line. These contributions lead to

$$
\begin{aligned}
\frac{1}{2} \cdot \frac{1}{3} \sum_{pol.} |M_I|^2 &= \frac{1}{6} \left(|M_{L\to LR}|^2 + |M_{L\to LL}|^2 + |M_{R\to RL}|^2 + |M_{R\to RR}|^2 \right) \\
&= \frac{1}{6} \cdot 2 \cdot 4g^2 p_\perp^2 \left(\frac{(D-2)(1-z)}{z^2} + \frac{4}{D-2}\ \frac{1-z}{z^2(1-z)^2} \right) \\
&\underset{D=4-2\epsilon}{=} g^2 C_F p_\perp^2 \left(\frac{2(1-\epsilon)(1-z)}{z^2} + \frac{2}{1-\epsilon}\ \frac{1-z}{z^2(1-z)^2} \right) \\
&\underset{\epsilon<<1}{=} 2g^2 C_F p_\perp^2 \left(\frac{(1-\epsilon)(1-z)}{z^2} + \frac{(1+\epsilon)(1-z)}{z^2(1-z)^2} \right) \\
&= 2g^2 C_F p_\perp^2 \left(\frac{(1-\epsilon)(1-z)^2 + 1 + \epsilon}{z^2(1-z)} \right) \\
&= \frac{2g^2 p_\perp^2}{z(1-z)} \left[C_F\ \frac{1 + (1-z)^2 - \epsilon(1-z)^2 + \epsilon}{z} \right] \\
&= \frac{2g^2 p_\perp^2}{z(1-z)} \left[\frac{4}{3} \left(\frac{1 + (1-z)^2}{z} - \epsilon z + \underbrace{2\epsilon}_{\to 0} \right) \right]
\end{aligned}
\tag{C.1}
$$

as the final result. The factor outside the angular brackets is commonly excluded from the splitting function because the denominator cancels in explicit computations of a cross section (see chapter 17.5 of [7]). For this reason, we ultimately state the splitting function

$$P^{<}_{g\leftarrow q}(z) = \frac{4}{3}\left(\frac{1+(1-z)^2}{z} - \epsilon z\right) \tag{C.2}$$

for quark $\rightarrow$ gluon splitting.

C.2. Quark $\rightarrow$ quark splitting $P^{<}_{q\leftarrow q}$

For this case all work is already done: Due to the fact that we exclude delta contributions since $z < 1$ we may directly adopt the latter result for quark $\rightarrow$ gluon splitting only performing the replacement $z \leftrightarrow 1-z$, thus

$$P^{<}_{q\leftarrow q}(z) = \frac{4}{3}\left(\frac{1+z^2}{1-z} - \epsilon(1-z)\right) \tag{C.3}$$

is the requested result.

C.3. Gluon $\rightarrow$ quark splitting $P^{<}_{q\leftarrow g}$

In the case of a gluon splitting into a quark-antiquark pair we assign the four-momentum q to the antiquark and k to the quark, z is the energy fraction of the gluon carried away by the antiquark. Assuming this the expressions of chapter C.1 have to be modified slightly. We have the right- and left-handed spinors

$$v_R(q) = \sqrt{2q^0}\begin{pmatrix}\xi(q)\\0\end{pmatrix}\ ,\ u_L(k) = \sqrt{2k^0}\begin{pmatrix}\xi(k)\\0\end{pmatrix}$$

for antiquark and quark, respectively, with

$$\xi(q) = \begin{pmatrix}-\frac{p_\perp}{2zp}\\1\end{pmatrix}\ ,\ \xi(k) = \begin{pmatrix}\frac{p_\perp}{2(1-z)p}\\1\end{pmatrix}$$

besides the two gluon polarizations

$$\varepsilon_L(p) = \frac{1}{\sqrt{2}}\begin{pmatrix}1\\-i\\0\end{pmatrix}\ ,\ \varepsilon_R(q) = \frac{1}{\sqrt{2}}\begin{pmatrix}1\\i\\0\end{pmatrix}$$

again for left- and right-handed channel. Parity invariance makes it possible anon to calculate only two of four possible helicity channels. Here, we calculate the contributions

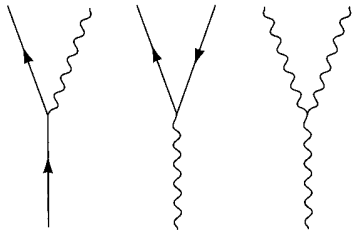

Figure C.1: Depiction of the splitting function vertices with the gluon characterized by waves [7]. $P_{q\leftarrow q}$, $P_{g\leftarrow q}$ (left), $P_{q\leftarrow g}$ (middle), $P_{g\leftarrow g}$ (right).

$$
\begin{aligned}
iM(g_L \to q_L\ \bar{q}_R) &= \bar{u}_L(k)\ (g\gamma_\mu T^a_{ij})\ v_R(q)\ \varepsilon^\mu_L(p) = \frac{\sqrt{2}gT^a_{ij}}{\sqrt{D-2}}\ \sqrt{2zp}\sqrt{2(1-z)p}\ \xi^\dagger(k)\ \sigma^i\varepsilon^i_L\ \xi(q) \\
&= \frac{2gT^a_{ij}\ p\sqrt{z(1-z)}\ \xi^\dagger(k)}{\sqrt{D-2}} \left[\begin{pmatrix} 0 & 1 \\ 1 & 0 \end{pmatrix} \cdot 1 - \begin{pmatrix} 0 & -i \\ i & 0 \end{pmatrix} \cdot i \right]\ \xi(q) \\
&= \frac{2gT^a_{ij}\ p\sqrt{z(1-z)}}{\sqrt{D-2}} \begin{pmatrix} \frac{p_\perp}{2(1-z)p} & 1 \end{pmatrix} \begin{pmatrix} 0 & 0 \\ 2 & 0 \end{pmatrix} \begin{pmatrix} -\frac{p_\perp}{2zp} \\ 1 \end{pmatrix} \\
&= \frac{2gT^a_{ij}\ p\sqrt{z(1-z)}}{\sqrt{D-2}} \begin{pmatrix} \frac{p_\perp}{2(1-z)p} & 1 \end{pmatrix} \begin{pmatrix} 0 \\ -\frac{p_\perp}{zp} \end{pmatrix} \\
&= -\frac{2gT^a_{ij}}{\sqrt{D-2}}\ \frac{\sqrt{z(1-z)}}{z}\ p_\perp
\end{aligned}
$$

and

$$
\begin{aligned}
iM(g_R \to q_L\ \bar{q}_R) &= \bar{u}_L(k)\ (g\gamma_\mu T^a_{ij})\ v_R(q)\ \varepsilon^\mu_R(p) = \frac{\sqrt{2}gT^a_{ij}}{\sqrt{D-2}}\ \sqrt{2zp}\sqrt{2(1-z)p}\ \xi^\dagger(k)\ \sigma^i\varepsilon^i_R\ \xi(q) \\
&= \frac{2gT^a_{ij}\ p\sqrt{z(1-z)}\ \xi^\dagger(k)}{\sqrt{D-2}} \left[\begin{pmatrix} 0 & 1 \\ 1 & 0 \end{pmatrix} \cdot 1 + \begin{pmatrix} 0 & -i \\ i & 0 \end{pmatrix} \cdot i \right]\ \xi(q) \\
&= \frac{2gT^a_{ij}\ p\sqrt{z(1-z)}}{\sqrt{D-2}} \begin{pmatrix} \frac{p_\perp}{2(1-z)p} & 1 \end{pmatrix} \begin{pmatrix} 0 & 2 \\ 0 & 0 \end{pmatrix} \begin{pmatrix} -\frac{p_\perp}{2zp} \\ 1 \end{pmatrix} \\
&= \frac{2gT^a_{ij}\ p\sqrt{z(1-z)}}{\sqrt{D-2}} \begin{pmatrix} \frac{p_\perp}{2(1-z)p} & 1 \end{pmatrix} \begin{pmatrix} 2 \\ 0 \end{pmatrix} \\
&= \frac{2gT^a_{ij}}{\sqrt{D-2}}\ \frac{\sqrt{z(1-z)}}{1-z}\ p_\perp
\end{aligned}
$$

which add up to

$$
\begin{aligned}
\frac{1}{2}\cdot\frac{1}{8}\sum_{pol.}|M_I|^2 &= \frac{1}{16}\left(|M_{L\to LR}|^2+|M_{R\to LR}|^2+|M_{R\to RL}|^2+|M_{L\to RL}|^2\right)\\
&= \frac{1}{16}\cdot 2\cdot 4g^2p_\perp^2\ \left(\frac{4}{D-2}\ \frac{1-z}{z}+\frac{4}{D-2}\ \frac{z}{1-z}\right)\\
&\underset{D=4-2\epsilon}{=}\ \frac{1}{2}g^2p_\perp^2\ \left(\frac{2}{1-\epsilon}\ \frac{1-z}{z}+\frac{2}{1-\epsilon}\ \frac{z}{1-z}\right)\\
&\underset{\epsilon<<1}{=}\ g^2p_\perp^2\ \left(\frac{(1+\epsilon)(1-z)}{z}+\frac{(1+\epsilon)z}{1-z}\right)\\
&= g^2p_\perp^2\ \left(\frac{z^2+(1-z)^2+\epsilon z^2+\epsilon(1-z)^2}{z(1-z)}\right)\\
&= \frac{2g^2p_\perp^2}{z(1-z)}\ \left[\frac{1}{2}\ \left(z^2+(1-z)^2-2\epsilon z(1-z)+\underbrace{\epsilon}_{\to\ 0}\right)\right]
\end{aligned}
\tag{C.4}
$$

in averaged shape where the splitting function

$$
P^<_{q\leftarrow g}(z)=\frac{1}{2}\ \left(z^2+(1-z)^2-2\epsilon z(1-z)\right) \tag{C.5}
$$

is already indicated.

C.4. Gluon → gluon splitting $P^<_{g\leftarrow g}$

For the gluon → gluon splitting the calculation procedure changes a bit because no fermionic spinors are involved. Instead, we must handle the three-gluon-vertex again considering all possible helicity states. Therefor, we need the vertex written with explicit polarization vectors which in our case already equals the desired matrix element. It holds

$$
iM = gf^{abc}\ \left[\varepsilon^*(q)\ \varepsilon(p)\ ((p+q)\ \varepsilon^*(k))+\varepsilon^*(q)\ \varepsilon^*(k)\ ((k-q)\ \varepsilon(p))-\varepsilon^*(k)\ \varepsilon(p)\ ((p+k)\ \varepsilon^*(q))\right] \tag{C.6}
$$

whereby the polarization vectors are specified by

$$
\begin{aligned}
\varepsilon_L(p) &= \frac{1}{\sqrt{2}}\begin{pmatrix}1\\-i\\0\end{pmatrix}\ ,\ \varepsilon_L(q)=\frac{1}{\sqrt{2}}\begin{pmatrix}1\\-i\\-\frac{p_\perp}{zp}\end{pmatrix}\ ,\ \varepsilon_L(k)=\frac{1}{\sqrt{2}}\begin{pmatrix}1\\-i\\\frac{p_\perp}{(1-z)p}\end{pmatrix}\ ,\\
\varepsilon_R(p) &= \frac{1}{\sqrt{2}}\begin{pmatrix}1\\i\\0\end{pmatrix}\ \ ,\ \varepsilon_R(q)=\frac{1}{\sqrt{2}}\begin{pmatrix}1\\i\\-\frac{p_\perp}{zp}\end{pmatrix}\ ,\ \varepsilon_R(k)=\frac{1}{\sqrt{2}}\begin{pmatrix}1\\i\\\frac{p_\perp}{(1-z)p}\end{pmatrix}
\end{aligned}
$$

for left- and right-handed gluons, respectively. Evaluating (C.6) is now straightforward while only half of all channels have to be calculated as before and terms of order $p_\perp^2$ are neglected due to $p_\perp << 1$. It should be noted that dimensions do not enter anymore due to absent Dirac structure. We obtain

$$
\begin{aligned}
&iM(g_L(p) \to g_L(q)\ g_L(k)) \\
&\quad = gf^{abc}\left[\begin{pmatrix} p_\perp \\ 0 \\ p+zp \end{pmatrix} \cdot \frac{1}{\sqrt{2}} \begin{pmatrix} 1 \\ i \\ \frac{p_\perp}{(1-z)p} \end{pmatrix} + \ldots \cdot \underbrace{\left(-\frac{p_\perp^2}{2zp(1-z)p}\right)}_{\approx 0} + \frac{1}{\sqrt{2}}\left(p_\perp + (p+(1-z)p)\cdot\frac{p_\perp}{zp}\right)\right] \\
&\quad = gf^{abc}\left[\frac{1}{\sqrt{2}}\left(p_\perp + \frac{p_\perp}{1-z} + \frac{zp_\perp}{1-z}\right) + \frac{p_\perp}{\sqrt{2}} + \frac{2p_\perp}{\sqrt{2}z} - \frac{p_\perp}{\sqrt{2}}\right] \\
&\quad = gf^{abc}\left[\frac{1}{\sqrt{2}}\left(\frac{(1-z)p_\perp + p_\perp + zp_\perp}{1-z}\right) + \frac{2p_\perp}{\sqrt{2}z}\right] \\
&\quad = gf^{abc}\left[\frac{1}{\sqrt{2}}\left(\frac{2p_\perp}{1-z} + \frac{2p_\perp}{z}\right)\right] \\
&\quad = \sqrt{2}gf^{abc}p_\perp\left(\frac{1}{1-z} + \frac{1}{z}\right)\ ,
\end{aligned}
$$

$$
\begin{aligned}
&iM(g_L(p) \to g_L(q)\ g_R(k)) \\
&\quad = gf^{abc}\left[\begin{pmatrix} p_\perp \\ 0 \\ p+zp \end{pmatrix} \cdot \frac{1}{\sqrt{2}} \begin{pmatrix} 1 \\ -i \\ \frac{p_\perp}{(1-z)p} \end{pmatrix} + (1 - \underbrace{\frac{p_\perp^2}{2zp(1-z)p}}_{\approx 0}) \cdot \begin{pmatrix} -2p_\perp \\ 0 \\ (1-z)p - zp \end{pmatrix} \cdot \frac{1}{\sqrt{2}} \begin{pmatrix} 1 \\ -i \\ 0 \end{pmatrix}\right] \\
&\quad = gf^{abc}\left[\frac{1}{\sqrt{2}}\left(\frac{2p_\perp}{1-z} - 2p_\perp\right)\right] \\
&\quad = \sqrt{2}gf^{abc}\left[\frac{p_\perp - p_\perp(1-z)}{1-z}\right] \\
&\quad = \sqrt{2}gf^{abc}p_\perp\left(\frac{z}{1-z}\right)\ ,
\end{aligned}
$$

$$
\begin{aligned}
&iM(g_L(p) \to g_R(q)\ g_L(k)) \\
&\quad = gf^{abc}\left[(1 - \underbrace{\frac{p_\perp^2}{2zp(1-z)p}}_{\approx 0}) \cdot \begin{pmatrix} -2p_\perp \\ 0 \\ (1-z)p - zp \end{pmatrix} \cdot \frac{1}{\sqrt{2}} \begin{pmatrix} 1 \\ -i \\ 0 \end{pmatrix} + \frac{p_\perp}{\sqrt{2}} + \frac{2p_\perp}{\sqrt{2}z} - \frac{p_\perp}{\sqrt{2}}\right]
\end{aligned}
$$

$$= g f^{abc} \left[\frac{1}{\sqrt{2}} \left(-2p_\perp + \frac{2p_\perp}{z} \right) \right]$$
$$= \sqrt{2} g f^{abc} p_\perp \left(\frac{1-z}{z} \right) \ ,$$

and finally

$$iM(g_L(p) \to g_R(q)\ g_R(k)) = (- \underbrace{\frac{p_\perp^2}{2zp(1-z)p}}_{\approx 0}) \cdot \begin{pmatrix} -2p_\perp \\ 0 \\ (1-z)p - zp \end{pmatrix} \cdot \frac{1}{\sqrt{2}} \begin{pmatrix} 1 \\ -i \\ 0 \end{pmatrix}$$
$$= 0$$

as defining contributions that lead to

$$\begin{aligned} \frac{1}{2} \cdot \frac{1}{8} \sum_{pol.} |M_I|^2 &= \frac{1}{16} \left(|M_{L\to LL}|^2 + |M_{L\to LR}|^2 + |M_{L\to RL}|^2 + |M_{R\to RR}|^2 + |M_{R\to RL}|^2 + |M_{R\to LR}|^2 \right) \\ &= \frac{1}{16} \cdot 2 \cdot \underbrace{24}_{f^{abc} f^{abc}} \cdot 2 g^2 p_\perp^2 \left(\left(\frac{1}{1-z} + \frac{1}{z} \right)^2 + \left(\frac{z}{1-z} \right)^2 + \left(\frac{1-z}{z} \right)^2 \right) \\ &= 6 g^2 p_\perp^2 \left(\frac{1}{(1-z)^2} + \frac{2}{z(1-z)} + \frac{1}{z^2} + \frac{z^2}{(1-z)^2} + \frac{1}{z^2} - \frac{2}{z} + 1 \right) \\ &= \frac{6 g^2 p_\perp^2}{z(1-z)} \left(\frac{z}{1-z} + 2 + \frac{1-z}{z} + \frac{z^3}{1-z} + \frac{1-z}{z} - 2(1-z) + z(1-z) \right) \\ &= \frac{2 g^2 p_\perp^2}{z(1-z)} \left[6\ \frac{(1-z+z^2)^2}{z(1-z)} \right] \end{aligned} \tag{C.7}$$

as ultimate result. According to this, the splitting function is read off to be

$$P^<_{g\leftarrow g}(z) = 6\ \frac{(1-z+z^2)^2}{z(1-z)} \ . \tag{C.8}$$

It is exactly the same as its more usual form

$$P^<_{g\leftarrow g}(z) = 6\ \left(\frac{z}{1-z} + \frac{1-z}{z} + z(1-z) \right) \tag{C.9}$$

what is shown with a few algebra.

References

[1] **NNLO Contributions to Jet Production in Deep Inelastic Scattering**. Thomas Biekötter; Master thesis, Westfälische Wilhelms-Universität Münster, Germany, July 2015; *https://www.uni-muenster.de/Physik.TP/research/klasen/teaching.shtml*

[2] **Next-to-next-to-leading order contributions to inclusive jet production in deep-inelastic scattering and determination of α_s.** T. Biekötter, M. Klasen, G. Kramer; Phys.Rev. D92, 074037 (2015); *arXiv:1508.07153 [hep-ph]*

[3] **JetVip 2.1: The hbook version**. B. Pötter; Comput.Phys.Commun. 133 (2000) 105-118; *arXiv:hep-ph/9911221 [hep-ph]*

[4] **A unified approach to NNLO soft and virtual corrections in electroweak, Higgs, QCD, and SUSY processes**. N. Kidonakis; Int.J.Mod.Phys. A19 (2004) 1793–1821; *arXiv:hep-ph/0303186*

[5] **Threshold Resummation for Dijet Cross Sections**. N. Kidonakis, G. Oderda, G. Sterman; Nucl.Phys. B525 (1998) 299-332; *arXiv:hep-ph/9801268*

[6] **Resummed Cross Section for Jet Production at Hadron Colliders**. D. de Florian, W. Vogelsang; Phys.Rev. D76 (2007) 074031; *arXiv:0704.1677 [hep-ph]*

[7] **An introduction to quantum field theory**. M. E. Peskin, D. V. Schroeder; Perseus Books Publishing; August 1995

[8] **Foundations of Quantum Chromodynamics**. T. Muta; World Scientific Publishing Co Pte Ltd, 1987

[9] **Introduction to QCD**. Michelangelo L. Mangano; CERN, TH Division, Geneva, Switzerland; *https://cds.cern.ch/record/454171/files/p53.pdf*

[10] **Inclusive Single- and Dijet Rates in Next-to-Leading Order QCD for $\gamma^* p$ and $\gamma^*\gamma$ Collisions**. B. Pötter; PhD thesis, University of Hamburg, 1997

[11] **Next-to-next-to-next-to-leading-order soft-gluon corrections in hard-scattering processes near threshold**. N. Kidonakis; Phys.Rev. D73 (2006) 034001; *arXiv:hep-ph/0509079*

[12] **Resummation for supersymmetric particle production at hadron colliders**.
Silja Christine Brensing; PhD thesis, RWTH Aachen University, Germany, May 2011; *https://publications.rwth-aachen.de/record/82641/files/3837.pdf*

[13] **Resummation for QCD Hard Scattering**.
N. Kidonakis, G. Sterman; May 1997; Nucl.Phys. B505 (1997) 321-348; *arXiv:hep-ph/9705234*

[14] **Precise predictions for supersymmetric particle production at the LHC**.
Marcel Rothering; PhD thesis, Westfälische Wilhelms-Universität Münster, Germany, 2016; *https://www.uni-muenster.de/Physik.TP/research/klasen/teaching.shtml*

[15] **Soft Gluon Resummation for Heavy Particle Production at the Large Hadron Collider**.
Vincent Michel Theeuwes; PhD thesis, Westfälische Wilhelms-Universität Münster, Germany, September 2015

[16] **Soft-gluon resummation and NNLO corrections for direct photon production**.
N. Kidonakis, J. F. Owens; Phys.Rev. D61 (2000) 094004; *arXiv:hep-ph/9912388*

[17] **Single inclusive jet production in polarized pp collisions at $\mathcal{O}(\alpha_s^3)$**.
B. Jäger, M. Stratmann, W. Vogelsang; Phys.Rev. D70 (2004) 034010; *arXiv:hep-ph/0404057*

[18] **Jet production in (un)polarized pp collisions: dependence on jet algorithm**.
A. Mukherjee, W. Vogelsang; Phys.Rev. D86, 094009 (2012); *https://journals.aps.org/prd/pdf/10.1103/PhysRevD.86.094009*

[19] **Next-to-leading order QCD corrections to high-p_T pion production in longitudinally polarized pp collisions**.
B. Jäger, A. Schäfer, M. Stratmann, W. Vogelsang; Phys.Rev. D67 (2003) 054005; *arXiv:hep-ph/0211007*

[20] **Hadron Fragmentation Inside Jets in Hadronic Collisions**.
T. Kaufmann, A. Mukherjee, W. Vogelsang; Phys.Rev. D92, 054015 (2015); *arXiv:1506.01415 [hep-ph]*

[21] **Regularized Unfolding of Jet Cross Sections in Deep-Inelastic *ep* Scattering at HERA and Determination of the Strong Coupling Constant**.
Daniel Andreas Britzger; PhD thesis, University of Hamburg, 2013; *https://www-h1.desy.de/psfiles/theses/h1th-831.pdf*

[22] **LHAPDF6: parton density access in the LHC precision era**.
A. Buckley et al.; Eur.Phys.J. C75 (2015) 3, 132; *arXiv:1412.7420 [hep-ph]*

[23] **Prompt Photon Production Predictions at NLO and in POWHEG**.
Florian König; PhD thesis, Westfälische Wilhelms-Universität Münster, Germany, December 2016;
https://www.uni-muenster.de/Physik.TP/research/klasen/teaching.shtml

Acknowledgements

We thank Werner Vogelsang (University of Tübingen) for his friendly support.

Declaration of academic integrity

I hereby confirm that this thesis on

Jet radius dependence in aNNLO in DIS and photoproduction

is solely my own work and that I have used no sources or aids other than the ones stated. All passages in my thesis for which other sources, including electronic media, have been used, be it direct quotes or content references, have been acknowledged as such and the sources cited.

Münster, 27 March 2018 _____

Jonas Potthoff

I agree to have my thesis checked in order to rule out potential similarities with other works and to have my thesis stored in a database for this purpose.

Münster, 27 March 2018 _____

Jonas Potthoff